SHIP DYNAMICS

TABLE OF CONTENTS

1. Maneuvering Motions.

The subject of *ship dynamics* is very broad and can be roughly divided into two categories: *maneuverability* or *controllability*, and *motions in waves* or *seakeeping*. Maneuvering involves motions that are inflicted upon the ship as a result of action taken by the autopilot or the helmsman and their characteristic time length spans over a few minutes. Seakeeping on the other hand is the study of motions that occur over a characteristic period of a few seconds as a result of wave action. Since the time scales of the two types of motions are vastly different, it is permissible to study them separately; i.e, study maneuvering when in calm waters, and seakeeping while the ship is maintaining straight course. Interactions between the two types of motions (for example, what happens to the rolling motion characteristics of a ship when turning in waves), are a matter of current research.

Maneuvering involves conflicting requirements. We wish to be able to steer the vessel on course and we wish to be able to turn when necessary. The first leads to consideration of controls fixed course stability. The second leads to consideration of the vessel's ability to turn. Slow speed operation and stopping are additional considerations. Course keeping and turning are conflicting objectives. A vessel which is extremely stable on course will be difficult to turn. A vessel which is unstable on course will be easy to turn and in fact it may decide to turn on its own due to external disturbances. Not too long ago the rule of thumb was that a vessel must be controls fixed course stable. With the development of fuller vessels and open sterns to improve propeller induced vibration, course unstable vessels have been built and operated successfully for some time. The question in control theory then is: how unstable can a ship be and still be controllable by the typical helmsman or by an autopilot?

Consideration of the generic control loop of Figure 1 shows that each of its elements plays a vital role in the overall response of the ship. The last element of the loop, the "ship", will be the main concern of this section, although the human factors present must be continually reviewed to develop a successful design. In the following sub–sections, we will attempt to quantify the block named "ship"; i.e, establish the response characteristics of the vessel due to rudder commands and other external forces. Whereas the directional loop of the figure functions to determine the path, a second loop of interest, the speed control loop, functions to regulate the speed along the path. In restricted and congested waters, orders to both control loops may have to be issued simultaneously, and with the development of automation, integration of these loops is becoming commonplace.

1.1 Linear equations in the horizontal plane.

The basic dynamics of maneuvering and coursekeeping can be described and analyzed using Newton's equations of motion. Basic equations in the horizontal plane can be considered first with reference to one set of axes fixed relative to the earth, and a second set fixed relative to the ship.

Figure 2 shows typical fixed and moving axes for a surface ship. The path is usually defined as the trajectory traced by the ship's center of gravity or some other reference point. Heading refers to the direction (ψ, yaw angle) of the ship's longitudinal axis with respect to one of the fixed axes. The difference between the heading and the actual course (or direction

of the velocity vector at the center of gravity) is the drift angle β. Writing Newton's law in the inertial (non–accelerating) reference frame (x_0, y_0) we have

$$\begin{aligned} m\ddot{x}_0 &= X_0 \,, \\ m\ddot{y}_0 &= Y_0 \,, \\ I_z\ddot{\psi} &= N \,, \end{aligned} \tag{1}$$

where

$$\begin{aligned} X_0 &= \text{total force in the } x_0 \text{ direction} \,, \\ Y_0 &= \text{total force in the } y_0 \text{ direction} \,, \\ N &= \text{turning moment around the } z_0 \text{ axis} \,, \\ m &= \text{ship's mass} \,, \\ I_z &= \text{mass moment of inertia of the ship about the } z_0 \text{ axis} \,, \\ \psi &= \text{yaw angle measured with respect to the } x_0 \text{ axis} \,. \end{aligned}$$

In spite of the apparent simplicity of equations (1), the motion of a ship is more conveniently expressed when referred to the (x, y) system of coordinates fixed with respect to the moving ship (the inertial system of coordinates which may have its origin in Kansas becomes an awkward frame of reference when the ship is not in Kansas any more). The ship fixed reference frame is always a right hand frame, with the x–axis pointing in the longitudinal direction, the y–axis positive starboard, and the z–axis positive down. We can transform coordinate systems using

$$\begin{aligned} X &= X_0 \cos\psi + Y_0 \sin\psi \,, \\ Y &= Y_0 \cos\psi - X_0 \sin\psi \,, \\ \dot{x}_0 &= u\cos\psi - v\sin\psi \,, \\ \dot{y}_0 &= u\sin\psi + v\cos\psi \,. \end{aligned}$$

Differentiating and substituting into equations (1) we obtain, using the fact that $\dot{\psi} = r$,

$$m\dot{u} - mvr = X \,, \quad \text{surge equation} \,, \tag{2}$$

$$m\dot{v} + mur = Y \,, \quad \text{sway equation} \,, \tag{3}$$

$$I_z\dot{r} = N \,, \quad \text{yaw equation} \,, \tag{4}$$

where u, v, r are the longitudinal or surge, lateral or sway, and rotational or yaw velocities of the moving ship. It is also convenient to write the above equations of motion with respect to a ship fixed reference frame at amidships instead of the center of gravity. If this is done we pick up a few additional terms

$$\begin{aligned} m\dot{u} - mvr - mx_G r^2 &= X \,, \\ m\dot{v} + mur + mx_G\dot{r} &= Y \,, \\ I_z\dot{r} + mx_G(\dot{v} + ur) &= N \,, \end{aligned} \tag{5}$$

assuming that $y_G = 0$. Note the existence of centrifugal forces in the above equations which exist when systems with moving axes are considered, but do not exist for inertial coordinate frames.

The forces and moments (right hand side) of the equations of motion (2) to (4) are build up of four types of forces that act on a ship during a maneuver:

1. Fluid forces acting on the hull due to the surrounding water, designated by the subscript F.
2. Forces due to control surfaces such as rudders, dive planes, bow planes, thrusters; subscript R.
3. Various environmental forces due to wind, current, or waves; subscript E.
4. Propulsion force, T.

Therefore, in general we can say

$$\begin{aligned} X &= X_F + X_R + X_E + T \ , & (6)\\ Y &= Y_F + Y_R + Y_E \ , & (7)\\ N &= N_F + N_R + N_E \ . & (8) \end{aligned}$$

The hydrodynamic forces X_F, Y_F, N_F depend on the motion of the ship through the water and are expected to be functions of the ship velocities and accelerations relative to the water. In other words, we can write

$$\begin{aligned} X_F &= X_F(u, v, \dot{u}, \dot{v}, r, \dot{r}) \ , & (9)\\ Y_F &= Y_F(u, v, \dot{u}, \dot{v}, r, \dot{r}) \ , & (10)\\ N_F &= N_F(u, v, \dot{u}, \dot{v}, r, \dot{r}) \ . & (11) \end{aligned}$$

The functional dependence of equations (9) through (11) can be quite complicated; however, for usual maneuvering studies a significant simplification occurs. We are interested in the ship response around a nominal equilibrium point designated by the subscript 1. Expanding the forces in a Taylor series around the nominal point and keeping the first order terms only, we have

$$\begin{aligned} Y_F &= Y_F(u_1, v_1, \dot{u}_1, \dot{v}_1, r_1, \dot{r}_1) + (u - u_1)\frac{\partial Y_F}{\partial u} + (v - v_1)\frac{\partial Y_F}{\partial v} \\ &\quad + \cdots + (\dot{r} - \dot{r}_1)\frac{\partial Y_F}{\partial \dot{r}} \ , \qquad (12) \end{aligned}$$

where all of the partial derivatives are evaluated at the nominal condition. Similar to (12) expressions hold for X_F and N_F as well.

Now the nominal condition is straight line motion at constant speed, or

$$u_1 = U, \ v_1 = \dot{u}_1 = \dot{v}_1 = r_1 = \dot{r}_1 = 0 \ . \qquad (13)$$

Because of port/starboard symmetry $\partial Y_F/\partial u = \partial Y_F/\partial \dot{u} = 0$ since a change in forward velocity or acceleration will produce no transverse force with ships that are symmetrical

about the xz–plane. Furthermore, if the ship is in fact in equilibrium in straight line motion, there can be no Y_F–force acting on it in that condition, therefore the first term in (12) is also zero. With these simplifications, equation (12) reduces to

$$Y_F = \frac{\partial Y_F}{\partial v}v + \frac{\partial Y_F}{\partial \dot{v}}\dot{v} + \frac{\partial Y_F}{\partial r}r + \frac{\partial Y_F}{\partial \dot{r}}\dot{r} \ , \tag{14}$$

and similarly the surge force and yaw moment can be written as

$$X_F = \frac{\partial X_F}{\partial \dot{u}}\dot{u} + \frac{\partial X_F}{\partial u}(u-U) + \frac{\partial X_F}{\partial v}v + \frac{\partial X_F}{\partial \dot{v}}\dot{v} + \frac{\partial X_F}{\partial r}r + \frac{\partial X_F}{\partial \dot{r}}\dot{r} \ , \tag{15}$$

$$N_F = \frac{\partial N_F}{\partial v}v + \frac{\partial N_F}{\partial \dot{v}}\dot{v} + \frac{\partial N_F}{\partial r}r + \frac{\partial N_F}{\partial \dot{r}}\dot{r} \ , \tag{16}$$

where the cross coupling derivatives $\partial Y_F/\partial r$, $\partial Y_F/\partial \dot{r}$, $\partial N_F/\partial v$, and $\partial N_F/\partial \dot{v}$ usually have small nonzero values because most ships are not symmetrical about the yz–plane even if that plane is at the midlength of the ship (bow and stern shapes are normally quite different). However, the cross coupling derivatives $\partial X_F/\partial v$, $\partial X_F/\partial \dot{v}$, $\partial X_F/\partial r$, and $\partial X_F/\partial \dot{r}$ are zero because of symmetry about the xz–plane and equation (13). Hence, equation (15) reduces to

$$X_F = \frac{\partial X_F}{\partial \dot{u}}\dot{u} + \frac{\partial X_F}{\partial u}(u-U) \ . \tag{17}$$

In standard notation, we call $\partial Y_F/\partial v = Y_v$, $\partial N_F/\partial r = N_r$, and so on. These are the so called *hydrodynamic derivatives*, and besides their mathematical definition in terms of first order partial derivatives, they carry a rather concrete physical meaning as well: Y_r, for example, is the force in the sway direction due to a unit change in the yaw angular velocity.

Using the above notation, and substituting into equations (5), the *linear* equations of motion in the horizontal plane in the absence of environmental disturbances and with the control surfaces at zero, become

$$(m - X_{\dot{u}})\dot{u} = X_u(u-U) \ , \tag{18}$$

$$(m - Y_{\dot{v}})\dot{v} - (Y_{\dot{r}} - mx_G)\dot{r} = Y_v v + (Y_r - mU)r \ , \tag{19}$$

$$(I_z - N_{\dot{r}})\dot{r} - (N_{\dot{v}} - mx_G)\dot{v} = N_v v + (N_r - mx_G U)r \ , \tag{20}$$

where we can see that within linearity the surge equation decouples from sway and yaw.

It is important to note that all of the terms of equations (19) and (20) must include the effect of the ship's rudder held at zero. On the other hand, if we want to consider the path of a ship with controls working, the equations of motion (19) and (20) must include terms on the right hand side expressing the control forces and moments created by rudder deflection (or any other control devices) as functions of time. Assuming that the rudder force and moment on the ship are functions of the rudder angle δ only, and not $\dot{\delta}$, we have

$$X_R(\delta) = X_R(\delta = 0) + \frac{\partial X_R}{\partial \delta}\delta = 0 \ , \tag{21}$$

$$Y_R(\delta) = Y_R(\delta = 0) + \frac{\partial Y_R}{\partial \delta}\delta = Y_\delta \delta \ , \tag{22}$$

$$N_R(\delta) = N_R(\delta = 0) + \frac{\partial N_R}{\partial \delta}\delta = N_\delta \delta \ , \tag{23}$$

where δ is the rudder deflection angle (see Figure 3) measured according to the right hand sign convention of Figure 2; positive rudder deflection corresponds to a turn to port for rudder located at the stern. Y_δ and N_δ are the rudder hydrodynamic derivatives. Including the rudder forces and moments, the linearized sway, (19), and yaw, (20), equations of motion become

$$(m - Y_{\dot{v}})\dot{v} - (Y_{\dot{r}} - mx_G)\dot{r} = Y_v v + (Y_r - mU)r + Y_\delta \delta \ , \tag{24}$$

$$(I_z - N_{\dot{r}})\dot{r} - (N_{\dot{v}} - mx_G)\dot{v} = N_v v + (N_r - mx_G U)r + N_\delta \delta \ . \tag{25}$$

Maneuvering work is commonly done in dimensionless form. Using the water density ρ, the ship length L, and the nominal forward speed U, we can nondimensionalize the variables as in

$$\begin{aligned}
&v' = \frac{v}{U} \ , \ r' = \frac{rL}{U} \ , \ \dot{v}' = \frac{\dot{v}L}{U^2} \ , \ \dot{r}' = \frac{\dot{r}L^2}{U^2} \ , \\
&t' = \frac{tU}{L} \ , \ m' = \frac{m}{\frac{1}{2}\rho L^3} \ , \ I_z' = \frac{I_z}{\frac{1}{2}\rho L^5} \ , \ x_G' = \frac{x_G}{L} \ , \\
&Y_{\dot{v}}' = \frac{Y_{\dot{v}}}{\frac{1}{2}\rho L^3} \ , \ Y_{\dot{r}}' = \frac{Y_{\dot{r}}}{\frac{1}{2}\rho L^4} \ , \ N_{\dot{v}}' = \frac{N_{\dot{v}}}{\frac{1}{2}\rho L^4} \ , \ N_{\dot{r}}' = \frac{N_{\dot{r}}}{\frac{1}{2}\rho L^5} \ , \\
&Y_v' = \frac{Y_v}{\frac{1}{2}\rho L^2 U} \ , \ Y_r' = \frac{Y_r}{\frac{1}{2}\rho L^3 U} \ , \ N_v' = \frac{N_v}{\frac{1}{2}\rho L^3 U} \ , \ N_r' = \frac{N_r}{\frac{1}{2}\rho L^4 U} \ , \\
&Y_\delta' = \frac{Y_\delta}{\frac{1}{2}\rho L^2 U^2} \ , \ N_\delta = \frac{N_\delta}{\frac{1}{2}\rho L^3 U^2} \ .
\end{aligned}$$

Note that the unit of time is now the time it takes to travel one ship length. The dimensionless form of the equations then turns out to be identical in the primed variables to that of (24) and (25) with $U' = 1$. In the following, we will always assume the dimensionless form of the equations, unless otherwise mentioned, and for convenience we will drop the primes.

In the next three sections, it will be shown how the linearized equations (24) and (25) can be used to analyze the problems of course stability and steady turning. In order to make numerical predictions it is necessary to obtain values for the hydrodynamic derivatives involved, and this is discussed in Section 1.6

1.2 Stability of straight line motion.

The concept of path keeping is strongly related to the concept of course stability or stability of straight line motion. The various kinds of motion stability associated with marine vehicles are classified by the attributes of their initial state of equilibrium that are retained in the final path of their center of gravity. For example, in each of the cases in Figure 4, a ship is initially assumed to be traveling at constant speed along a straight path. In Case I, termed straight line or *dynamic* stability, the final path after release from a disturbance retains the straight line attribute of the initial state of equilibrium, but not its direction. In Case II, *directional* stability, the final path after release from a disturbance retains not only the straight line attribute of the initial path, but also its direction. Case III is similar to Case II except that the ship does not oscillate after the disturbance, but passes smoothly

to the same final path as Case II. This implies complex conjugate characteristic roots with negative real parts for Case III and real negative for Case II. Finally, in Case IV, *positional* motion stability, the ship returns to the original path with the same direction as well as position.

The foregoing kinds of stability have been defined in a kind of ascending order. A ship that is directionally stable must also possess straight line stability. A ship that possesses positional motion stability must possess both directional and straight line stability. Straight line stability or instability is indicated by the solution to a second order differential equation, directional stability or instability is indicated by the solution to a third order differential equation, and positional stability or instability is indicated by the solution to a fourth order differential equation.

In ship and submarine usage the term stability usually implies controls fixed stability; however, the term can also have meaning with the controls working. The following examples indicate the distinctions:

(a) A surface ship on a calm sea possesses positional stability in the vertical plane with controls fixed. In this case, hydrostatic forces and moments introduce a unique kind of stability which in the absence of these forces could only be introduced either by very sophisticated automatic controls or by manual control.

(b) Hydrofoil boats with submerged foils do not possess this kind of stability with controls fixed, and must rely on an automatic control system to provide stability in pitch, heave, or roll.

(c) Neutrally buoyant submarines possess directional stability in the vertical plane with controls fixed. This is because of the existence of the metacentric restoring moment $\Delta\overline{BG}\sin\theta$, as discussed in Part I. Positional stability can be achieved only with suitable bow and/or dive plane action.

(d) In the horizontal plane in the open sea, a self propelled ship cannot possess either positional or directional stability with controls fixed because the changes in buoyancy that stabilize in the vertical plane are nonexistent in the horizontal plane. However, a ship must possess both of these kinds of stability with controls working either automatic or manual.

(e) An exception to this is the case of a sailing ship. Sailing ships can possess controls fixed directional stability (with respect to the wind direction) in the horizontal plane. This is because their propulsive force, the wind here, can introduce stabilizing forces and moments which tend to return the path of the ship to its original direction after a momentary disturbance.

(f) An other exception is the case of a towed ship. A towed ship can possess controls fixed positional stability (with respect to the tugboat direction of motion) because of the towline restoring forces and moments.

(g) The only kind of motion stability possible with self propelled ships in the horizontal plane with controls fixed is straight line stability. As noted in the beginning of Section 1, this kind of stability is desirable but not mandatory. In fact, many ships do not possess it. In the remaining of this section, whenever controls fixed stability is mentioned, the intended meaning is, unless otherwise specified, controls fixed straight line stability.

With each of the kinds of controls fixed stability, there is associated a numerical index which by its sign designates whether the body is stable or unstable in that particular sense and its magnitude designates the degree of stability or instability. To show how such an index

is determined, and to be able to evaluate the dynamic stability of a ship in a quantitative sense, we must resort to the differential equations of motion (19) and (20). This homogeneous set of differential equations will have a solution of the form

$$v(t) = v_1 e^{\sigma_1 t} + v_2 e^{\sigma_2 t} , \tag{26}$$
$$r(t) = r_1 e^{\sigma_1 t} + r_2 e^{\sigma_2 t} , \tag{27}$$

where the constants v_1, v_2, r_1, r_2 are determined from the initial conditions. Differentiation and substitution of (26) and (27) into (19) and (20) yields the characteristic equation

$$A\sigma^2 + B\sigma + C = 0 , \tag{28}$$

where

$$A = (I_z - N_{\dot{r}})(m - Y_{\dot{v}}) - (Y_{\dot{r}} - mx_G)(N_{\dot{v}} - mx_G) , \tag{29}$$
$$B = -(I_z - N_{\dot{r}})Y_v - (m - Y_{\dot{v}})(N_r - mx_G U) - (Y_r - mU)(N_{\dot{v}} - mx_G) - (Y_{\dot{r}} - mx_G)N_v , \tag{30}$$
$$C = (N_r - mx_G U)Y_v - (Y_r - mU)N_v , \tag{31}$$

with roots

$$\sigma_1, \sigma_2 = \frac{1}{2}\left(-\frac{B}{A} \pm \sqrt{\left(\frac{B}{A}\right)^2 - 4\left(\frac{C}{A}\right)} \right) . \tag{32}$$

Stability on course with controls fixed requires that both σ_1 and σ_2 have negative real parts. In such a case, it can be seen from (26) and (27) that both $v(t)$ and $r(t)$ will go to zero for increasing time, which means that the path of the ship will eventually resume a new straight line direction at a different, in general, heading. This corresponds to Case I of Figure 4. The stability requirement

$$\Re\{\sigma_1, \sigma_2\} < 0 ,$$

translates to

$$A > 0 , \quad B > 0 , \quad C > 0 , \tag{33}$$

i.e., all coefficients of the quadratic (28) to be positive. To evaluate whether conditions (33) are satisfied we have to check the signs of the hydrodynamic derivatives that enter in the definitions of A, B, C in equations (29) through (31). In order to do that we have to resort to the physical interpretation of the hydrodynamic derivatives as forces or moments acting on the hull due to the various hull motions with respect to the water.

A careful analysis of the various derivatives, Figure 5, shows the following (the reader is expected to spend some time studying the figure before reaching some of the conclusions that folow):

$Y_{\dot{v}}$ is always negative and large ,
Y_v is always negative and large ,
$N_{\dot{r}}$ is always negative and large ,

N_r is always negative and large ,
$Y_{\dot{r}}$ is small and of uncertain sign ,
Y_r is small and of uncertain sign ,
$N_{\dot{v}}$ is small and of uncertain sign ,
N_v is small and of uncertain sign ,
x_G is small and of uncertain sign ,
I_z is always positive and large ,
m is always positive and large .

This shows that A and B are always positive for ships, so stability requires

$$C = (N_r - mx_G U)Y_v - (Y_r - mU)N_v > 0 \ , \tag{34}$$

which is the *stability criterion*. The more positive C is the more stable the ship will be, and it will be increasingly difficult to turn. The more negative C is the more unstable the ship, and it will require continuous use of the rudder to keep course. One may observe from (34) that for stability, it is desirable to have $x_G > 0$; i.e, the center of gravity forward of amidships, a result which agrees with everyday experience.

The stability condition (34) can also be written in the form

$$\frac{N_r - mx_G U}{Y_r - mU} > \frac{N_v}{Y_v} \ , \tag{35}$$

since $Y_r - mU < 0$ and $Y_v < 0$. Inequality (35) can be viewed as a relationship between the lever arms of forces due to yaw and due to sway. If N_v is positive, we see that C is positive and stability is assured. If N_v is negative, however, as is usually the case with ships due to longer and finer fore bodies and fuller sterns, its magnitude will be the ultimate determination for ship straight line stability. The weathervane, by comparison, will seek the wind if N_v is positive, making it useful for its intended purpose. Weathervanes are designed with large tail surfaces to ensure a positive N_v. Ships have another degree of freedom and, in any case, could not maneuver well with a large positive value of N_v.

1.3 Stability and control.

Although the previous section arrived at a quantitative index, C, designating the stability of a ship, it is not always easy to evaluate particularly in a preliminary design phase. For this reason several simplified models have appeared, most notably Nomoto's K–T model. This uses two indices, K and T, which can be easily estimated from standard full scale sea trials. They are useful in comparing coursekeeping as well as turning abilities.

The steering equations of motion (24) and (25) can be manipulated to produce a pair of decoupled second order equations in r and v,

$$T_1 T_2 \ddot{r} + (T_1 + T_2)\dot{r} + r = K\delta + KT_3\dot{\delta} \ , \tag{36}$$
$$T_1 T_2 \ddot{v} + (T_1 + T_2)\dot{v} + v = K_v\delta + K_v T_4\dot{\delta} \ . \tag{37}$$

The first of these is now commonly called Nomoto's equation. The coefficients in these two equations are related to the hydrodynamic derivatives by the following:

$$
\begin{aligned}
T_1 T_2 &= \frac{(Y_{\dot{v}} - m)(N_{\dot{r}} - I_z) - (Y_{\dot{r}} - mx_G)(N_{\dot{v}} - mx_G)}{Y_v(N_r - mx_G U) - N_v(Y_r - mU)} \,, \\
T_1 + T_2 &= \frac{(Y_{\dot{v}} - m)(N_r - mx_G U) + (N_{\dot{r}} - I_z)Y_v}{Y_v(N_r - mx_G U) - N_v(Y_r - mU)} \\
&\qquad + \frac{-(Y_{\dot{r}} - mx_G)N_v - (N_{\dot{v}} - mx_G)(Y_r - mU)}{Y_v(N_r - mx_G U) - N_v(Y_r - mU)} \,, \\
T_3 &= \frac{(N_{\dot{v}} - mx_G)Y_\delta - (Y_{\dot{v}} - m)N_\delta}{N_v Y_\delta - Y_v N_\delta} \,, \\
T_4 &= \frac{(N_{\dot{r}} - I_z)Y_\delta - (Y_{\dot{r}} - mx_G)N_\delta}{(N_r - mx_G U)Y_\delta - (Y_r - mU)N_\delta} \,, \\
K &= \frac{N_v Y_\delta - Y_v N_\delta}{Y_v(N_r - mx_G U) - N_v(Y_r - mU)} \,, \\
-K_v &= \frac{(N_r - mx_G U)Y_\delta - (Y_r - mU)N_\delta}{Y_v(N_r - mx_G U) - N_v(Y_r - mU)} \,.
\end{aligned}
$$

Equation (36) expresses the relationship between the ship turning rate, r, and the rudder angle, δ, through a second order transfer function

$$
\frac{r}{\delta} = \frac{K + KT_3 s}{T_1 T_2 s^2 + (T_1 + T_2)s + 1} \,. \tag{38}
$$

Performing the synthetic division in (38), we can arrive at a simplified first order transfer function

$$
\frac{r}{\delta} = \frac{K}{Ts + 1} \,, \tag{39}
$$

or in differential equation form

$$
T\dot{r} + r = K\delta \,, \tag{40}
$$

where

$$
T = T_1 + T_2 - T_3 \,. \tag{41}
$$

Equation (40) is the so called Nomoto's first order equation, which captures the fundamental turning performance. It requires only two parameters, K and T, instead of the plethora of hydrodynamic derivatives of more accurate models.

Physically, the indices K and T represent ratios of nondimensional coefficients,

$$
T = \frac{\text{yaw inertia}}{\text{yaw damping}} \,,
$$

is the time constant of the system, and

$$
K = \frac{\text{turning moment}}{\text{yaw damping}} \,,
$$

is related to the rudder effectiveness or strength. For a simple case where the rudder is put hard over suddenly to an angle δ and held there, the solution for r is given, in terms of K and T, by

$$r = K\delta\left(1 - e^{-t/T}\right) \ . \tag{42}$$

This shows that the yaw rate r increases exponentially with time but at a declining rate dependent on T and approaches a steady value $K\delta$. A larger K thus provides greater steady state turning ability, and a smaller value of T provides a quicker initial response to the helm. Since quick response is obviously valuable in course keeping (steering), it is thus consistent with a smaller T. The above discussion of equation (42) shows that T has no effect at all on steady turning rate, but a small T would reduce the time required to reach a steady turn. The steady turning radius, R, is by definition

$$R = \frac{U}{r} = \frac{1}{r} \ , \tag{43}$$

since $U = 1$ (dimensionless) and, therefore,

$$R = \frac{1}{K\delta} \ . \tag{44}$$

This relation shows that with a large value of K a smaller rudder angle may be used in achieving a given turning radius.

The main maneuvering qualities of a ship using linear analysis can thus be characterized using only the indices K and T, where increasing values indicate improving performance:

$$\begin{aligned} 1/T \ , &\qquad \text{course stability} \ , \\ 1/T \ , &\qquad \text{responsiveness to rudder} \ , \\ K \ , &\qquad \text{turning ability} \ . \end{aligned}$$

The parameters of the first order Nomoto's equation give a good basis for comparison with similar vessels. They can be estimated early in design and also obtained in standard sea trial maneuvers. A typical K–T diagram is shown in Figure 6. On the left the rays from the origin are lines of constant rudder area A_R/LT. Suppose you have a ship at point P_1 and wish to change it to improve course stability. If you add deadwood near the stern with no change in rudder area, the ratio K/T will remain constant and the design will shift to point P_2. Course stability will be better but turning will be worse. If the turning is not to be degraded, rudder area must be added so the design will move to point P_3. Notice on the right that most ships have a linear relationship between A_R/KLT and $1/T$.

When a ship is course unstable, it is entirely feasible for a man to successfully control the ship. It all depends upon the speed of the man's response and the speed of response of the steering gear, refer to Figure 1. People of course vary considerably but if the system without the man in the loop is not too unstable, the typical helmsman should be able to successfully maintain course. Elementary control theory can be used to evaluate the question of "too unstable". A common measure of relative stability is the phase margin. In linear models, control systems are usually designed with 45–50 degrees phase margin. This is selected for good time response but also to give some margin against going unstable since the linear

model is only approximate and the assumed parameters will change and degrade in service. If a ship is course unstable it will have a negative phase margin. A helmsman can make up for some negative phase margin for the ship and the steering engine if this is not too excessive. A typical helmsman can overcome 20–30 degrees of negative phase margin, and in such a case we can have confidence that with the man in the control loop the total system will be stable.

1.4 Turning characteristics.

The most fundamental ship maneuver is the turning maneuver. The response of the ship to rudder deflection, and the resulting forces and moments produced by the rudder, can be divided into two parts:

1. An initial transient in which significant surge, sway, and yaw accelerations occur.
2. A steady turning phase in which rate of turn and forward speed are constant and the path of the ship is circular.

Figure 7 is a definition diagram for the turning path of a ship. Generally, the turning path of a ship is characterized by four measures: advance, transfer, tactical diameter, and steady turning radius. The figure also shows the position of the so called pivot point in a steady turn. This point is of interest because to an observer aboard a turning ship it appears as if the ship were pivoting about a point usually somewhat aft of the bow and foreward of amidships. The bow deviates inward of the turning circle while the stern deviates outward of it. According to Figure 7, the distance between the pivot point and the center of gravity of the ship is $x_c = R\sin\beta$, where β is the drift angle. Because small radius turns are usually associated with large drift angles, the product $R\sin\beta$ does not vary significantly for different ships or for the same ship at different turning radius. For most ships the pivot point is somewhere between the bow and about $0.2L$ of the bow. Based on empirical data, the drift angle, β, in degrees, generally falls within the following range of values: $\beta = 22.5L/R + 1.45$ and $\beta = 18L/R$. The former relationship yields values of x_c from 0.4 to $0.5L$ depending on the L/R ratio. The latter relationship yields values of $x_c = 0.3L$.

Suppose that the ship is advancing on a straight path when its rudder is deflected and held at a fixed angle δ as in Figure 7. The resulting path of the ship can be divided into three distinct phases.

The first phase starts at the instant that the rudder is placed hard over at δ. During this period, the ship's mass and inertia prevent the lateral velocity, v, and rotational velocity, r, from instantaneously increasing. Therefore, initially $v = r = 0$, and equations (24) and (25) can be solved for the *initial* accelerations

$$\dot{r} = \frac{(m - Y_{\dot{v}})N_\delta + (N_{\dot{v}} - mx_G)Y_\delta}{(m - Y_{\dot{v}})(I_z - N_{\dot{r}}) - (Y_{\dot{r}} - mx_G)(N_{\dot{v}} - mx_G)}\,, \tag{45}$$

$$\dot{v} = \frac{(I_z - N_{\dot{r}})Y_\delta + (Y_{\dot{r}} - mx_G)N_\delta}{(m - Y_{\dot{v}})(I_z - N_{\dot{r}}) - (Y_{\dot{r}} - mx_G)(N_{\dot{v}} - mx_G)}\,. \tag{46}$$

Looking back at Figure 3, we can see that a positive rudder (clockwise, turn to port for rudder at the stern) produces a positive sway force (so $Y_\delta > 0$) and a negative yaw moment (so $N_\delta < 0$). In other words, the ship initially turns out of the turn, Figure 7.

The first phase lasts only momentarily since the accelerations $\dot{v}$ and $\dot{r}$ will soon give rise to velocities v and r. With the introduction of these parameters the ship enters the second phase of turning. Here accelerations coexist with velocities and all of the terms in equations (24) and (25) are equally important. Since we are analyzing a starboard turn, negative δ, we have a positive $\dot{r}$ and negative $\dot{v}$, in other words the ship is skidding. A positive drift, or side slip angle β is developed and a positive (to starboard, same as direction of turn) force $Y_v v$ is developed. Eventually this force overcomes the ruder force $Y_\delta \delta$ and $\dot{v}$ dies out. The angular acceleration $\dot{r}$ may persist a bit longer but it eventually it too goes to zero, Figure 8.

After some possible oscillation, the second phase of turning ends with the establishment of the final equilibrium of forces. When this equilibrium is reached, the ship settles down to a turn of constant radius R as shown in Figure 7. This is the third, or steady, phase of the turn. Here v and r have nonzero values, but $\dot{v}$ and $\dot{r}$ are zero. Using equations (24) and (25) the *steady state* values of v and r are computed as

$$r = -\frac{Y_v N_\delta - N_v Y_\delta}{Y_v(N_r - mx_G U) - N_v(Y_r - mU)}\delta \,, \tag{47}$$

$$v = -\frac{(Y_r - mU)N_\delta + (N_r - mx_G U)Y_\delta}{Y_v(N_r - mx_G U) - N_v(Y_r - mU)}\delta \,, \tag{48}$$

and, therefore, within linear theory the final values of the yaw and sway velocities are proportional to the rudder deflection δ. If we consider the signs in equations (47) and (48) we can see that a negative δ (rudder to starboard) will eventually produce a positive r (to starboard) and a negative v (to port or out of the turn). The resulting ship speed is

$$V = U\cos\beta + v\sin\beta \approx U \,, \tag{49}$$

in other words, within linear theory, there is no speed loss due to turning. The final value of the side slip angle β is

$$\tan\beta \approx \beta = -\frac{v}{U} \,, \tag{50}$$

with v given by (48). Equation (50) shows that the drift angle, β, is directly proportional to δ. This, of course, establishes some of the linear theory limitations: high δ means large β and this implies increased ship resistance with a resulting loss of speed and, therefore, rudder effectiveness.

Because of the angular velocity r, since the ship speed is constant the ship is executing a circular path with radius

$$R = \frac{U}{r} \,, \tag{51}$$

with r given by (47). It can be seen that the steady turning radius R is inversely proportional to δ, whereas the drift angle β is directly proportional to δ. This means that the pivot point mentioned in the beginning of this section

$$x_c = R\sin\beta \approx R\beta \,, \tag{52}$$

remains approximately constant since large R is associated with small β and vice versa. This pivot point can also be computed from the fact that the total angle of attack is zero there,

$$v + rx_c = 0 \quad \Rightarrow \quad x_c = -\frac{v}{r} \approx \frac{\beta}{r} \approx R\beta \,. \tag{53}$$

It is interesting to note that, using equations (51), (47), and (34),

$$R = -\frac{1}{\delta} \cdot \frac{C}{Y_v N_\delta - N_v Y_\delta} \ , \tag{54}$$

where C is the stability index. Now since $Y_v N_\delta - N_v Y_\delta > 0$ we can see that for a stable ship ($C > 0$), a negative δ (rudder to starboard) will produce a positive R (turn to starboard), as it should. Furthermore, as C increases so does R; another demonstration of the fact that a very stable ship is also very sluggish in turning. We can see that if x_G is large and positive (i.e., LCG significantly forward of amidships), the turning radius R will increase for a given δ. For an unstable ship equation (54) claims that for $\delta < 0$ (rudder to starboard) the ship ought to turn port side ($R < 0$), which means that the above analysis is not valid. The small motions assumption breaks down in such a case and so does our linear model; we need to resort to nonlinear equations. Before we go nonlinear, though, a look at the roll angle during a turn is in order.

Heel angle in a turn. While use of the rudder is intended mainly to produce motions only in the xy–plane, motions are also induced by cross coupling into the pitch (xz) and roll (yz) planes. The unwanted motions in the roll plane, particularly, are likely to be large enough to be of significance (although submariners may argue that the pitch angles induced in turning by the rudder are of greater concern). Consider a ship into a starboard turn, Figure 9. During the first phase of the turn, equilibrium of forces produces in the sway direction

$$Y_\delta \delta + (Y_{\dot v} - m)\dot v + (Y_{\dot r} - m x_G)\dot r = 0 \ .$$

Now since $\delta < 0$, $\dot v < 0$ we have $Y_\delta \delta < 0$, $Y_{\dot v}\dot v > 0$, $Y_{\dot r}\dot r$ is small, $-m\dot v > 0$ (inertial force), and $-m x_G \dot r$ is small. Therefore, by considering the moments with respect to CG we can see that the initial heel angle is inboard (to starboard), Figure 10.

During the third phase, equilibrium of forces produces

$$Y_\delta \delta + Y_v v + (Y_r - mU) r = 0 \ ,$$

and we can see that since the term $Y_v v + Y_r r$ is much larger than $Y_\delta \delta$ in order to maintain the turn, the roll angle is to port (outboard). For submarines, the bridge fairwater contributes heavily to both the magnitude and location of the $Y_v v$ force of Figure 9, thereby, increasing the rolling moment. It is clear that if the $Y_v v + Y_r r$ force is raised sufficiently high, the heel in the third phase of a turn will be in the same direction as in the first phase, into the turn.

1.5 Nonlinear aspects.

Linear theory as discussed in the previous sections is useful for analyzing the influence of ship features on controls fixed stability and on the turning ability of directionally stable ships in the linear range. However, it fails to predict accurately the characteristics of the tight maneuvers that most ships are capable of performing, and it cannot predict the maneuvers of directionally unstable ships. Furthermore, it can be seen from equations (18), (19), and (20) that, within linear models, the surge equation decouples from sway and yaw which means that the ship forward speed is unaffected by the rest of horizontal plane motions. A speed

reduction in a turn nevertheless exists and can be relatively small for slow moving tankers but can reach as much as 40% for high speed destroyers. Figure 11 shows typical speed reductions while turning for different $R/2L$ and C_B values. To evaluate these effects we need to introduce nonlinear cross coupling between surge, sway, and yaw.

One popular technique of introducing nonlinear terms in the previously derived equations of motion is to keep second and third order velocity dependent terms in the Taylor expansions (12). Terms beyond third order and cross coupling of velocity and acceleration terms are not typically included since their effect is insignificant in practice. This way, equations (24) and (25) are restated as

$$(m - Y_{\dot{v}})\dot{v} - (Y_{\dot{r}} - mx_G)\dot{r} = Y_v v + (Y_r - mU)r + Y_\delta \delta + f_2'(u, v, r, \delta) \ , \tag{55}$$

$$(I_z - N_{\dot{r}})\dot{r} - (N_{\dot{v}} - mx_G)\dot{v} = N_v v + (N_r - mx_G U)r + N_\delta \delta + f_3'(u, v, r, \delta) \ , \tag{56}$$

where f_2' and f_3' contain higher order terms in u, v, r, δ. To arrive at an expression for $f_2'(u, v, r, \delta)$ we observe that because of port/starboard symmetry $Y(u) = 0$, i.e., $Y_u = Y_{uu} = Y_{uuu} = 0$, where the same notation as before is adopted $Y_{uu} = \partial^2 Y/\partial u^2$ and so on. Even powers of v, r, δ are zero, for example $Y_{vv} = 0$ since the sway force should respect the sign of the sway velocity. Odd powers will survive only. Therefore, the sway equation (55) becomes

$$(m - Y_{\dot{v}})\dot{v} - (Y_{\dot{r}} - mx_G)\dot{r} = f_2(u, v, r, \delta) \ , \tag{57}$$

where

$$\begin{aligned} f_2(u, v, r, \delta) = {} & Y_0 + Y_{0u}(u - U) + Y_{0uu}(u - U)^2 + Y_v v + \tfrac{1}{6}Y_{vvv}v^3 + \tfrac{1}{2}Y_{vrr}vr^2 + \\ & \tfrac{1}{2}Y_{v\delta\delta}v\delta^2 + Y_{vu}v(u - U) + \tfrac{1}{2}Y_{vuu}v(u - U)^2 + (Y_r - mU)r + \tfrac{1}{6}Y_{rrr}r^3 + \\ & \tfrac{1}{2}Y_{rvv}rv^2 + \tfrac{1}{2}Y_{r\delta\delta}r\delta^2 + Y_{ru}r(u - U) + \tfrac{1}{2}Y_{ruu}r(u - U)^2 + Y_\delta \delta + \\ & \tfrac{1}{6}Y_{\delta\delta\delta}\delta^3 + \tfrac{1}{2}Y_{\delta vv}\delta v^2 + \tfrac{1}{2}Y_{\delta rr}\delta r^2 + Y_{\delta u}\delta(u - U) + \tfrac{1}{2}Y_{\delta uu}\delta(u - U)^2 + \\ & Y_{vr\delta}vr\delta \ . \end{aligned} \tag{58}$$

Similarly for the yaw equation we have

$$(I_z - N_{\dot{r}})\dot{r} - (N_{\dot{v}} - mx_G)\dot{v} = f_3(u, v, r, \delta) \ , \tag{59}$$

where the expression for $f_3(u, v, r, \delta)$ is similar to (58) with the exception of $(N_r - mx_G U)$ instead of $(Y_r - mU)$. The terms with subscript 0 represent the influence of the propeller on the lateral force and turning moment.

Following similar arguments, the surge equation is written as

$$(m - X_{\dot{u}})\dot{u} = f_1(u, v, r, \delta) \ . \tag{60}$$

Because of symmetry, $f_1(u, v, r, \delta)$ contains even powers in v, r, δ. All odd powers are zero, for example $X_{vvv} = 0$ since the same surge force should develop for either port or starboard motions. Therefore,

$$\begin{aligned} f_1(u, v, r, \delta) = {} & T - R + \tfrac{1}{2}X_{vv}v^2 + \left(\tfrac{1}{2}X_{rr}r^2 + mx_G\right)r^2 + \tfrac{1}{2}X_{\delta\delta}\delta^2 + \tfrac{1}{2}X_{vvu}v^2(u - U) + \\ & \tfrac{1}{2}X_{rru}r^2(u - U) + \tfrac{1}{2}X_{\delta\delta u}\delta^2(u - U) + (X_{vr} + m)vr + X_{v\delta}v\delta + \\ & X_{r\delta}r\delta + X_{vru}vr(u - U) + X_{v\delta u}v\delta(u - U) + X_{r\delta u}r\delta(u - U) \ . \end{aligned} \tag{61}$$

The terms T and R represent the propeller thrust and ship resistance, respectively, as developed in Part III. The rest of the terms in (61) model the added surge force (added resistance) due to horizontal plane ship motions and rudder action. These terms will cause speed loss during turning, unless the propulsive thrust changes.

The terms in the right hand side of equations (58) and (61) are usually called "coefficients of the equations of motion" as opposed to "hydrodynamic derivatives" for the linear equations. The reason is that they are obtained through curve fitting of actual data and do not necessarily correspond to an actual derivative at equilibrium in the pure sense of the term.

Equations (57), (59), and (61) can be solved for the accelerations $\dot{u}$, $\dot{v}$, $\dot{r}$ as

$$\begin{aligned} \dot{u} &= \frac{f_1(u,v,r,\delta)}{m - X_{\dot{u}}} \,, \\ \dot{v} &= \frac{(I_z - N_{\dot{r}}) f_2(u,v,r,\delta) + (Y_{\dot{r}} - m x_G) f_3(u,v,r,\delta)}{(m - Y_{\dot{v}})(I_z - N_{\dot{r}}) - (N_{\dot{v}} - m x_G)(Y_{\dot{r}} - m x_G)} \,, \\ \dot{r} &= \frac{(m - Y_{\dot{v}}) f_3(u,v,r,\delta) + (N_{\dot{v}} - m x_G) f_2(u,v,r,\delta)}{(m - Y_{\dot{v}})(I_z - N_{\dot{r}}) - (N_{\dot{v}} - m x_G)(Y_{\dot{r}} - m x_G)} \,. \end{aligned} \tag{62}$$

Equations (62) can be solved numerically for any possible time history of $\delta(t)$ and provide then a fairly accurate time simulation of the actual ship maneuver. An easy and popular numerical integration technique is the Euler or rectangular integration in which values of u, v, r at time $t + \Delta t$ are obtained from knowledge of the values of u, v, r, δ at time t using a simple first order expansion; that is

$$\begin{aligned} u(t + \Delta t) &= u(t) + \dot{u}(t)\Delta t \,, \\ v(t + \Delta t) &= v(t) + \dot{v}(t)\Delta t \,, \\ r(t + \Delta t) &= r(t) + \dot{r}(t)\Delta t \,. \end{aligned} \tag{63}$$

This method is found to give adequate accuracy for the present type of differential equations because the accelerations $\dot{u}$, $\dot{v}$, $\dot{r}$ vary slowly with time, owing to the large mass or inertia of a ship compared to the relatively small forces and moments produced by its rudder. Any desired accuracy can be easily obtained computationally by using a smaller time step Δt. The so derived $u(t)$, $v(t)$, $r(t)$ can be utilized to obtain the ship orientation $\psi(t)$ and inertial positions $x_0(t)$, $y_0(t)$ by using (refer to Figure 2)

$$\begin{aligned} \dot{\psi} &= r \,, \\ \dot{x}_0 &= u\cos\psi - v\sin\psi \,, \\ \dot{y}_0 &= u\sin\psi + v\cos\psi \,, \end{aligned} \tag{64}$$

and integrating

$$\begin{aligned} \psi(t + \Delta t) &= \psi(t) + \dot{\psi}(t)\Delta t \,, \\ x_0(t + \Delta t) &= x_0(t) + \dot{x}_0(t)\Delta t \,, \\ y_0(t + \Delta t) &= y_0(t) + \dot{y}_0(t)\Delta t \,. \end{aligned} \tag{65}$$

As a final word of caution on the applicability of our maneuvering model, it should be mentioned that the most basic (and rather bold) assumption of the Taylor series expansions for the hydrodynaic forces and moments is that they can be expressed through the instantaneous values of motions, velocities and accelerations of the body, neglecting higher order time derivatives. Although this is not exact when a free surface is present (due to memory effects), it can be taken as a good approximation provided the motions are "slow". This is the reason why the hydrodynamic derivatives are often referred to as "slow motion derivatives". The above assumption is no longer valid when dealing with "fast" motions in waves (seakeeping) and we will not be entitled to using it once this section is over. As the hydrodynamic forces and moments induced by ship motions are affected by the presence of a free surface, the coefficients in the equations of motion should be functions of the frequency of motion. For slow motions (ordinary steering) we can use the values at zero frequency and consider them constant. Frequency dependence corresponds to incorporating convolution integrals in the equations of motion. The equations of motion as expressed in the previous sections contain no convolution integrals, which is equivalent to assuming that the history of the motion plays no role in the determination of u, v, and r. It has been, in general, shown that the dominant frequency range to determine the maneuvering response is so slow that to make use of the constant stability derivatives at very low frequency does not bring any serious errors in the computations.

1.6 Determination of hydrodynamic derivatives.

Success of the previous models depends heavily on our knowledge of the hydrodynamic derivatives. There are four main ways to achieve this and we will briefly discuss them here:

1. Experiments with model tests.
2. Full scale sea trials and system identification techniques.
3. Theoretical prediction methods.
4. Regression analysis results from similar designs.

There are five main types of *model tests* that can be performed

- straight line tests in a towing tank,
- rotating arm tests,
- planar motion mechanism tests,
- oscillator tests,
- free running (radio controlled) tests.

Straight line tests in a towing tank (Figure 12) are used to measure Y_v and N_v; the model is towed at Froude scaling U and at different angles of attack β, and its sway velocity is, therefore, given by $v = -U \sin \beta$. A dynamometer is used to measure the force Y and

moment N at each angle β and these are then plotted versus v. The slopes of these curves at zero provide Y_v, N_v, and with curve fitting we can get nonlinear coefficients as well. Then nondimensionalize the values as in Section 1.1 and use the same dimensionless coefficients for the ship. Since the propeller has an effect on the hydrodynamic derivatives, these tests should be conducted with propellers operating, preferably at the ship propulsion point. An undeflected rudder model should also be included in the model. Similar tests can be performed to get Y_δ and N_δ. The model is run at zero angle of attack but for different rudder deflections δ.

The rotating arm technique is used to measure the rotary derivatives Y_r, N_r where during rotation we would like to have $v = 0$ and $r \neq 0$ only. The dynamometer will measure Y and N, and we plot these versus r for a constant reference speed U. Since $r = U/R$ and $U = \text{const.}$ we need to vary the radius R, Figure 12. We then get Y_r, N_r by taking the slopes of $Y(r)$ and $N(r)$ at $r = 0$. The rotating arm technique has two basic drawbacks:

- The model must be accelerated and data obtained within a single revolution. Otherwise, the model will be in its own wake and its velocity with respect to the water will not be accurately known.

- The most useful data points are close to $r = 0$ and this requires very large R. Therefore, expensive set–up and special tanks are needed (we cannot use existing long and narrow towing tanks).

By performing tests at nonzero drift angles β and cross plotting the results, we can get values for Y_v, N_v, Y_δ, N_δ but such predictions are not as reliable as with straight line tests.

The planar motion mechanism tests were developed in order to avoid the large expense of a rotating arm facility. Say we have a model towed down a towing tank at a constant speed U — Froude number scaled always — and suppose we can impose a small lateral sinusoidal motion

$$y = y_0 \sin \omega t \ ,$$

as in Figure 13. The resisting hydrodynamic force is then

$$Y = Y_v v + Y_{\dot{v}} \dot{v} + Y_{\ddot{v}} \ddot{v} + \cdots \ ,$$

and since $\dot{y} = v$ we have

$$\begin{aligned} Y &= (Y_v - \omega^2 Y_{\ddot{v}} + \cdots)(y_0 \omega \cos \omega t) + (Y_{\dot{v}} - \omega^2 Y_{\ddot{v}} + \cdots)(-y_0 \omega^2 \sin \omega t) \\ &= \widetilde{Y_v} v + \widetilde{Y_{\dot{v}}} \dot{v} \ . \end{aligned}$$

In the last expression, $\widetilde{Y_v} v$ is the force component of Y at a 90° phase with the motion y, and $\widetilde{Y_{\dot{v}}} \dot{v}$ is the force component in phase with y. Both are measurable using dynamometers. The usefulness of these sinusoidal coefficients $\widetilde{Y_v}$ and $\widetilde{Y_{\dot{v}}}$ is due to the fact

$$\lim_{\omega \to 0} \widetilde{Y_v} = Y_v \quad \text{and} \quad \lim_{\omega \to 0} \widetilde{Y_{\dot{v}}} = Y_{\dot{v}} \ ,$$

according to what was mentioned in the previous section on the frequency dependency of the hydrodynamic coefficients. This idea of imposing translational and/or rotational motions to

the model, superimposed on a straight line reference motion, led to the development of the Planar Motion Mechanism, PMM. It can be used to measure velocity dependent derivatives Y_v, N_v, rotary derivatives Y_r, N_r, as well as acceleration derivatives $Y_{\dot{v}}$, $N_{\dot{v}}$, $Y_{\dot{r}}$, $N_{\dot{r}}$. The PMM consists of two oscillators, one of which produces a transverse oscillation at the bow, and the other a transverse oscillation at the stern. It also needs transducers to measure the forces and special instrumentation for the proper resolution of forces. This procedure can give the hydrodynamic coefficients as functions of frequency, a very useful information for motions in rough seas and transient maneuvers. The PMM results can be used to determine nonlinear and cross coupling effects; as well as hydrodynamic coefficients in all six degrees of freedom motions.

The oscillator technique, Figure 14, is a simpler mechanism than PMM but it requires more elaborate analysis techniques. The model motion is combined yaw and sway, and rotation is always combined with translation. The procedure is to measure Y_v and N_v by straight line tests, and then estimate the remaining six derivatives Y_r, N_r, $Y_{\dot{v}}$, $N_{\dot{v}}$, $Y_{\dot{r}}$, $N_{\dot{r}}$ by solving a system of simultaneous equations. The results are usually not as reliable as PMM.

Finally, radio controlled model tests are essentially system identification tests and can be used for full scale sea trials as well. We start with a prescribed input and measure the output. Then by a systematic trial–and–error procedure we pick values of the coefficients such that close agreement between predicted and measured output is achieved.

Full scale test techniques are required during ship sea trials and delivery. They are used not only to evaluate hydrodynamic characteristics but also to check whether design specifications have been met. The main full scale sea trials are the following:

1. Spiral test: In this we measure the steady turning rate r that corresponds to a specified rudder angle δ. A steady state r–δ curve is thus constructed and its deviation from a straight line shows the effect of nonlinearities at high rudder angles, Figure 15. For an unstable ship the initial slope of the curve is located in the first and third quadrant. In the reverse spiral test we measure the required rudder angle δ to give a specified turning rate r. In this way we can get the full r–δ curve for an unstable ship even within the hysteresis loop.

2. Turning maneuver: The rudder is set at a constant angle and the ship executes a full 360^o heading change. We measure and characterize quantities like the tactical diameter, advance and transfer, drift angle, heel angle, and speed loss.

3. Zig–zag maneuver: Set the rudder at constant δ_0 as quickly and as smoothly as possible until the ship heading becomes ψ_0; then rudder at $-\delta_0$ until heading becomes $-\psi_0$, and repeat, Figure 16. We measure and characterize quantities like the overshoot, period, and time to overshoot. The traditional zig–zag maneuver is with $\delta_0 = \psi_0$, for example 20^o–20^o test. In the case of course unstable ships the results of zig–zag maneuvers at small rudder angles, say 5^o–5^o, tend to diverge and will not give steady results. For this reason we often use the modified zig–zag test with $\psi_0 < \delta_0$, say 5^o–2^o or 10^o–1^o test.

4. Sinusoidal maneuver: This method involves a sinusoidal change in rudder angle and is used to obtain frequency response characteristics. It is useful at relatively high frequencies whereas it is not very practical at low frequencies.

5. Parallel shift maneuver: The ship is steered to a new course parallel to the original. It can be used to estimate frequency response characteristics at very low frequencies.

6. System identification techniques: System identification determines, from a given input/output data record of vehicle test response, an estimate of the physical model which relates to the observed data. The process is schematically shown in Figure 17 and it consists mainly of a dynamic iterative process in which the values of the hydrodynamic coefficients are continously changed until convergence between predicted and actual output.

Theoretical prediction methods are based on the principles of hydrodynamics for the evaluation of added mass (acceleration dependent derivatives) and damping (velocity dependent derivatives) coefficients for three dimensional bodies. Since damping depends to a great extent on viscous effects, the hydrodynamic calculations (usually based on potential theory) are more reliable for the acceleration dependent hydrodynamic coefficients. While theoretical approaches such as slender body and strip theory have had some success in aircraft where body geometry is dominated by wings and fins, results for ships have not been as accurate since there are no flat stabilizing surfaces and the flow around the hull is greatly altered by fluid viscosity. The rudder coefficients Y_δ, N_δ, $X_{\delta\delta}$ can be evaluated from existing lift and drag coefficient data for standard foil sections.

Empirical regression analysis results have been obtained to express the main hydrodynamic coefficients as functions of principal dimensions:

$$
\begin{aligned}
Y_{\dot{v}} &= -\pi \left(\frac{T}{L}\right)^2 \left[1 + 0.16 C_B \frac{B}{T} - 5.1 \left(\frac{B}{L}\right)^2\right] , \\
Y_{\dot{r}} &= -\pi \left(\frac{T}{L}\right)^2 \left[0.67 \frac{B}{L} - 0.0033 \left(\frac{B}{T}\right)^2\right] , \\
N_{\dot{v}} &= -\pi \left(\frac{T}{L}\right)^2 \left(1.1 \frac{B}{L} - 0.041 \frac{B}{T}\right) , \\
N_{\dot{r}} &= -\pi \left(\frac{T}{L}\right)^2 \left(\frac{1}{12} + 0.017 C_B \frac{B}{T} - 0.33 \frac{B}{L}\right) , \\
Y_v &= -\pi \left(\frac{T}{L}\right)^2 \left(1 + 0.40 C_B \frac{B}{T}\right) , \\
Y_r &= -\pi \left(\frac{T}{L}\right)^2 \left(-\frac{1}{2} + 2.2 \frac{B}{L} - 0.080 \frac{B}{T}\right) , \\
N_v &= -\pi \left(\frac{T}{L}\right)^2 \left(\frac{1}{2} + 2.4 \frac{T}{L}\right) , \\
N_r &= -\pi \left(\frac{T}{L}\right)^2 \left(\frac{1}{4} + 0.039 \frac{B}{T} - 0.56 \frac{B}{L}\right) .
\end{aligned}
$$

Such formulas have statistical significance only and should be used with caution only when studying variations from a known similar design.

2. Sea Waves.

A rather unique feature of ships and floating bodies is the importance of wave effects on the free surface. The most common and important wave phenomena for our purposes are the surface waves that exhibit typical periods of a few seconds, Figure 18. Other waves like subsurface or internal waves are found in internal regions of density stratification beneath the free surface and are typically of lower frequency with periods on the order of several minutes. The influence of such waves on ships is generally negligible unless the body has an unusually low frequency resonance, as mentioned in Part III. Waves of even lower frequencies exist, including inertial waves associated with the Coriolis acceleration due to the earth's rotation, and tides generated by changes in the potential energy of heavenly bodies. At the high frequency of the spectrum are capillary waves and ripples, but these do not affect large vessels or structures.

In Ship Motions we are concerned with the effects of surface waves on ships and fixed structures. The problem is treated here (and in most cases and places) based on the assumptions that the fluid is ideal and that wave and body motions are sufficiently small to linearize.

2.1 Plane progressive waves.

The simplest free surface wave formation, which nevertheless has great practical significance, is the plane progressive wave system. This motion is two dimensional, sinusoidal in time with angular frequency ω, and propagates with phase velocity c_p such that to an observer moving with this velocity the wave appears to be stationary. A Cartesian coordinate system (x, y, z) is adopted, see Figure 19, with $z = 0$ the plane of the undisturbed free surface and the z–axis *positive upwards*. The vertical elevation of any point on the free surface may be defined by a function $z = \eta(x, y, t)$. In the special case of two dimensional fluid motion parallel to the x–z plane, the dependence on y will be deleted. Thus, the free surface elevation must be of the general form

$$\eta(x,t) = A\cos(kx - \omega t) \ , \tag{66}$$

where the positive x–axis is chosen to coincide with the direction of wave propagation. Here A is the wave amplitude, and the parameter

$$k = \frac{\omega}{c_p} \ , \tag{67}$$

is the *wavenumber*, the number of waves per unit distance along the x–axis. Clearly

$$k = \frac{2\pi}{\lambda} \ , \tag{68}$$

where the *wavelength* λ is the distance between successive points on the wave with the same phase, Figure 19.

The solution of this problem is expressed in terms of a two dimensional velocity potential $\phi(x, z, t)$ which must satisfy Laplace's equation

$$\nabla^2\phi = 0 \ , \tag{69}$$

and appropriate boundary conditions. Furthermore, ϕ must yield the wave elevation (66) from

$$\eta = -\frac{1}{g} \cdot \frac{\partial \phi}{\partial t} \, . \tag{70}$$

Equation (70) is the so called linearized dynamic boundary condition on the free surface and is an expression of the fact, through Bernoulli's equation, that the pressure on the free surface must be the same as the ambient atmospheric pressure. An appropriate boundary condition on the sea bottom is

$$\frac{\partial \phi}{\partial z} = 0 \, , \quad \text{at} \quad z = -h \, , \tag{71}$$

i.e., the bottom at depth h is a rigid impermeable plane. Finally, the free surface boundary condition is

$$\frac{\partial^2 \phi}{\partial t^2} + g \frac{\partial \phi}{\partial z} = 0 \, , \quad \text{on} \quad z = 0 \, . \tag{72}$$

Equation (72) is a combined dynamic and kinematic free surface boundary condition. The dynamic condition was mentioned before, while the kinematic condition simply states

$$\frac{\partial \eta}{\partial t} = \frac{\partial \phi}{\partial z} \, , \tag{73}$$

i.e, the vertical velocities of the free surface and fluid particles are the same. Combining (70) and (73) we arrive at (72), ignoring the small departures of the free surface η from the horizontal orientation $z = 0$.

Clearly the velocity potential ϕ must be sinusoidal in the same sense as (66); therefore we seek a solution of the form

$$\phi(x, z, t) = \Re \left\{ Z(z) e^{-ikx + i\omega t} \right\} \, . \tag{74}$$

Substituting (74) into (69), Z must satisfy the ordinary differential equation

$$\frac{d^2 Z}{dz^2} - k^2 Z = 0 \, , \tag{75}$$

throughout the domain of the fluid. The most general solution of (75) is given in terms of exponential functions in the form

$$Z = C e^{kz} + D e^{-kz} \, . \tag{76}$$

For now we assume that the water depth is infinite (deep water), hence (75) must hold for $-\infty < z < 0$. To avoid an unbounded motion deep beneath the free surface, the constant D in (76) must be zero

$$Z = C e^{kz} \, , \tag{77}$$

or, if we substitute into (74)

$$\phi = \Re \left\{ C e^{kz - ikx + i\omega t} \right\} \, . \tag{78}$$

Now if we substitute (78) into (70) with $z = 0$, and compare the result with (66) we can find

$$C = \frac{igA}{\omega} \ ,$$

and

$$\phi = \frac{gA}{\omega} e^{kz} \sin(kx - \omega t) \ . \tag{79}$$

An additional relation between the wavenumber k and the frequency ω can be obtained by substituting (79) into (72). This relation, called a *dispersion* relation is

$$k = \frac{\omega^2}{g} \ . \tag{80}$$

Of course, the frequency ω can be replaced by the wave period $T = 2\pi/\omega$, just as the wavenumber k can be replaced by the wavelength $\lambda = 2\pi/k$.

The phase velocity c_p can be determined from (67), and using (80) it follows that

$$c_p = \frac{\omega}{k} = \frac{g}{\omega} = \sqrt{\frac{g}{k}} = \sqrt{\frac{g\lambda}{2\pi}} \ . \tag{81}$$

The last equation (81) states that surface waves in deep water are dispersive, longer waves travel faster than short waves, unlike, for instance, electromagnetic waves in deep space which travel at the same speed regardless of their color.

While the wave moves with the phase velocity c_p, the fluid itself moves with a much smaller velocity given by the gradient of the potential (79). The velocity components (u, w) of the fluid are

$$u = \frac{\partial \phi}{\partial x} = \omega A e^{kz} \cos(kx - \omega t) \ , \tag{82}$$

$$w = \frac{\partial \phi}{\partial z} = \omega A e^{kz} \sin(kx - \omega t) \ . \tag{83}$$

It can be seen that the fluid particles move through circular orbits, see Figure 19. The horizontal velocity component is maximum beneath the crest and trough. Beneath the crest the velocity is positive, in the same direction as the wave propagation, and beneath the trough the flow is in the opposite direction. The vertical velocity component is a maximum beneath the nodes $\eta = 0$, rising or falling with the free surface. Within linear theory, the fluid particles move in small circular orbits proportional to the wave amplitude; they remain in the same mean position as the wave propagates through the fluid with a phase velocity independent of the wave amplitude. Some nonlinear effects that modify this situation are discussed in Section 2.4, but for most practical purposes the linear results described here are extremely accurate. As the depth of submergence beneath the free surface increases, the fluid velocities (82) and (83) are attenuated exponentially — a hydrofoil boat with its foils deeply submerged is relatively insensitive to free surface wave action. For a submergence of half a wavelength, $kz = -\pi$, the exponential factor is reduced to 0.04. Thus, waves in deep water are confined to a relatively shallow layer near the free surface, with negligible motion

beneath a depth of about 0.5λ. On this basis one can anticipate that if the fluid depth is finite, but greater than half a wavelength, the effects of the bottom will be negligible.

For a fluid at constant depth h, the boundary condition (71) is imposed. Returning to the general solution (76), both exponential functions are retained, with the constants C and D suitably chosen to satisfy (71). In this case, the velocity potential (79) becomes

$$\phi = \frac{gA}{\omega}\frac{\cosh k(z+h)}{\cosh kh}\sin(kx-\omega t)\ , \tag{84}$$

and the dispersion relation (80) is now

$$k\tanh kh = \frac{\omega^2}{g}\ , \tag{85}$$

where we can see that as $h \to \infty$ we get the previous deep water results. The fluid velocity commponents can be computed as in (82), (83), and for finite depth it follows that

$$u = \frac{\partial\phi}{\partial x} = \frac{gAk}{\omega}\frac{\cosh k(z+h)}{\cosh kh}\cos(kx-\omega t)\ , \tag{86}$$

$$w = \frac{\partial\phi}{\partial z} = \frac{gAk}{\omega}\frac{\sinh k(z+h)}{\cosh kh}\sin(kx-\omega t)\ . \tag{87}$$

It can be seen that now the trajectories of the fluid particles are elliptical. The major axis of the ellipses is horizontal, and the velocity distribution is also shown in Figure 19.

From (67) and (85) the phase velocity for finite depth can be expressed in the form

$$c_p = \frac{\omega}{k} = \sqrt{\frac{g}{k}\tanh kh}\ . \tag{88}$$

This tends to the deep water limit (81) for $kh \gg 1$. The opposite limit, where $kh \ll 1$, is the regime of shallow water waves. In this case (88) can be approximated using the Taylor series expansion for the hyperbolic tangent, and the leading order approximation for the phase velocity is

$$c_p = \sqrt{gh}\ , \quad \text{for} \quad kh \ll 1\ . \tag{89}$$

As we mentioned before, water waves are generally dispersive, long waves travel faster than shorter waves. The shallow water limit (89) is an exception, where the phase velocity depends only on the depth, and the resulting wave motion is nondispersive.

A very interesting, for those of us who live along the coast of California, shallow water wave is the tsunami. "Tsunami" is a Japanese word for sea waves produced by earthquakes. A typical such wave has a frequency of 10^{-3} Hz (10–20 minute period) and a wave length of about 100 km, see Figure 18. At such wave numbers the ocean is effectively "shallow" and waves are no longer dispersive but travel at a unique speed $\sqrt{gh}$ where h is the ocean depth, see equation (89). A typical speed of such a wave is 800 km/h. These waves are only a few centimeters high in mid ocean, and are therefore very difficult to detect; they are also very harmless at that stage. However, they contain tremendous energy and can build up to amplitudes of 30 m when slowed down by a shelving beach or focussed by off shore topography. This is because of the "dragging" of water particles close to land at the sea bed

(see Figure 19, shallow water case) there is a net transfer towards the beach regardless of the original wave direction; the wave length decreases and, by continuity, the wave height will increase until breaking. Tsunamis can echo around the oceans with decreasing energy levels for many days after their initial generation.

The plane progressive wave described so far is a single, discrete wave system, with a prescribed monochromatic component of frequency ω and wavenumber k, moving in the postive x–direction. More general wave motions, which are no longer monochromatic, can be obtained by superimposing plane waves of different k and ω. In the two dimensional case we can begin by forming a discrete sum of waves

$$\eta = \sum_{n=1}^{N} \Re\{A_n \exp(-ik_n x + i\omega t)\} \ , \tag{90}$$

where n refers to the n–th sinusoidal wave component. If the total number of discrete waves N tends to infinity, while the difference between adjacent frequencies and wave numbers reduces to zero, the sum (90) will become an integral over the continuous spectrum of frequencies

$$\eta(x,t) = \Re \int_{-\infty}^{\infty} A(\omega) \exp[-ik(\omega)x + i\omega t]\, d\omega \ . \tag{91}$$

Here $k(\omega) > 0$ must satisfy the appropriate dispersion relation, and negative values of frequency have been admitted under the integral to allow for the possibility of plane waves moving in the negative x–direction. These distributions of wave systems can be extended from two to three dimensions by introducing an oblique wave and summing or integrating over all possible directions θ (see Figure 19). In the most general case of a continuous distribution, a two dimensional integral representation follows of the form

$$\eta(x,y,t) = \Re \int_0^{\infty} d\omega \int_0^{2\pi} d\theta A(\omega,\theta) \exp[-ik(\omega)(x\cos\theta + y\sin\theta) + i\omega t] \ . \tag{92}$$

This expressin can be used to analyze ship generated waves (the Kelvin wave system mentioned in Part III), and this is done in Section 2.3. It can also be utilized, with $A(\omega,\theta)$ being a random variable, to represent a spectrum of ocean waves, and this is discussed in Section 2.5.

2.2 Group velocity and wave energy.

Consider a group of two adjacent components of the discrete wave system (90)

$$\begin{aligned} \eta &= \Re\left\{A_1 \exp(-ik_1 x + i\omega_1 t) + A_2 \exp(-ik_2 x + i\omega_2 t)\right\} \\ &= \Re\left\{A_1 \exp(-ik_1 x + i\omega_1 t)\left[1 + \frac{A_2}{A_1}\exp(-i\delta k x + i\delta\omega t)\right]\right\} \ , \end{aligned} \tag{93}$$

where $\delta k = k_2 - k_1$ and $\delta\omega = \omega_2 - \omega_1$. Here, the factor in brackets represents an amplitude modulation which is slowly varying in space and time. The wave form (93) is similar to the beat–frequency effect in electromagnetic wave motions, where one refers to the first exponential factor in (93) as the carrier wave. The wavelength and period of the carrier are the usual parameters $\lambda = 2\pi/k_1$ and $T = 2\pi/\omega_1$. By analogy, the wavelength of the group is

$2\pi/\delta k$, and its period in time is $2\pi/\delta\omega$. Of particular interest is the *group* velocity c_g, given by the ratio

$$c_g = \frac{\delta\omega}{\delta k} \ . \tag{94}$$

In the limiting case where $\delta\omega \to 0$ and $\delta k \to 0$, (93) will tend to a monochromatic wave but if x and t are large, the amplitude modulation in (93) will persist so long as the products $x\delta k$ and $t\delta\omega$ are finite. Under this condition, the group velocity (94) will approach the finite limit

$$c_g = \frac{d\omega}{dk} \ , \tag{95}$$

in accordance with the classical definition of a derivative. Thus, a group of waves of nearly equal frequency and wavenumber will propagate with the group velocity $c_g = d\omega/dk$ as opposed to the phase velocity $c_p = \omega/k$ of the individual wave components in the group.

In general, the phase and group velocities differ, unless $\omega/k = d\omega/dk$. This exception occurs in the shallow water limit $kh \ll 1$. In deep water, the group velocity can be evaluated by solving the dispersion relation (80) for $\omega(k)$ and substituting this into (95). Thus

$$c_g = \frac{1}{2}\sqrt{\frac{g}{k}} = \frac{1}{2}\frac{\omega}{k} = \frac{1}{2}c_p \ , \tag{96}$$

and the group velocity is precisely half of the phase velocity. In finite depth, the dispersion relation (85) can be combined with (95) to give

$$c_g = \left(\frac{1}{2} + \frac{kh}{\sinh 2kh}\right) c_p \ . \tag{97}$$

This expression reduces to (96) if kh is large, whereas in the shallow water limit the factor in parenthesis in (97) reduces to unity.

That individual waves move faster than the group implies that in a wave system with a *front*, propagating into otherwise calm water, the individual waves will overtake the front and vanish. At first glance it appears that the energy within the wave system is destroyed in some sense, contrary to the principle of conservation of energy. In fact there is no contradiction, since the wave energy moves not with the phase velocity but with the group velocity as we discuss in the following. For all it matters, the phase velocity can exceed the speed of light, this won't bother Einstein a bit as long as the group velocity does not exceed it.

In order to confirm the last statement we have to look at the wave energy and an alternative approach to the group velocity based upon the rate of energy flux in a plane progressive wave system. Water waves are the result of balance between kinetic and potential energy in the fluid, and the total energy is the sum of these two components. Thus, in a prescribed volume V, the total energy is given by the integral

$$KE + PE = \rho \iiint_V \left[\tfrac{1}{2}(u^2 + w^2) + gz\right] \, dV \ . \tag{98}$$

If we focus our attention on a vertical column, extending throughout the depth of the fluid and bounded above by the free surface, the energy density E, per unit area of the mean free surface above this column, is given by

$$E = \rho \int_{-h}^{\eta} \left[\tfrac{1}{2}(u^2 + w^2) + gz\right] \, dz = \tfrac{1}{2}\rho \int_{-h}^{\eta} (u^2 + w^2) \, dz + \tfrac{1}{2}\rho g(\eta^2 - h^2) \ . \tag{99}$$

Substituting the deep water expressions (82), (83) in (99) and neglecting the term $-1/2\rho g h^2$ (the potential energy of the fluid below $z = 0$ is of no interest since it is a constant unrelated to wave motion) we get

$$E = \frac{\rho\omega^2 A^2}{4k} e^{2k\eta} + \tfrac{1}{2}\rho g\eta^2 \ . \tag{100}$$

For small amplitude waves, the exponential in (100) may be set equal to one, and using the dispersion relation (80) and wave elevation (66) we get

$$E = \tfrac{1}{4}\rho g A^2 + \tfrac{1}{2}\rho g A^2 \cos^2(kx - \omega t) \ . \tag{101}$$

The first and second terms on the right hand side of (101) represent the kinetic and potential energies, respectively. If these are averaged with respect to time over one cycle of wave motion, their contributions are identical, and the total mean energy density is given by the expression

$$\overline{E} = \tfrac{1}{2}\rho g A^2 \ , \tag{102}$$

where a bar denotes the time average.

A vertical control surface is then employed to measure the rate of energy flux. Utilizing Bernoulli's equation, the final result is that the rate of energy flux across a fixed control surface is the product of the energy density and the group velocity,

$$\frac{d\overline{E}}{dt} = c_g \overline{E} \ . \tag{103}$$

Equations (102) and (103) can be used to predict the change in height of a sinusoidal wave as it propagates through a region of gradually changing depth. Provided the change in depth is small over distances on the order of a wavelength, these relations can be applied locally at each depth, and it can be assumed that the reflected energy is negligible. It then follows that the energy flux (103) is constant for all depths, and since the frequency ω remains constant, the local wave height must be inversely proportional to the square root of the group velocity. Simultaneously, the wavelength and phase velocity will decrease with depth (why?). Taking both effects into account, the steepness of the waves will increase as the waves near the beach, leading ultimately to wave breaking when the wave height is comparable to the local depth. Of course, every surfer knows this even without the supporting mathematics.

Since the group velocity is less than the phase velocity, the energy in a plane progressive wave system will be propagated at a slower speed than the individual wave crests and will be "left behind" in the fluid. This seems physically reasonable and explains why ship waves are observed downstream of the disturbance that generates them.

2.3 The ship wave system.

Now that we are better equipped we can briefly go back to the wave system generated by a moving ship; the Kelvin wave pattern discussed in Part III. The most general wave distribution in three dimensions is given by the double integral (92). If this is transformed to a reference system moving with the ship in the positive x–direction with steady velocity

U, the appropriate expression with x replaced by $x + Ut$ is given by

$$\eta(x,y,t) = \Re \int_0^\infty d\omega \int_0^{2\pi} d\theta\, A(\omega,\theta) \exp[-ik(x\cos\theta + y\sin\theta) + i(\omega - kU\cos\theta)t] \,. \tag{104}$$

Here $k(\omega)$ is the wavenumber corresponding to a given frequency ω in accordance with the dispersion relation (80) for infinite depth.

If the ship motion is steady state in the reference system that moves with the ship, the expression (104) must be independent of time. This requires that

$$kU\cos\theta - \omega = 0 \,, \tag{105}$$

which means that the phase velocity of each amplitude wave component is given by

$$c_p = \frac{\omega}{k} = U\cos\theta \,. \tag{106}$$

In this sense (see Figure 19), a system of plane progressive waves moving at an oblique angle θ with respect to the x–axis will appear to be stationary to an observer moving along the x–axis with velocity $c_p/\cos\theta$. We can use equation (105) to eliminate one of the variables of integration in (104) and thereby replace it by a single integral

$$\eta(x,y) = \Re \int_{-\pi/2}^{\pi/2} d\theta\, A(\theta) \exp\left[-ik(\theta)(x\cos\theta + y\sin\theta)\right] \,, \tag{107}$$

where for the deep water case we have from (80) and (105)

$$k(\theta) = \frac{g}{U^2\cos^2\theta} \,. \tag{108}$$

Expression (107) is known as the free wave distribution of a given ship. This is characterized by the amplitude and phase of the complex function $A(\theta)$ which depends on the hull shape and its forward velocity, and is ultimately related to the wave making resistance, refer to equation (28) of Part III. If the distance downstream from the position of the ship is large (far field), the integral (107) can be simplified and the classical ship wave pattern can be obtained. Kelvin did this in 1887 rigorously using the method of stationary phase, but here we do it in a heuristic manner using the previous concept of group velocity.

If x' is a local coordinate, normal to the wave crests as in Figure 19 and defined with respect to a fixed reference frame, the significant waves will travel in groups such that $x'/t = c_g$ is determined by

$$\frac{d}{dk}(kx' - \omega t) = 0 \,. \tag{109}$$

If this expression for the derivative of the phase of the local waves is transformed into the frame of reference of (107), the significant waves will satisfy the equation

$$\frac{d}{dk}\left[k(\theta)(x\cos\theta + y\sin\theta)\right] = 0 \,. \tag{110}$$

Since k and θ are related by (108), condition (110) is equivalent to

$$\frac{d}{d\theta}\left(\frac{x\cos\theta + y\sin\theta}{\cos^2\theta}\right) = 0\ , \tag{111}$$

except for the isolated points $\theta = 0, \pm\pi/2$ where $d\theta/dk$ is infinite or zero, respectively. Ignoring these singular points and evaluating the derivatives in (111) yields

$$x\sec^2\theta\sin\theta + y\sec^3\theta(1+\sin^2\theta) = 0\ . \tag{112}$$

Thus, the significant waves, moving in a direction θ, will be situated along the radial line

$$\frac{y}{x} = -\frac{\cos\theta\sin\theta}{1+\sin^2\theta}\ . \tag{113}$$

A plot of (113) is shown in Figure 20, where the maximum value of the ratio y/x is defined by

$$\frac{y}{x} = 2^{-3/2} \approx \tan(19^{\circ}28')\ , \tag{114}$$

and this maximum occurs when the wave angle is

$$\theta = \pm\sin^{-1}\left(\frac{\sqrt{3}}{3}\right) = \pm 35^{\circ}16'\ . \tag{115}$$

Thus, the waves are confined to a sector symmetrical about the negative x–axis, with included semiangles of $19^{\circ}28'$. Within this sector, for a given point (x, y) two solutions of (113) exist; hence two waves with distinct angles θ move in different directions. By requiring that the phase function in parentheses in (111) be a constant, we can calculate the loci of the crests as shown in Figure 20.

The waves on the negative x–axis move in the same direction as the ship with $\theta = 0$. As the lateral coordinate y is increased, the angle of these *transverse* waves changes, in accordance with (113) and Figure 20, reaching a value of $\pm 35^{\circ}$ on the boundaries. Larger values of θ correspond to *diverging* waves; these have shorter wavelength and converge towards the origin as shown in Figure 20. A departure from the above linearized far field potential theory that appears in practical ship wave systems is a pronounced breaking wave, originating at the bow and trailing aft on either side of the ship into the wake. The effect of this breaking wave on the resistance of a ship, a particularly interesting topic in contemporary naval architecture, was discussed in Part III of the notes.

2.4 Second order Stokes waves.

In this section we consider briefly some of the simpler effects that were neglected in the linearized theory. The most significant nonlinearities enter through the free surface boundary conditions. The linearized kinematic condition was stated in equation (73) where the free surface elevation η was assumed to be sufficiently small so that it does not differ much from the undisturbed position $z = 0$. The exact kinematic free surface boundary condition can

be obtained by requiring that the substantial derivative of the quantity $(z-\eta)$ vanish on the free surface

$$\frac{D}{Dt}(z-\eta)=0\ . \tag{116}$$

The substantial derivative D/Dt is defined by

$$\frac{D}{Dt}=\frac{\partial}{\partial t}+\nabla\phi\cdot\frac{\partial}{\partial x}\ , \tag{117}$$

and it expresses the rate of change of a quantity in a moving coordinate frame following the fluid particles. Using the definition (117), equation (116) becomes

$$\frac{\partial\phi}{\partial z}-\frac{\partial\eta}{\partial t}-\frac{\partial\phi}{\partial x}\cdot\frac{\partial\eta}{\partial x}-\frac{\partial\phi}{\partial z}\cdot\frac{\partial\eta}{\partial z}=0\ . \tag{118}$$

The last two terms in (118) are of second order, and upon linearization, equation (118) reduces to (73).

The dynamic free surface boundary condition can be obtained from Bernoulli's equation. For an unsteady, irrotational flow this is

$$\frac{\partial\phi}{\partial t}+\frac{1}{2}\nabla\phi\cdot\nabla\phi+\frac{p}{\rho}+gz=\text{const.} \tag{119}$$

If we require that the pressure on the free surface is the same as the atmospheric pressure p_a, which is assumed to be independent of the actual position on the free surface, we get from (119)

$$-\frac{1}{\rho}(p-p_a)=\frac{\partial\phi}{\partial t}+\frac{1}{2}\nabla\phi\cdot\nabla\phi+gz\ . \tag{120}$$

Substituting the free surface elevation η for z, and solving for η

$$\eta=-\frac{1}{g}\left(\frac{\partial\phi}{\partial t}+\frac{1}{2}\nabla\phi\cdot\nabla\phi\right)\ . \tag{121}$$

If we neglect the last term, which is a second order quantity in the fluid velocity, the linearized condition (70) can be obtained. If (121) is substituted into (118), the combined free surface boundary condition becomes

$$\frac{\partial^2\phi}{\partial t^2}+g\frac{\partial\phi}{\partial z}+2\nabla\phi\cdot\nabla\frac{\partial\phi}{\partial t}+\tfrac{1}{2}\nabla\phi\cdot\nabla(\nabla\phi\cdot\nabla\phi)=0\ . \tag{122}$$

Of course it is not necessary to memorize this! We can see that upon linearization, the first two terms of (122) will survive only, and the linearized condition (72) follows. The free surface boundary condition (122) is exact and explicit, except that it must be applied on the unknown surface $z=\eta$ defined by (121) instead of $z=0$ as in the linear case.

With the exception of the above two boundary conditions, the procedure for solving the problem is similar, to a certain extent, to the linear case of Section 2.1, and it follows the so called *Stokes expansions*. The unknown velocity potential can be expanded in a Taylor series around the undisturbed plane $z=0$

$$\phi(x,\eta,y,t)=\phi(x,0,y,t)+\eta\left(\frac{\partial\phi}{\partial z}\right)_{z=0}+\tfrac{1}{2}\eta^2\left(\frac{\partial^2\phi}{\partial z^2}\right)_{z=0}+\cdots\ , \tag{123}$$

and using this perturbation scheme we can obtain, by substituting into (121) and (122), a sequence of boundary conditions valid on the known plane $z = 0$. Keeping up to second terms only, the final result for the wave profile in deep water is

$$\eta = A\cos(kx - \omega t) + \tfrac{1}{2}kA^2\cos 2(kx - \omega t) \; . \tag{124}$$

The last term in (124), which represents the second order correction to the free surface profile, is positive both at the crests $(kx - \omega t) = 0, 2\pi, 4\pi, \ldots$ and at the troughs $(kx - \omega t) = \pi, 3\pi, 5\pi, \ldots$ As a result of this nonlinear correction the crests will be steeper and the troughs flatter, a water waves feature that is easily detectable in practice, see Figure 21.

From the early days of naval architecture it has been customary to make use of a trochoidal wave in some ship design problems. The trochoidal wave, shown in Figure 22, represents the trace of a point on a rolling circle, it has a convenient form from the geometrical point of view and it is much easier to analyze than the previous Stokes waves. Naturally it is nothing more than a trick, and it cannot be derived from the principles of hydrodynamics; a neat trick, we have to admit though, since its profile is almost identical to the second order Stokes wave.

The deep water dispersion relation (80) corrected for second order effects is

$$\omega^2 = gk(1 + k^2A^2) \; . \tag{125}$$

This can be combined with (67) to obtain the corresponding correction for the phase velocity

$$c_p = \left(\frac{g}{k}\right)^{1/2}\left(1 + \tfrac{1}{2}k^2A^2\right) + O(k^3A^3) \; . \tag{126}$$

It can be seen that the phase velocity depends weakly on the wave amplitude, and waves of large height travel faster than small waves. By analogy with the more significant dependence of the phase velocity on wave length, this dependence on amplitude is known as amplitude dispersion.

Finally, one of the more interesting nonlinear features of plane progressive waves is the occurrence of a second order mean drift of the fluid particles. The orbital motion of a particular fluid particle can be computed in terms of the Lagrangian coordinates $[x_0(t), z_0(t)]$ which define the position of a particle. These must satisfy the relations

$$\frac{dx_0}{dt} = u(x_0, z_0, t) \; , \tag{127}$$

$$\frac{dz_0}{dt} = w(x_0, z_0, t) \; . \tag{128}$$

If x_0 and z_0 differ by a small amount, of order A, from the fixed position (x, z), Taylor series can be used to expand (127), (128) in the form

$$\frac{dx_0}{dt} = u(x, z, t) + (x_0 - x)\frac{\partial u}{\partial x} + (z_0 - z)\frac{\partial u}{\partial z} \; , \tag{129}$$

$$\frac{dz_0}{dt} = w(x, z, t) + (x_0 - x)\frac{\partial w}{\partial x} + (z_0 - z)\frac{\partial w}{\partial z} \; . \tag{130}$$

Now it can be shown that the deep water velocity potential (79) is exact to second order in the wave amplitude, and if we integrate (82) and (83) with respect to time we get the first order trajectories

$$x_0 - x = \int u\, dt = -Ae^{kz} \sin(kx - \omega t) \,, \tag{131}$$

$$z_0 - z = \int w\, dt = -Ae^{kz} \cos(kx - \omega t) \,. \tag{132}$$

If these expressions are substituted with (82), (83) in (129), (130), it follows that

$$\frac{dx_0}{dt} = \omega A e^{kz} \cos(kx - \omega t) + \omega k A^2 e^{2kz} \,, \tag{133}$$

$$\frac{dz_0}{dt} = \omega A e^{kz} \sin(kx - \omega t) \,. \tag{134}$$

It can be seen that the second order vertical motion of a given particle of fluid is strictly periodic, with the velocity given by (134), but the horizontal velocity (133) contains a steady Stokes' drift. Integrating (133) vertically with respect to all particles of fluid $-\infty < z_0 < 0$ yields the total mean flux

$$Q = \tfrac{1}{2}\omega A^2 = \tfrac{1}{2} k A^2 c_p \,. \tag{135}$$

The presence of a mean drift is obvious from the observation of small vessels floating in waves and it may become a serious consideration for accurate positional control of large floating offshore platforms. In the latter case, computation of the steady or slowly varying drift is a much more complex problem.

2.5 Description of the seaway.

Wave patterns in an open sea are ever changing with time and space, in a manner that appears to defy analysis be it linear or second order Stokes. Ambient waves on the surface of the sea are dispersive as well as *random*. The generating mechanism is, predominantly, the effect upon the water surface of wind in the atmosphere. The wind is itself random, especially when viewed from the standpoint of the turbulent fluctuations and eddies which are important in generating waves. The randomness of sea waves is subsequently enhanced by their propagation over large distances in space and time and their exposure to the random nonuniformities of the water and air.

In principle, one could use the superposition principle in the form of equation (92) and attempt a description of the seaway deterministically accounting for each one of the individual wave components. Leaving aside the issue of whether such an approach is possible or not (advocates of chaos theory may well argue that it is impossible), it is clearly a highly impractical task. Fortunately, it is not required either. It would suffice to represent sea waves in a *probabilistic* manner.

If $X(t)$ represents a random process, say the wave elevation at a particular observation station, all we will be able to record is *one* form of $X(t)$ as it unfolds over time. We call this a *realization* $X^{(1)}(t)$ of the random process $X(t)$. Notice that it is not possible to observe the random process itself — only one realization of it. From Figure 23 it can be seen that there exist two possible ways of defining the statistical properties of the random process $X(t)$. We

can consider the statistical properties taken "across the ensemble" at fixed values of time $t = t_1$, $t = t_2$, etc., or we may consider the properties of the random process taken "along the ensemble" where t_1, t_2, etc., are assumed to vary. Description of a random process so general would require an enormous amount of information. Fortunately, for certain random processes such as sea waves, it is possible to assume that the process is of a special form: it is "stationary", "homogeneous", and "ergodic". For sea waves it should be adequate to describe the wave environment over a period of a few hours (or before the next weather report comes in), and to assume that the wave motion is *stationary* (its statistics remain the same over time) during this interval of time. Likewise, we have no interest in describing the wave environment simultaneously throughout the world, a small area of operations is all we need, and we can assume that the wave motion is *homogeneous* (its statistics remain the same in that area) in space over the area in question. These statements have meaning only in a statistical sense, since for a random wave system it would be funny to suggest that the precise wave motion is the same at different points in space or time. Finally, it is reasonable to assume that the statistical properties of the waves measured over time, should be "typical" of the random process; i.e., they should be the same even if we were able to sample all possible realizations of the wave motion at a fixed time. Such random processes are said to be *ergodic*.

To arrive at a statistical description of the seaway we start with the general representation (92), which we write in the form

$$\eta(x, y, t) = \Re \iint dA(\omega, \theta) \exp[-ik(x \cos\theta + y \sin\theta) + i\omega t] \; . \tag{136}$$

Here the wave number k is defined in terms of the frequency ω by the appropriate dispersion relation, and the differential wave amplitude dA is a complex quantity of random phase and magnitude proportional to the square root of the differential energy $d\overline{E}$, see equation (102). The average energy density can be computed by squaring (196) and taking its average value. The only contribution to this average will be from combinations of the form $(\omega, \theta) = (\omega', \theta')$, with the final result

$$\overline{\eta^2} = \tfrac{1}{2} \iint dA(\omega, \theta) dA^*(\omega, \theta) \equiv \int_0^\infty \int_0^{2\pi} S(\omega, \theta) \, d\omega \, d\theta \; , \tag{137}$$

where $(*)$ denotes the complex conjugate. This approach to random sea waves is motivated by the deterministic distribution of plane waves and the desire to extend that representation to the random case. The function $S(\omega, \theta)$ is called the *spectral density* and more rigorously can be defined as the Fourier transform of the correlation function for the free surface elevation. Comparing (137) and (102) we can see that the total mean energy of the wave system per unit area of the free surface is equal to

$$\overline{E} = \rho g \int_0^\infty \int_0^{2\pi} S(\omega, \theta) \, d\theta \, d\omega \; . \tag{138}$$

It is customary to ignore the factor ρg and to refer to the function $S(\omega, \theta)$ as the *spectral energy density* or simply the *energy spectrum*. More specifically, this is a *directional* energy spectrum; it can be integrated over all wave directions to give the *frequency* spectrum

$$S(\omega) = \int_0^{2\pi} S(\omega, \theta) \, d\theta \; . \tag{139}$$

If it is desired to visualize the amplitudes A_i of the wave components we can use

$$\tfrac{1}{2}A_i^2 = S(\omega_i)\,\delta\omega_i \ ,$$

so that a component amplitude is

$$A_i = \sqrt{2S(\omega_i)\,\delta\omega_i} \ , \tag{140}$$

in the limit as $\delta\omega_i \to 0$. Of course, this cannot be evaluated directly, but it can be approximated when $\delta\omega_i$ is taken to be very small, see Figure 24. Using equations (138) and (139) we can see that

$$\overline{E} = \int_0^\infty S(\omega)\,d\omega \ , \tag{141}$$

i.e., the area under the spectrum $S(\omega)$ of Figure 24 is equal to (within the constant ρg) the mean energy stored in that particular wave system.

If one attempts to find the sea wave spectrum from measurements of the free surface elevation at a single point in space, for instance by recording the heave motion of a buoy, the directional characteristic of the waves will be lost. Only the frequency spectrum (139) can be determined from such a restricted set of data. A limited amount of directional information follows if one measures the slope of the free surface, for example by measuring the angular response of the buoy as well as its heave. A complete description of the directional wave spectrum requires an extensive array of measurements at several adjacent points in space, and there are practical difficulties associated with task.

As a simpler alternative, one can assume that the waves are *unidirectional*, with the energy spectrum proportional to a delta function in θ. Wave spectra of this form are called *long crested*, since the fluid motion is two dimensional and the wave crests are parallel. If one assumes that the spectrum is of this character, with the direction prescribed, the frequency spectrum (139) is sufficient to describe the wave environment.

If the waves are generated by a single storm, far removed from the point of observation, it might be presumed that these waves would come from the direction of the storm in a long crested manner. The limitations of this assumption are obvious to anyone who has observed the sea surface. While a preferred direction may exist, especially for long swell that has traveled large distances, even these long waves will be distributed in their direction, and for short steep waves the directional variation is particularly significant. Since the superposition of such waves from a range of different directions appears in space as a variation of the free surface elevation in all directions, these waves are known as *short crested* waves.

Usually in the fields of ocean engineering and naval architecture it is customary to assume that the waves are long crested. With such a simplification it is possible to use existing information for the frequency spectrum (139), which is based on a combination of theory and full scale observations. Sea wave spectra depend on the velocity of the wind as well as its duration in time and the distance over which the wind is acting on the free surface. This distance is known as the *fetch*. Wave spectra that have reached a steady state of equilibrium, independent of the duration and fetch are said to be *fully developed*. A semi–empirical expression for the frequency spectrum of fully developed seas is

$$S(\omega) = \frac{\alpha g^2}{\omega^5} \exp\left[-\beta\left(\frac{g}{U\omega}\right)^4\right] \ . \tag{142}$$

Here α and β are nondimensional parameters defining the spectrum, and U is the wind velocity at a standard height of 19.5 meters above the free surface. This two parameter spectrum is sufficiently general to fit quite a few observations and is consistent with theoretical predictions of the high frequency limit. The most common values for the parameters in (142) are

$$\alpha = 8.1 \times 10^{-3} \quad \text{and} \quad \beta = 0.74 \,, \tag{143}$$

and with these values, (142) is known as the *Pierson–Moskowitz* spectrum. the resulting family of curves is shown in Figure 25 for wind speeds of 20 to 50 knots. It can be seen that the energy in the wave system increases as the wind speed increases. A typical actual wave spectrum, fetch limited, is also shown in Figure 25 where it can be observed that the main difference with (142) is the existence of a twin peak — usually associated with swells where two distinct wave systems dominate.

Directional characteristics can be introduced into the fully developed spectrum (142) by

$$S(\omega, \theta) = S(\omega)\Theta(\theta) \,, \tag{144}$$

where $\Theta(\theta)$ is an appropriate *spreading function* typically of the form

$$\Theta(\theta) = \frac{2}{\pi} \cos^2 \theta \,. \tag{145}$$

A comparison between such an idealized and an actual directional specrtum is also shown in Figure 25.

Now that we are equipped with a suitable description of the sea we can proceed with the statistical properties of the sea waves. If the spectrum is assumed to be of narrow bandwidth, the wave amplitudes follow a *Rayleigh distribution*. The probability that the wave amplitude A lies within the differential increment $(A, A + dA)$ is $p(A)\, dA$, where the normalized *probability density function* is given by

$$p(\zeta) = \zeta \exp(-\zeta^2/2) \,. \tag{146}$$

Here $\zeta = A/m_0^{1/2}$ is the normalized wave amplitude, and m_0 is the total energy of the spectrum, or the integral of $S(\omega)$ over all frequencies. More generally, the *moments* m_i of the spectrum are defined by

$$m_i = \int_0^\infty \omega^i S(\omega)\, d\omega \,, \quad i = 0, 1, 2, \ldots \tag{147}$$

Statistics for the *wave height* $H = 2A$ can be derived using the probability density function (146). Thus, the average wave height $\overline{H}$ is given by

$$\overline{H} = 2 \int_0^\infty A p(\zeta)\, d\zeta = (2m_0)^{1/2} \,. \tag{148}$$

For most purposes, however, we are interested primarily in the larger waves. The most common parameter that takes this into account is the *significant wave height*, $H_{1/3}$, defined as the average of the highest one third of all waves. This is computed by

$$H_{1/3} = \frac{2 \int_{\zeta_0}^\infty A p(\zeta)\, d\zeta}{\int_{\zeta_0}^\infty p(\zeta)\, d\zeta} \,, \tag{149}$$

where the lower limit of the integration is defined by

$$\int_{\zeta_0}^{\infty} p(\zeta)\, d\zeta = \frac{1}{3}\ . \tag{150}$$

Using (150) we can find

$$H_{1/3} = 4.0(m_0)^{1/2}\ . \tag{151}$$

Other important parameters of the wave system are defined in Figure 26 and can be computed as follows. An average frequency of the spectrum can be defined as the expected number of zero upcrossings per unit time, that is, the number of times the wave amplitude passes through zero with positive slope. The final result here is

$$\omega_z = \left(\frac{m_2}{m_0}\right)^{1/2}\ . \tag{152}$$

The moments m_0 and m_2 can be computed without difficulty for the two parameter spectrum (142), and it follows that

$$H_{1/3} = (2.0)\frac{U^2}{g}\left(\frac{\alpha}{\beta}\right)^{1/2}\ , \tag{153}$$

and

$$\omega_z = (\pi\beta)^{1/4}\left(\frac{g}{U}\right)\ . \tag{154}$$

Substituting the values (143) for the Pierson–Moskowitz spectrum gives the results shown in the table that accompanies Figure 26. Also shown in the table is the approximate Beaufort scale of the sea states for each wind speed and the average value of the wave length. The results shown in the table are based on the assumption of a fully developed sea. It is unusual for a storm of 50 knots intensity to last long enough for the sea to develop fully. Thus, while wind speeds of this intensity are not uncommon, the corresponding wave height and length shown in the table are rare.

The average period between zero upcrossings is

$$T_z = \frac{2\pi}{\omega_z} = 2\pi\sqrt{\frac{m_0}{m_2}}\ , \tag{155}$$

while the average period between peaks (maxima) or hollows (minima) is computed by

$$T_c = \frac{2\pi}{\omega_c} = 2\pi\sqrt{\frac{m_2}{m_4}}\ . \tag{156}$$

For a narrow banded process, T_c and T_z do not differ by much.

Much of the uncertainty regarding the process by which the wind speed is related to the waves can be avoided by identifying the Pierson–Moskowitz spectrum in terms of the significant wave height rather than the wind speed or sea state. However, if the sea is not fully developed, the corresponding wave lengths will be shorter since dispersion has less opportunity to occur. Thus, the Pierson–Moskowitz spectrum underestimates the peak frequency for the higher spectra and conversely for smaller waves. To account for this

problem, the two parameter spectrum (142) is used together with full scale observations of the significant wave height and period. The parameters α and β are then determined from (153) and (154). The significant wave height, $H_{1/3}$, and the frequency ω_z can be easily computed from an experimental record of wave elevations at a given point. It is interesting to note that $H_{1/3}$ and T_z are closely correlated to human observations from the deck of a ship; the human mind disregards the smaler waves and pays closer attention to the largest.

The significant wave height is relevant as an indication of the most likely waves to be encountered, but for design purposes a more conservative estimate is needed. Thus we are led to consider the statistics of *extreme values*.

From the Rayleigh distribution (146), the cumulative probability of a single wave being less than $A = \zeta(m_0)^{1/2}$ is

$$P(\zeta) = \int_0^\zeta p(\zeta')\, d\zeta' = 1 - \exp(-\zeta^2/2) \; . \tag{157}$$

The probability that the amplitudes of N statistically independent waves are all less than A is P^N, and the probability that at least one wave amplitude will exceed this value is

$$1 - P^N = 1 - [1 - \exp(-\zeta^2/2)]^N \; . \tag{158}$$

The negative derivative of (158) gives the probability density of the extreme value in N cycles, in the form

$$g(\zeta) = Np(\zeta)[P(\zeta)]^{N-1} \; . \tag{159}$$

The wave amplitude for which this probability density function is a maximum can be found by setting the derivative of (159) equal to zero. Simplifying the resulting expression for $N \gg 1$, the *most probable extreme value* in N waves is given by

$$A = (2m_0 \ln N)^{1/2} \; . \tag{160}$$

It has been shown that the probability of exceeding (160), for large N, is $1 - e^{-1} = 0.632$. Thus a more conservative criterion is required, and for this purpose we define the *design extreme value* as the wave amplitude that will be exceeded in N encounters with a probability of only 1 percent. From (158) it follows that

$$1 - P^N = 0.01 \; , \tag{161}$$

so that

$$P = (0.99)^{1/N} = e^{(1/N)\ln(0.99)} \simeq e^{-0.01/N} \simeq 1 - \frac{0.01}{N} \; . \tag{162}$$

Combining (162) with (157) and solving for the wave amplitude, we get

$$A = \left(2m_0 \ln \frac{N}{0.01}\right)^{1/2} \; . \tag{163}$$

This is the design extreme value, or the maximum wave amplitude in N encounters that will not be exceeded with probability 99%. Since the significant wave amplitude is half the wave height (151), the design extreme value exceeds the significant value by the ratio

$$\frac{\text{Design Extreme}}{\text{Significant}} = \left(\frac{1}{2} \ln \frac{N}{0.01}\right)^{1/2} \; . \tag{164}$$

This factor is not sensitive to the value of N, nor to the arbitrary choice of 0.01 as the probability that the extreme wave will exceed this value. For example, with $N = 100$, (164) is equal to 2.15; for $N = 10^6$ this factor increases to 2.63. Since (162) is much more sensitive to the value of m_0 than to $(N/0.01)$, the most important factor to estimate correctly is the total wave energy.

3. Ship Motions in Waves.

A subject of great concern to us is the effect suffered by a ship or a near–surface submarine in the presence of sea waves. The most common responses of concern are ship motions and structural loading. In the simplest case it may be assumed that the waves incident upon the body are plane progressive waves oof small amplitude, with sinusoidal time dependence, as described in the previous Section. Ship motions are assumed to be sufficiently small so that linear theory holds. In the context of these notes we will try to keep the discussion at a rather informal level, and after a general inrtoduction to the problem we will study the heave and pitch motions of a floating body in regular waves coming from the bow in Section 3.1. Derived responses such as velocities, accelerations, added resistance in waves, and bending moments in waves are discussed in Section 3.2. The results that are obtained in regular waves are not without physical interest, but their practical value might be questioned given the highly irregular nature of actual waves in the sea. Fortunately, the statistical description of the seaway of Section 2.5 makes the study of ship motions in irregular seas a rather straight forward extension of the regular waves case, and this is done in Section 3.3. A discussion of computational aspects of the problem is the subject of Section 3.4, and some seakeeping considerations in ship design are delayed until Section 3.5.

3.1 Motions in regular waves.

In the problem to be formulated here, plane progressive waves of amplitude A and direction θ are incident upon a *stationary* body, which moves in response to these waves, in general, with six degrees of freedom as illustrated in Figure 27. We define three translational motions parallel to (x, y, z) as *surge*, *heave*, and *sway*, and three rotational motions about the same axes as *roll*, *yaw*, and *pitch*, respectively. The corresponding velocities $U_j(t)$ will be sinusoidal in time, with the same frequency (for linear motions) as the incident waves, therefore

$$U_j(t) = \Re\left(i\omega\eta_j e^{i\omega t}\right) , \quad j = 1, 2, \ldots, 6 . \tag{165}$$

Here the complex amplitude is employed in preference to the body velocity, since the hydrostatic restoring forces that will be encountered are proportional to the amplitudes of heave, roll, and pitch. These restoring forces are analogous to the familiar "spring constant" of a mechanical oscillator.

If the incident wave is sufficiently small in amplitude and the ship is stable, the resulting motion will be proportionally small, so we can utilize linear theory. The total velocity

potential ϕ can be written, using the superposition principle, in the form

$$\phi(x,y,z,t) = \Re\left\{\left(\sum_{j=1}^{6}\eta_j\phi_j(x,y,z) + A\phi_A(x,y,z)\right)e^{i\omega t}\right\} . \tag{166}$$

In this decomposition, the function ϕ_j represents the velocity potential of a rigid body motion with unit amplitude, in the absence of the incident waves. For example, if the body is forced by an external mechanism to oscillate in heave with unit amplitude, in otherwise calm water, the resulting fluid motion will be represented by the potential ϕ_2. A similar interpretation applies for each mode of rigid body motion. The appropriate boundary conditions to be imposed on the ship surface S are obtained by equating the normal derivative of (166) to the normal component of the body velocity

$$\frac{\partial\phi_j}{\partial n} = i\omega n_j , \qquad j = 1,2,3, \tag{167}$$

$$\frac{\partial\phi_j}{\partial n} = i\omega(\mathbf{r}\times\mathbf{n})_{j-3} , \quad j = 4,5,6, \tag{168}$$

on S. Here $\mathbf{n}$ is the unit normal vector on the body surface, directed into the body, and $\mathbf{r}$ is the position vector (x,y,z). The forced motion potentials ϕ_j, $j = 1,2,\ldots,6$, are generally known as solutions of the *radiation* problem.

The remaining potential represented by the last term in (166) is due to the incident waves and their interaction with the body. Given the assumption of linear superposition, this potential is independent of the body motions and may be defined with the body fixed in position. The appropriate boundary condition on the body surface is

$$\frac{\partial\phi_A}{\partial n} = 0 , \quad \text{on} \quad S . \tag{169}$$

The problem so defined is known as a *wave diffraction* problem.

The presence of the body in the fluid results in diffraction of the incident wave system and the addition of a disturbance to the incident wave potential associated with the *scattering* effect of the body. This process can be emphasized by the additional decomposition

$$\phi_A = \phi_0 + \phi_7 , \tag{170}$$

where ϕ_0 is the incident wave potential and ϕ_7 is the scattering potential that must be introduced to represent the disturbance of the incident waves by the fixed body. The incident wave potential is known, from (79) for infinite depth or (84) for finite depth, and the scattering potential must satisfy the boundary condition

$$\frac{\partial\phi_7}{\partial n} = -\frac{\partial\phi_0}{\partial n} , \quad \text{on} \quad S . \tag{171}$$

In addition to the above body boundary conditions, each potential ϕ_j must satisfy Laplace's equation

$$\nabla^2\phi_j = 0 , \quad j = 0,1,\ldots,7 , \tag{172}$$

throughout the domain of the fluid, and condition (71) on the bottom for finite depth, or alternatively $\phi_j \to 0$ as $z \to \infty$ for deep water. On the free surface, the linearized boundary condition follows from (72) and (166) in the form

$$-\frac{\omega^2}{g}\phi_j + \frac{\partial \phi_j}{\partial z} = 0 \ , \quad \text{on} \quad z = 0 \ , \quad j = 0, 1, \ldots, 7 \ . \tag{173}$$

Finally, an appropriate radiation condition at infinity is imposed, which states that the waves on the free surface, other than those due to the incident potential itself, are due to the presence of the body; and, therefore, the waves associated with the potentials ϕ_j, $j = 1, 2, \ldots, 7$ must be radiating *away* from the body.

At this stage the problem formulation is complete and the velocity potential ϕ in (166) can be found. A general discussion of some popular solution techniques can be found in Section 3.4. Once the velocity potential is determined we can obtain the oscillatory force and moment acting on the body by substituting (166) into Bernoulli's equation. Retaining only the first order linear terms in (119), the total pressure is given by

$$\begin{aligned} p &= -\rho\left(\frac{\partial \phi}{\partial t} + gz\right) \\ &= -\rho \Re\left\{\left(\sum_{j=1}^{6} \eta_j \phi_j + A(\phi_0 + \phi_7)\right) i\omega e^{i\omega t}\right\} - \rho g z \ . \end{aligned} \tag{174}$$

The force $\mathbf{F}$ and moment $\mathbf{M}$ on the body can then be determined by integrating the fluid pressure (174) over the wetted surface S

$$\mathbf{F} = \iint_S p\mathbf{n}\, dS \ , \tag{175}$$

$$\mathbf{M} = \iint_S p(\mathbf{r} \times \mathbf{n})\, dS \ . \tag{176}$$

Substituting (174) into (175) we get an expression of the form

$$\begin{aligned} \mathbf{F} = & -\rho g \iint_S \mathbf{n} z \, dS \\ & -\rho \Re\left(\sum_{j=1}^{6} i\omega \eta_j e^{i\omega t} \iint_S \mathbf{n}\phi_j \, dS\right) \\ & -\rho \Re i\omega A e^{i\omega t} \iint_S \mathbf{n}(\phi_0 + \phi_7)\, dS \ . \end{aligned} \tag{177}$$

The three integrals in (177) represent distinctly different contributions to the total force; the development for the moment is similar. The first is the *hydrostatic* component and produces terms that are proportional to body displacements. The second produces components that are proportional to body velocities (these are called *damping* terms) and body accelerations (called *added mass* terms). Finally, the third integral represents the *wave exciting* force which is further broken down into the *Froude–Krylov* force (the contribution from the incident potential ϕ_0 alone), and the *diffraction* force (the contribution from the scattering potential

ϕ_7). These forces and moments are substituted then into Newton's law and the six degree of freedom equations for the body motions are obtained.

As a more down to earth case, consider the motions of a body that is allowed to heave and pitch only. Such motions are usually decoupled, for typical ships, from the horizontal plane motions in sway or yaw. The final coupled form of the heave and pitch equations of a ship in regular waves is then

$$\begin{aligned}(m + A_{33})\ddot{\eta}_3 + B_{35}\dot{\eta}_3 + C_{33}\eta_3 + A_{35}\ddot{\eta}_5 + B_{35}\dot{\eta}_5 + C_{35}\eta_5 &= F_3 e^{i\omega t} , \qquad (178)\\ (I_{55} + A_{55})\ddot{\eta}_5 + B_{55}\dot{\eta}_5 + C_{55}\eta_5 + A_{53}\ddot{\eta}_3 + B_{53}\dot{\eta}_3 + C_{53}\eta_3 &= F_5 e^{i\omega t} , \qquad (179)\end{aligned}$$

where m is the ship's mass and I_{55} the mass moment of inertia with respect to the y axis. The A_{jk} terms correspond to added mass, in phase with vertical accelerations, and physically A_{jk} represents the force component in the j–th mode of motion per unit acceleration in the k–th mode of motion. The B_{jk} terms correspond to hydrodynamic damping, in phase with vertical velocity, and physically B_{jk} represents the force component in the j–th mode of motion per unit velocity in the k–th mode of motion. Terms involving the coefficients C_{jk} are the restoring forces and moments, representing the net hydrostatic buoyancy effects of the ship motions. These terms are related to the hydrostatic coefficients used in the calculations of Part I; i.e., C_{33}, C_{35}, and C_{55} are related to tons per cm immersion, change in displacement per cm, and moment to trim one cm, respectively. The right hand side represent the heave, F_3, and pitch, F_5, Froude–Krylov and diffraction excitation forces as mentioned before. F_3 and F_5 are taken to be the complex exciting force and moment amplitudes, containing both amplitude and phase information. Expressions for the above coefficients are presented in Fig. 28.

The previous equations of motion are valid for a ship with zero forward speed. If the ship possesses a forward speed U, this can be assumed, within linearity, constant. The only change in such a case is in the frequency ω due to a Doppler shift effect. If we consider the case of head seas, or waves from directly ahead, we can assume that both the wave excitation forces and the resultant oscillatory motions are linear and harmonic, acting at the frequency of wave encounter

$$\omega_e = \omega + \frac{2\pi}{\lambda/U} = \omega + kU = \omega + \frac{\omega^2}{g}U . \qquad (180)$$

For the general case of waves at a direction θ, where $\theta = 180^o$ corresponds to head seas and $\theta = 0^o$ to following seas, the *frequency of encounter* ω_e becomes

$$\omega_e = \omega - \frac{\omega^2}{g}U\cos\theta = \omega - kU\cos\theta . \qquad (181)$$

In linear theory, the harmonic responses of the vessel, $\eta_j(t)$, will be proportional to the amplitude of the exciting forces and at the same frequency, which is now ω_e instead of ω. Consequently, the ship motions will have the form

$$\begin{aligned}\eta_j(t) &= \overline{\eta}_j e^{i\omega_e t} ,\\ \dot{\eta}_j(t) &= i\omega_e\overline{\eta}_j e^{i\omega_e t} , \quad j = 3, 5 , \qquad (182)\\ \ddot{\eta}_j(t) &= -\omega_e^2\overline{\eta}_j e^{i\omega_e t} ,\end{aligned}$$

where $\overline{\eta}_j$ is the complex response amplitude, and $j = 3$ for heave and $j = 5$ for pitch. Substituting equations (182) in (178) and (179), the $e^{i\omega_e t}$ terms cancel out and the resulting equations are

$$[-\omega_e^2(m + A_{33}) + i\omega_e B_{33} + C_{33}]\overline{\eta}_3 + (-\omega_e^2 A_{35} + i\omega_e B_{35} + C_{35})\overline{\eta}_5 = F_3 \ , \tag{183}$$

$$[-\omega_e^2(I_{55} + A_{55}) + i\omega_e B_{55} + C_{55}]\overline{\eta}_5 + (-\omega_e^2 A_{53} + i\omega_e B_{53} + C_{53})\overline{\eta}_3 = F_5 \ , \tag{184}$$

where A_{jk} is the added mass coefficient in j–th direction due to k–th motion, B_{jk} is the damping coefficient in j–th direction due to k–th motion, C_{jk} is the hydrostatic restoring force coefficient in j–th direction due to k–th motion, and F_j is the complex exciting force amplitude in j–th direction. Note than in equations (183) and (184) the origin is at the center of gravity, which is assumed to lie on the waterline. In the more general case, the term $m\ddot{\eta}_3$ is substituted by $m\ddot{\eta}_3 - mx_G\ddot{\eta}_5$, and the term $I_{55}\ddot{\eta}_5$ by $I_{55}\ddot{\eta}_5 + m(z_G\ddot{\eta}_1 - x_G\ddot{\eta}_3)$, where η_1 is the surge motion amplitude. In other words, a coordinate coupling is introduced similar to the maneuvering case.

Equations (178) and (179) are similar to the coupled equations of motion for a classical two degree of freedom spring–mass–damper system. This similarity is only on the surface though, and the analogy should not be pushed too far. The coefficients and the excitation terms in the equations of motion here are functions of the frequency of motion. This introduces *memory effects* and the correct solution of these equations of motion in the time domain requires the addition of complicated convolution integrals. Only in slowly moving reference motions we can assume the coefficients effectively constant and equal to their zero frequency limit, and thus eliminate such convolution integrals in the differential equations. This was the case during the maneuvering motions in the first section of this part. In order to overcome this difficulty here it is necessary to consider the equations in the frequency domain as was done in (183) and (184). Note that this is valid for linear motions though; nonlinear seakeeping is *not* a straightforward extension of linearized motions as in the case of ship maneuvering.

The determination of the coefficients and exciting forces and moments amplitudes represents the major problem in ship motion calculations. The problem can be simplified by applying a strip theory (see Section 3.4) approach, where the ship is divided into transverse strips, or segments. The added mass and damping for each strip are relatively easily calculated, using two dimensional potential theory or by suitable two dimensional experiments (in which case the results for damping are contaminated by viscous damping too). The sectional values are then appropriately combined to yield values for A_{jk}, B_{jk}, C_{jk}, and F_j. For the case of heave and pitch in head seas the table on page 203 lists the formulas for calculating the coefficients and the exciting forces.

As we mentioned previously, the exciting forces and moments are usually subdivided into the Froude–Krylov and diffraction excitations. The Froude–Krylov excitations represent the integration of the pressure over the body surface that would exist in the incident wave system if the body were not present. The diffraction exciting forces and moments are caused by the diffraction or modification of the incident waves due to the presence of the vessel. The Froude–Krylov forces and moments are sometimes used to approximate the total exciting

forces, and this is a considerably simpler task than diffraction force computations. This is a good approximation if the wave length is much larger than the vessel length, such as in the case of a small underwater vehicle in waves. For shorter wave lengths the approximation is increasingly inaccurate because the diffraction force becomes significant, for example in the case of a near surface submarine. For short waves the diffraction force may become approximately one–half of the total exciting force. For the expressions in the table, the terms in brackets proportional to c_{33} are the Froude–Krylov exciting force and moment, and the terms involving a_{33} and b_{33} represent the hydrodynamic diffraction forces. That these forces are given in terms of the same added mass and damping coefficients used in calculating the radiation force coefficients, A_{ij} and B_{ij}, is the result of the so called *Haskind relations*. These relations relate the diffraction exciting force to the incident wave and radiation potentials. They allow the computation of the diffraction force without having to solve for the diffraction potential. This is important because it means substantial savings in computer time for ship motion prediction programs.

The factor e^{ikx} in the expressions accounts for the wave profile along the length of the ship. Both the Froude–Krylov and diffraction parts of the exciting forces and moments are multiplied by the term $e^{-kT^*(x)}$, where k is the wave number and $T^*(x)$ is the mean draft for the section, assumed to be $S(x)/B(x)$, where $S(x)$ is the sectional area and $B(x)$ is the local beam at the waterline. This is the result of the exponential decay of the dynamic pressure in the incident wave as one moves deeper below the free surface. This effect is often called the Smith Effect. For depths greater than approximately one wave length no variation in pressure due to the incident waves can be felt. This decay in the incident wave dynamic pressure results in an equivalent reduction in the magnitude of the exciting forces.

To solve equations (183) and (184) for the complex amplitudes, the equations are written in the form

$$P\overline{\eta}_3 + Q\overline{\eta}_5 = F_3 \,, \tag{185}$$
$$R\overline{\eta}_3 + S\overline{\eta}_5 = F_5 \,, \tag{186}$$

where

$$\begin{aligned} P &= -\omega_e^2(m + A_{33}) + i\omega_e B_{33} + C_{33} \,, \\ Q &= -\omega_e^2 A_{35} + i\omega_e B_{35} + C_{35} \,, \\ R &= -\omega_e^2 A_{53} + i\omega_e B_{53} + C_{53} \,, \\ S &= -\omega_e^2(I_{55} + A_{55}) + i\omega_e B_{55} + C_{55} \,. \end{aligned}$$

The solution to the coupled equations (185) and (186) is then given by

$$\overline{\eta}_3 = \frac{F_3 S - F_5 Q}{PS - QR} \,, \tag{187}$$
$$\overline{\eta}_5 = \frac{F_5 P - F_3 R}{PS - QR} \,. \tag{188}$$

The limiting forms of the solutions for $\overline{\eta}_3$ and $\overline{\eta}_5$ are easily determined from (187) and (188). At the high frequency limit, the exciting forces go to zero (a large number of very short waves give individual contributions that cancel out when integrated along the length

of the hull), and therefore the motions must also approach zero. Thus, a ship in waves can be viewed as a low pass filter. In the low frequency limit, P, Q, R, and S approach the values of their hydrostatic restoring force coefficients. The low frequency limit of F_3 and F_5 are found by using only the Froude–Krylov terms and expanding the e^{ikx} term for small k. The net result is that in the limit of low frequency

$$\overline{\eta}_3 \to \overline{\zeta} \ , \tag{189}$$

$$\overline{\eta}_5 \to -ik\overline{\zeta} \ . \tag{190}$$

Thus, for very long waves the heave amplitude approaches the wave amplitude (the ship is riding the waves) and the pitch amplitude is the same as the maximum wave slope. The phasing is such that the ship contours the waves. At intermediate frequencies the ship motions may peak. Depending on hull form and speed, as well as wave direction, typical peak values are in the range of 1 to 2 times the wave amplitude for heave and 1 to 1.5 times the wave slope for pitch.

The cross coupling between heave and pitch results from the coefficients with subscripts 35 or 53. For a fore and aft symmetric ship, such as a barge, at zero forward speed the cross coupling is zero; heave and pitch occur independent of each other. Even though typical ships are almost fore and aft symmetric, the cross coupling between heave and pitch is very important and must be retained in order to correctly predict the motions in head seas at some forward speed. Although in hydrostatics we were able to treat parallel sinkage and trim independently, for small displacements, we cannot in general do the same in seakeeping due to the forward speed coupling effects.

The previous equations of motion for a floating body can be generalized for the six degree of freedom case. In general, the equations will take the following form, where the overbars have been dropped for brevity,

$$\sum_{j=1}^{6} \eta_j[-\omega_e^2(M_{ij} + A_{ij}) + i\omega_e B_{ij} + C_{ij}] = AF_i \ , \tag{191}$$

where F_i is the exciting force per unit wave amplitude A and M_{ij} the appropriate mass matrix element. These are six simultaneous linear equations, which can be solved for the body motions η_j by standard matrix inversion techniques. Thus, in general, the body motion η_j will be given by an expression of the form

$$\eta_j = A\sum_{j=1}^{6}[D_{ij}]^{-1}F_i \ , \tag{192}$$

where D_{ij} denotes the total matrix in square brackets on the left side of (191). The ratio (η_j/A) is a quantity of fundamental significance, and is defined separately by

$$Z_j(\omega, U, \theta) \equiv \frac{\eta_j}{A} = \sum_{j=1}^{6}[D_{ij}]^{-1}F_i \ . \tag{193}$$

Physically, this is the complex amplitude of body motion in the j–th mode, in response to an incident wave of unit amplitude, frequency ω, and direction θ. The body itself moves

with forward speed U. This ratio is generally known as the *transfer function*, or the *response amplitude operator*, RAO. The RAO can be calculated from (193) once the added mass, damping, exciting, and hydrostatic forces are known.

To illustrate the nature of the RAO, we return to the special case of heave for a body with port/starboard and fore/aft symmetry at zero forward speed in head seas. Here there are no cross coupling effects, and equation (187) reduces to

$$Z_3(\omega) = \frac{F_3}{D_{33}} = \frac{F_3}{-\omega^2(m + A_{33}) + i\omega B_{33} + C_{33}} \ . \tag{194}$$

We can see from (194) that $Z_3(\omega) \to 1$ as $\omega \to 0$, and $Z_3(\omega) \to 0$ as $\omega \to \infty$, as we mentioned before. For intermediate frequencies, the most significant feature of the motions will be a resonant response at approximately the natural frequency where

$$\omega_n = \left(\frac{C_{33}}{m + A_{33}}\right)^{1/2} \ . \tag{195}$$

At or near this resonant frequency, the body will experience a response of large amplitude and a phase shift increasing from zero for lower frequencies to 180 degrees for $\omega \gg \omega_n$.

As in the case of a classical mechanical oscillator, the resonant response will be inversely proportional to the damping coefficient, but once more we must point out that this analogy is a bit deceptive. Unlike a mechanical oscillator, here there is a connection between the exciting force and the damping coefficient (this comes from the Haskind relations). Small exciting forces are associated with light damping as well. In particular, for a two dimensional or axisymmetric body the damping coefficient is proportional to the square of the exciting force, and the resonant response will then be *inversely* proportional to the exciting force! Thus, bodies deliberately designed with small exciting forces (small waterplane areas for instance) will experience a large resonant response, in a highly tuned manner. Vertical spar buoys are important examples of this category, as well as SWATH ships.

As a final remark on equation (194), we can see that for very long waves (low frequency ω) the problem is predominantly hydrostatics: the response is dominated by the hydrostatics coefficient C_{33} and the exciting force F_3. In the other extreme case of short waves the response is dominated by the exciting force F_3, the virtual mass $(m + A_{33})$, and the damping B_{33}; this is in the realm of ship vibrations. Ship motions in waves concentrate mainly on the intermediate regime where F_3, A_{33}, B_{33}, and C_{33} are all equally important. A typical plot of the exciting forces and motions in heave and pitch is shown in Figure 28. This corresponds to a particular RAO for a fixed ship forward speed and wave direction. A typical sketch of how the heave RAO may vary with the ship Froude number is shown in Figure 29. For certain ranges of speed and wave lengths there may be resonance with the development of excessive ship motions. This leads to a voluntary speed reduction in a seaway, as discussed in Section 3.5.

3.2 Derived responses.

Several aspects of ship response to waves are generally of greater importance in evaluating the seakeeping performance of the ship. These are responses that can in principle be derived

from the basic six modes of motion analyzed in the previous section. They include linear motions such as

- Vertical and/or lateral motions, velocities, and accelerations at specific points.
- Relative motions between a location in the ship and the encountered waves.

Nonlinear effects arise in connection with

- Steering and maneuvering in waves.
- Added resistance and powering in waves.
- Wave bending moments and loads on the ship.

The *absolute* vertical displacement at a point x along the length of the hull, due to heave and pitch, is given by

$$\xi_{VA} = \eta_3 - x\eta_5 \ , \tag{196}$$

and since η_3 and η_5 are the complex amplitudes in heave and pitch motion, respectively, ξ_{VA} contains both magnitude and phase information. The absolute vertical velocity is computed from

$$\dot{\xi}_{VA} = i\omega_e \xi_{VA} \ , \tag{197}$$

and the acceleration

$$\ddot{\xi}_{VA} = -\omega_e^2 \xi_{VA} \ . \tag{198}$$

From equations (196) to (198) we can find the response amplitude operator for motion, velocity, or acceleration at a particular point once the RAO's for heave $Z_3(\omega_e)$ and pitch $Z_5(\omega_e)$ are known. For this we only need the magnitude of the corresponding complex quantity. It should be mentioned that equations (197) and (198) are valid for zero forward speed. For a nonzero forward speed U, they become

$$\dot{\xi}_{VA} = i\omega_e(\eta_3 - x\eta_5) + U\eta_5 \ , \tag{199}$$

$$\ddot{\xi}_{VA} = -\omega_e^2(\eta_3 - x\eta_5) + 2i\omega_e U\eta_5 \ . \tag{200}$$

Also of interest is the *relative* vertical motion between a point in the ship and the surface of the encountered wave. This relative motion in regular waves is found by subtracting the free surface motion from the vertical ship motion at the desired point, taking account of their phase relationship. The free surface motion is composed of the incident wave, the diffracted wave, the radiated wave, and the Kelvin wave due to the ship's steady forward speed. The traditional assumption is that the principal component is the incident wave; i.e., the incident wave is not distorted by the presence of the ship. Then the amplitude of the relative vertical motion in general is given by

$$\xi_{VR} = \xi_{VA} - Ae^{ikx} \ , \tag{201}$$

where A is the wave amplitude and k the wave number. Then the RAO which requires only the scalar or absolute magnitude is

$$\left|\frac{\xi_{VR}}{A}\right| = \left|\frac{\eta_3 - x\eta_5}{A} - e^{ikx}\right| \ . \tag{202}$$

The significance of the relative motion response is that, as we will see in the next section, the moments of their spectrum provide probability measures related to anticipated deck wetness, bow slamming, and propeller racing.

The problem of *steering and maneuvering in waves* depends upon systems for ship path control as well as the ship sway, yaw, and roll motions including important nonlinear behavior. Analysis of the problem goes beyond the scope of these notes and we briefly mention here some of the potential dangers. In order to analyze the resulting motions we have to include the wave exciting forces and moments for the horizontal plane in the maneuvering equations of Section 1, and to take into account the important memory effects through complicated convolution integrals. Furthermore, in the horizontal modes of motion the ship will experience steady drift motions in addition to periodic motions, because of the lack of hydrostatic restoring forces and moments in the horizontal plane. Similarly, in irregular seas the ship will experience slowly varying surge, sway, and yaw motions with non zero means in addition to motion with frequency components equal to the frequency of encounter of the individual wave components. In quartering seas, the wave encounter frequencies are much lower and good steering is particularly important. At very low encounter frequencies, i.e, when the wave and ship speeds are nearly equal, the danger of loss of control and broaching arises. Here the pressures may actually turn the ship broadside to the waves, and excessive rolling or structural damage, or even the capsizing of small vessels, may result. In general, broaching is more probable for a ship that is unstable on course in calm water than for one that is stable.

The increase in required power resulting from ship motions in heavy seas arises from the combined effect of several factors:

1. *Added resistance* caused by
   (a) Direct wind and wave action.
   (b) Indirect effects associated with ship motions.
2. *Reduced propulsive efficiency* caused by
   (a) Increased propeller loading.
   (b) Propeller racing.
   (c) Unsteady propeller effects.
   (d) Reduced hull efficiency.

When a ship is subject to heaving and pitching, the effect of the motions on resistance may be significant. The added resistance in head seas may be considered to be made up of three components:

1. One corresponding to that experienced by a ship forced to oscillate in calm water, generating damping waves that dissipate energy.
2. Another caused by the phase shift between wave excitation and ship motions.
3. One resulting from the reflection and refraction of the incident waves by the ship.

The following conclusions are generally considered to be valid for head seas

1. The added resistance is independent of the still water resistance.
2. The added resistance is proportional to the square of the wave height.
3. The pitching motion has a dominating effect upon the resistance increase.
4. The direct effect of the reflection of sea waves is relatively small.
5. The maximum added resistance occurs at a higher speed than that for pitch resonance, if the natural pitching period is longer than the natural heaving period.

Equating added resistance to energy radiated by the pitching and heaving ship, we can arrive at a simple expression for the mean added resistance of a ship in regular head seas

$$\delta R = \frac{\pi}{L_w \omega_e} \int b(x) |\dot{\xi}_{VR}|^2(x)\, dx \ , \tag{203}$$

where

$$b(x) = b_{33}(x) - U \frac{da_{33}(x)}{dx} \ ,$$

and where $a_{33}(x)$ and $b_{33}(x)$ are the sectional heave added mass and damping coefficients, respectively. Assuming that a_{33} goes to zero at the ends of the ship, after partial differentiation and substitution, the mean added resistance at U and ω_e becomes

$$\delta R = \frac{\pi}{L_w \omega_e} \int \left[b_{33}(x) |\dot{\xi}_{VR}| + 2U a_{33}(x) \frac{d|\dot{\xi}_{VR}|}{dx} \right] |\dot{\xi}_{VR}|\, dx \ . \tag{204}$$

Since $|\dot{\xi}_{VR}|$ represents the amplitude of relative velocity, it must be calculated by combining the effects of pitch, heave, and wave elevation, considering their phase relationships, as discussed previously. Figure 30 gives a broad overall picture obtained from service records of speed versus power relationships in rough seas for a large containership. It shows a series of average power curves corresponding to different degrees of sea severity. The limit lines indicate the upper limits of attainable speed (based on wet decks, slamming, etc.) that provide cut–off points for each power curve. The plot also shows the effect of the ship's heading to the waves.

Although *wave loads* enter implicitly into the calculation of ship motions, they are considered here under the heading of derived responses because, in order to determine the loads at a particular instant of time, a solution to the ship motions must first be obtained. There are three different levels at which wave loads may be needed for structural design purposes:

1. Instantaneous local hydrodynamic pressures on the surface of the hull as a result of ship motions and ship wave interactions. These pressures may be needed over the entire hull surface or only some portion of it.
2. Integrated instantaneous pressures yielding the longitudinal and torsional bending moments and shear force at amidships or other stations.

3. Impulsive pressures on local areas of the hull which can cause vibratory hull response.

The vertical shear force on the ship is given by

$$V_3(x) = I_3(x) - H_3^S(x) - H_3^D(x) - F_3(x) \ , \tag{205}$$

where

$$I_3(x) = \int_0^x m(x)(\ddot{\eta}_3 - x\ddot{\eta}_5)\, dx \ ,$$

is the inertial force;

$$H_3^S(x) = -\rho g \int_0^x B(x)(\ddot{\eta}_3 - x\ddot{\eta}_5)\, dx \ ,$$

is the hydrostatic restoring force;

$$H_3^D(x) = -\int_0^x [a_{33}(x)(\ddot{\eta}_3 - x\ddot{\eta}_5) + b_{33}(\dot{\eta}_3 - x\dot{\eta}_5)]\, dx \ ,$$

is the hydrodynamic radiation (added mass and damping) force; and $F_3(x)$ is the wave exciting (Froude–Krylov and diffraction) force, as discussed previously. Equation (205) is valid for zero forward speed. A similar expression holds for nonzero forward speed as well as bending moment in waves. These relations can be used to obtain a rational determination of the loading of a ship's hull and its structural response in regular waves.

3.3 Motions in a seaway.

Any conclusions drawn on the seakeeping behavior of a ship based on the critical examination of motion response in regular waves can, at best, assume only academic significance. The establishment of the seakeeping behavior of a ship and the determination of explicit design parameters such as bending moments or added resistance, has to be done in a realistic seaway. With the spectral description of sea waves given in Section 2.5, we can return to the subject of body motions and generalize the results of the previous two sections in regular harmonic waves. If the sea waves are described by the random distribution (136), and if the response of the body to each component wave is defined by a response amplitude operator $Z(\omega, \theta)$, the body response will be

$$\eta_j(t) = \Re \iint Z_j(\omega, \theta) e^{i\omega t}\, dA(\omega, \theta) \ . \tag{206}$$

The principal assumption here is that linear superposition applies, as it must in any event for the underlying development of the RAO and the spectrum.

Like the waves themselves, the response (206) is a random variable. The statistics of the body response are identical to the wave statistics as analyzed in Section 2.5, except that the wave energy spectrum S is multiplied by the square of the RAO (this is a property of linear systems). Thus, if the subscript R represents any body response, we have

$$S_R(\omega) = |Z_R(\omega)|^2 S(\omega) \ , \tag{207}$$

where $Z_R(\omega)$ is the RAO of the response R, and $S(\omega)$ the spectrum of the seaway. Equation (207) can then be utilized to obtain the spectrum of the response R, and the formulas of Section 2.5 can be used to provide the statistics of this response in the particular sea state.

To a large extent, equation (207) provides the justification for studying regular wave responses. The transfer function $Z_R(\omega)$ is valid not only in regular waves, where it has been derived, but also in a superposition of regular waves, and ultimately in a spectrum of random waves. Generally speaking, a vessel with favorable response characteristics in regular waves will be good in irregular waves, and vice versa. This statement is oversimplified, however, and the relative shape of the energy spectrum and the transfer function is very crucial. For example, a large resonant response of the body will be of importance only if the resonant frequency is located close to the peak of the wave energy spectrum, and vice versa.

The average period between zero upcrossings was determined by equation (155), and the number between zero upcrossings per unit time is

$$N_z^R = \frac{1}{2\pi}\sqrt{\frac{m_2^R}{m_0^R}}\,, \tag{208}$$

where m_0^R, m_2^R are the moments of the particular response R, whose spectral density is given by (207). Equation (208) can be generalized for the case of the average number of upcrossings above a specified level α as in

$$N_{z,\alpha}^R = \frac{1}{2\pi}\sqrt{\frac{m_2^R}{m_0^R}}\exp\left(-\frac{\alpha^2}{2m_0^R}\right)\,. \tag{209}$$

Equation (209) can be utilized to determine such events as propeller emergence, deck wetness, and bow slamming. If f represents the available freeboard (see Figure 31) at the wetness station (say Station 1), the number of deck wetness events per hour is

$$N_p = 3600\cdot\frac{1}{2\pi}\sqrt{\frac{m_2}{m_0}}\exp\left(-\frac{f^2}{2m_0}\right)\,, \tag{210}$$

where m_0, m_2 are the moments of the vertical relative motion spectrum at Station 1. Naturally, we can use a different parameter in equation (210), for instance $f' = 1.25f$ and find how often there will be excessive water on deck. The same equation can be used to estimate the frequency of propeller racing, with f substituted by the depth at the propeller h. Of course, m_0, m_2 are now the moments of the relative motion spectrum at the propeller. A similar equation can be used to evaluate the frequency of bow slamming in a seaway. For bow slamming to occur two things must happen simultaneously: the ship bottom at the slamming station (say Station 1) must be out of the water and the relative velocity of the ship bottom must exceed a certain threshold U_{th}, which is usually determined by experience. In this case, the number of bow slammings per hour is given by

$$N_{sp} = 3600\cdot\frac{1}{2\pi}\sqrt{\frac{m_2}{m_0}}\exp\left[-\left(\frac{H^2}{2m_0}+\frac{U_{th}^2}{2m_2}\right)\right]\,, \tag{211}$$

where m_0, m_2 are the moments of the vertical relative motion spectrum at the slamming station.

Equation (210) is based on the fact that the probability of event 1 to exceed the threshold value f_1 is

$$P_1 = \exp\left(-\frac{f_1^2}{2m_{0,1}}\right)\,, \tag{212}$$

where $m_{0,1}$ is the area under the spectrum of event 1. Equation (211) is based on the fact that the probability that two statistically independent events 1 and 2 exceed the thresholds f_1 and f_2, respectively is

$$P_{1,2} = P_1 P_2 = \exp\left[-\left(\frac{f_1^2}{2m_{0,1}} + \frac{f_2^2}{2m_{0,2}}\right)\right] , \tag{213}$$

and

$$m_{0,\text{velocity}} = m_{2,\text{motion}} , \tag{214}$$

$$m_{0,\text{acceleration}} = m_{4,\text{motion}} . \tag{215}$$

This is because the spectrum of the derivatives of a random process is given in terms of the spectrum of the process by

$$S^{(n)}(\omega) = \omega^{2n} S(\omega) . \tag{216}$$

In case where the ship has a nonzero forward speed equation (207) is still valid with the frequency of encounter ω_e substituted for ω

$$S_R(\omega_e) = Z_R^2(\omega_e) S(\omega_e) . \tag{217}$$

Now the RAO spectrum of the response $Z_R(\omega_e)$ is derived precisely at the frequency of encounter, while the spectrum of the seaway is known as $S(\omega)$ at the original frequency ω. We can convert $S(\omega)$ to $S(\omega_e)$ by noting that the energy of the seaway must remain unchanged regardless of whether is viewed from a stationary point or from a moving ship, in other words

$$S(\omega)\, d\omega = S(\omega_e)\, d\omega_e . \tag{218}$$

Using equation (218) and the definition for the frequency of encounter (181), we can write equation (217) as

$$S_R(\omega_e) = Z_R^2(\omega_e) S(\omega) \left(1 - \frac{2\omega}{g} U \cos\theta\right)^{-1} . \tag{219}$$

The process by which $S(\omega)$ is transformed to $S(\omega_e)$

$$S(\omega_e) = S(\omega) \left(1 - \frac{2\omega}{g} U \cos\theta\right)^{-1} , \tag{220}$$

is schematically depicted in Figure 32 for the case of head ($\theta = 180^o$) and following ($\theta = 0^o$) seas.

3.4 Computational aspects.

Obtaining the RAO of a ship in regular waves is a relatively easy task, provided the body added mass and damping coefficients, and the exciting forces and moments are known as functions of frequency of motion. Computation of these coefficients is the most difficult part of the problem. As we mentioned in Section 3.1, a popular solution technique is the *strip theory.*

While the details of the mathematical formulation of strip theory are still being debated, the physical motivations are relatively easy to describe. First, it must be assumed that the ship is a slender body (i.e., its beam and draft are much less than the length and changes in cross section vary gradually along the length). Restricting the discussion to zero forward speed and high frequencies, we would find that the fluid flow velocities in the transverse direction are much greater than the longitudinal direction. Consequently, the flow field at any cross section of the ship may be approximated by the two dimensional flow in that "strip". To obtain the total effect on the ship, the effects of each strip are integrated along the length. For example, the strip theory approximation for the heave added mass is

$$A_{33} = \int_L a_{33}(x)\, dx \ , \tag{221}$$

where $a_{33}(x)$ is the two dimensional added mass, and L denotes that the integration is over the entire ship length. Expressions similar to (221) were presented in the table on page 203 for heave and pitch motions. The sectional added mass, a_{33}, is computed by solving a two dimensional hydrodynamic problem. The essence of strip theory is thus to reduce a three dimensional hydrodynamic problem to a series of two dimensional problems which are easier to solve.

For low frequencies and ships with forward speed the strip theory approximation is no longer straight forward and different initial assumptions lead to different formulations. A mathematically consistent analysis using slender body theory has revealed that the leading order terms involve only the zero speed pure strip theory coefficients. The effects of forward speed are of a slightly higher order and are present only in the cross coupling coefficients.

The key to a successful strip theory computer program for ship motions is to have a good method to solve the corresponding two dimensional problem, the evaluation of integrals such as (221) is trivial. In ship hydrodynamics the two most popular methods for solving the two dimensional problem are boundary integral and multipole methods.

A typical boundary integral method is Frank's method which consists of dividing the ship section into a series of straight line segments. Over each segment fluid sources with constant, but unknown, strengths are distributed. The form of the source potential is chosen so that the boundary conditions on the free surface and at infinity are met. The unknown source strengths are found by satisfying the body boundary conditions at the center point of each segment. Knowing the source strength, the velocity potential can be found, and the sectional added mass and damping coefficients by appropriate integrations around the section.

The advantages of Frank's method are that it is computationally fast and any ship cross section can be approximated with as much accuracy as desirable. Typically, 8 to 10 segments on a half section are enough to get accurate added mass and damping coefficients for heave and pitch motions. Slightly more segments seem to be needed for the transverse motions, particularly for roll. The primary disadvantage of Frank's method is the presence of the so called irregular frequencies. Most of the boundary integral methods are plagued by irregular frequencies when the cross section penetrates the free surface. The irregular frequencies are a set of discrete frequencies at which the solution obtained from the boundary integral method is not unique or "blows up". For most ship types the irregular frequencies are often above the range of practical interest. However, for certain section types such as transom sterns or offshore transport barges, the irregular frequencies can cause calculation difficulties. Several

techniques for circumventing the problem of the irregular frequencies have been proposed, and research in the subject is continuing.

The multipole method consists of the superposition of potential functions that all satisfy the Laplace equation, the free surface boundary condition, and the condition at infinity. The potential functions represent a source and dipole at the origin, which give the radiated waves at infinity, and a series of multipole potentials that die off rapidly as one moves away from the origin. The strengths of the source, dipole, and multipoles are all determined such that the body boundary condition is met. The problem can be solved for the circular section case, and for sections that are not circular in shape conformal mapping is used. In conformal mapping the actual section is mapped through a change in variables in a circular section, the problem is solved there, and then the solution is transferred back to the original section through the inverse mapping. The difficulty of the technique here is to determine the appropriate mapping function for each section. The most common mapping uses the so called Lewis forms. This uses a two parameter mapping function based on the sectional beam to draft ratio, $B(x)/T(x)$, and the sectional area coefficient $\beta_n = S(x)/(T(x)B(x))$. Lewis forms turn out to be ship–like, and the principal dimensions of each section (beam and draft) and its sectional area (and hence the ship's displacement) remain the same through the transformation. Figure 33 shows the section shapes for various Lewis sections for different beam to draft ratios and sectional area coefficients. In the same figure it can be seen how well Lewis forms approximate the sections of a Mariner–type hull. Note that most of the stations are fairly well approximated. The bottom is not exactly flat, but this makes little difference in the added mass and damping. The bulb sections near the bow and the wine glass sections near the stern are not well approximated, however.

Lewis forms cannot fit all ship sections. For any given beam to draft ratio there is a permissible range for the sectional area coefficient. For ship sections outside of the permissible range, modifications must be made. Some ship motions programs artificially modify B/T or β_n until it fits into the range. This may sound alarming, but for strip theory calculations this approach is not too bad because the final computed motions are hardly affected. Another approach is to alter the mapping function slightly to give a different section shape for the same two parameters. Such a modification exists and is used for mapping bulbous–type sections. A different technique involves the use of a third parameter in the family, the local centroid of each section. We have then a three parameter extended Lewis family which can map either U or V–shaped sections for the same area and beam to draft ratio. An example of this extended Lewis family is shown in Figure 34 where two extreme variations of the same parent hull for a general purpose corvette are created with the same section dimensions and areas and different values of the vertical center of buoyancy. This allows comparative studies of changes in the underwater hull geometry while keeping the ship's displacement the same.

In summary, Frank's method and conformal mapping techniques are the two most common approaches to computing the two dimensional coefficients for use in strip theory. Of course it should be borne in mind that in all of these models the problem is formulated in the frequency domain leading to equations that have meaning only if the body motions are sinusoidal in time. In more general situations, such as a ship performing a maneuver with varying speed, the frequency domain approach is meaningless. An alternative approach here is to formulate the problem directly in the time domain. The flow created by the body motions is represented by a singularity (source and sink) distribution on the body surface.

The body surface is usually approximated by an ensemble of plane quadrilateral elements of constant strength. The resulting integral equations are satisfied at selected collocation points giving a system of algebraic equations for the singularity strengths. The technique is used to compute the impulse response function of the body, and then the dynamic equations of motion can be solved for any initial conditions or excitation by convolution. As a closing remark of this section, we must point out a rather important peculiarity of the problem. Since the ultimate goal is to find the hydrodynamic forces on the hull, we only need the values of the velocity potential and its derivatives on the hull (this through Bernoulli's equation will yield pressures and when integrated forces and moments). The values of the velocity potential inside the fluid domain are of no immediate interest as far as ship motions are concerned. This feature combined with the fact that the fluid domain may well extend to infinity explains why finite difference or finite element techniques are rarely used in this type of problem. What is considered more efficient is replacing the body by a suitable distribution of source singularities.

3.5 Seakeeping considerations in design.

Unfortunately, seakeeping design is not generally carried out well, if any attention is given to it at all in a preliminary design phase. There is no excuse for this situation, as the tools are at hand to do an excellent job. Furthermore, a preliminary investigation of the seakeeping qualities of a ship at a given sea environment does not demand a geometric hull description as accurate as other aspects of ship design, for example hydrostatic calculations. Using for example Lewis forms, all that one needs is sectional beams, drafts, and areas; the particular geometry associated with these quantities being of no interest. There is no reason for there to ever be any surprise in the seakeeping qualities of a ship. The experimental and computational tools, while having some important deficiencies, are sufficiently advanced so that the designer can can have a clear idea of the seakeeping qualities of his ship. Further, he can direct his design in the very critical early stages in such a way as to avoid some of the most serious problems. The subject of "Design for seakeeping" can be roughly divided into three areas:

- Habitability
- Operability
- Survivability

Habitability is concerned with providing the crew with an environment which permits them to function effectively and without performance degrading. *Operability* may include some spects of habitability, but the concern here goes further: the ability of the ship with all of its mechanical equipment to be operated by the crew to carry out the assigned mission in the ocean environments in which it is expected to function. This includes such things as gun accuracy, helicopter take–off and landing operations, keeping instruments operating, towing devices for oceanographic research, ensuring the safety of deck equipment, holding course in quartering seas, and so on. *Survivability* takes us beyond operability. It is concerned with what happens to the ship when conditions become so rough that the ship or any of its major

subsystems is in danger of damage or destruction. The environment is now one of those very severe storms (or Exocets) that a ship sees only once or twice in its lifetime. Habitability is no longer a factor of primary concern and operability is important only with respect to the most essential subsystems.

Even though these three qualities are quite different in nature, they are all affected by the following:

- Average or characteristic motions in all 6 degrees of freedom.
- Characteristic accelerations in all 6 degrees of freedom.
- Extreme motions and accelerations.
- Increase in required power.
- Green water and spray.
- Stability on course including tendency to broach.
- Slamming and slamming loads.
- Hull girder bending moments.
- Wave induced vibrations.
- Local sea loads.
- Hull deflection.
- Propeller racing and tail shaft loading.

The list is quite extensive and every item has its own effect. As an example, standard NATO criteria for comparative assessment of frigate seakeeping qualities in joint operations, with regard to helicopter operations are shown in Fig. 36.

The criteria levels for continuous responses are given as significant single amplitudes. It can be seen that each of the items in the table can be calculated according to the discussion in the previous sections. The results are usually presented in the following form: Suppose that the ship will be operating in a sea environment characterized by a significant wave height and a certain modal period, so that the sea spectrum is defined. For all around the clock ship headings and for ship speeds up to 30 knots, a polar plot similar to the one in Figure 35 is prepared. The shaded areas in the plot show that one or more of the performance criteria is exceeded. Letting the polar area of the disk in the figure be A_0 and the subset of A_0 within which the ship can conduct helicopter operations be A, a performance index characterizing the ability of the ship to perform this specific operation in the specified sea condition can be defined by $100(A/A_0)$. For the case of the figure, this performance index is 44%. Such computations can be performed for different sea spectra, for example varying the significant wave height within the observed limits for the particular area. The performance indices can then be added (in a weighted sum to account for the probability of occurrence of a particular wave height in the area) so that a combined performance index is obtained.

If this is repeated for a number of different ships or design options, an optimal hull with respect to some critical seakeeping related operation can be obtained. It should be clear now that such computations can be routinely performed using the principles in the previous sections and a good regular waves hydrodynamics solver.

Assuming that the designer can establish acceptable ranges for the parameters of his design, it is possible for him to determine at a very early stage what the range in seakeeping qualities will be, and what influence he can exert over these qualities. There are three critical phases in the design process, which are:

1. The definition of the environment in which the ship is expected to operate.

2. Establishing quantitative and qualitative requirements for seakeeping performance based on the intended mission of the ship.

3. The evaluation of the design to establish whether or not it meets the requirements, and to modify the design if it should become necessary.

Most ships are expected to operate in a relatively well defined portion of the ocean, and sea statistics are generally available throughout the world. The conversion of the mission profile for a ship design into hard quantitative and qualitative measures, such as those presented in the previous table, is one of the most difficult problems the ship designer will face. Not only experience is limited here, but people and weapon systems change all the time, which makes the establishment of universally accepted criteria a task next to impossible. Fortunately, for comparative evaluations this does need to be exact. The evaluation of the design can only be performed by taking into account the crucial operational restrictions and specifications of the ship and its mission. As an example, suppose that the Navy needs a small aircraft carrier intended to have as its primary operating area the waters between northern Great Britain and Iceland. Assume that the hull shape and size have been selected and the designer is concerned with one final problem, the plan form of the flight deck. Because of the small size of the carrier, space on the flight deck is at a premium, and the operators consider that the carrier will be far more usable if the flight deck maintains its midship width all the way to the bow. However, this would imply a very large flare at the bow and suggests that flare slamming could affect both operability and survivability. The designer has the option of tapering the flight deck in order to reduce the flare at the bow and greatly reduce the danger of damage if slam occurs. Tapering is clearly a solution to slamming, but would not be accepted by the operators unless they are convinced that the rectangular plan form would seriously compromise the ship. Deck operations is not the only reason for keeping an amount of bow flare, though. A sufficient amount of flare is helpful in deflecting water outward as the bow moves downward into a wave to decrease the occurrences of deck wetness and to increase effective freeboard. The final form of the flight deck in this case would have to be determined from a rational examination of which criterion is the most limiting factor in the particular sea environment.

Besides ship motions, another factor that influences the behavior of a ship in waves is the speed loss. Speed loss in waves takes one of the two forms that are schematically shown in Figure 36. The involuntary speed reduction is due to the added drag in waves and the decrease in propulsive efficiency due to the interactions of the propulsor and the waves. The

attainable speed of large low–powered ships in rough seas is determined primarily by this involuntary speed reduction. In fact, large supertankers are usually slowed down sufficiently by rough seas to avoid problems of severe motions. But for moderate to high–speed ships there is also a voluntary speed reduction related to ship motions. Figure 36 shows how attainable speed varies with head seas of different significant wave heights. It illustrates both the involuntary speed reduction, caused by added required power and reduced available power, and the voluntary speed reduction caused by slamming (at the lighter draft) and by deck wetness (at the deep draft).

An easy to compute in a preliminary design stage index which ranks destroyer type hulls with regards to their seakeeping behavior is Bales' seakeeping rank estimator, R. The basis for this is that ship motions are not usually very sensitive to details of the ship form. Section characteristics as used in strip theory are essentially determined by beam, draft, and area. The actual shape of the section has only secondary significance. Therefore, quite crude representations of the section shape can result in good estimates of ship behavior in waves. In the seakeeping rank estimator only a few crucial parameters are used to tie down the magnitude of the ship motions. These parameters in dimensionless form are:

1. Waterplane coefficient forward of amidships, $C_{WF} = 2A_{WF}/LB$.
2. Waterplane coefficient aft of amidships, $C_{WA} = 2A_{WA}/LB$.
3. Draft to length ratio, T/L.
4. Cut–up ratio, c/L, where c is the distance from the forward perpendicular to the cut–up point, typically close to the stern.
5. Vertical prismatic coefficient forward of amidships, $C_{VPF} = V_F/A_{WF}T$.
6. Vertical prismatic coefficient aft of amidships, $C_{VPA} = V_A/A_{WA}T$.

By a systematic series of numerical calculations and experiments, the following expression for R was established

$$\begin{aligned} R &= 8.422 + 45.104C_{WF} + 10.078C_{WA} - 378.465(T/L) + 1.273(c/L) \\ &\quad -23.501C_{VPF} - 15.875C_{VPA} \, . \end{aligned}$$

A value of R close to 10 corresponds to the best hull from the seakeeping point of view and a value close to 1 for the worst. Although the seakeeping rank estimator does not substitute detailed calculations it might be useful as a tool in preliminary design for destroyers, light cruisers, and frigates. Naturally, a seakeeping optimal hull may be far from an overall successful design, for its still water resistance for instance may be too high. Nevertheless, seakeeping *is* a very important factor in an overall ship design methodology as is evident by the many ships that have become white elephants because they cannot perform their missions effectively due to a deficiency in seakeeping qualities.

LIST OF FIGURES

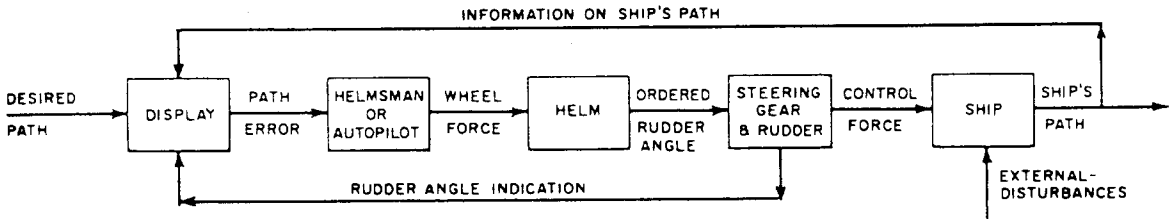

Figure 1: Ship controllability and maneuverability loop.

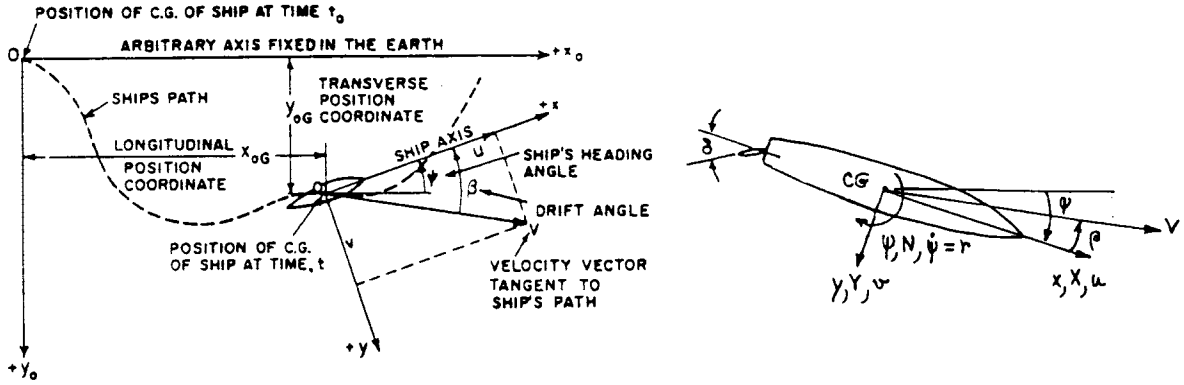

Figure 2: Orientation of fixed axes and moving axes.

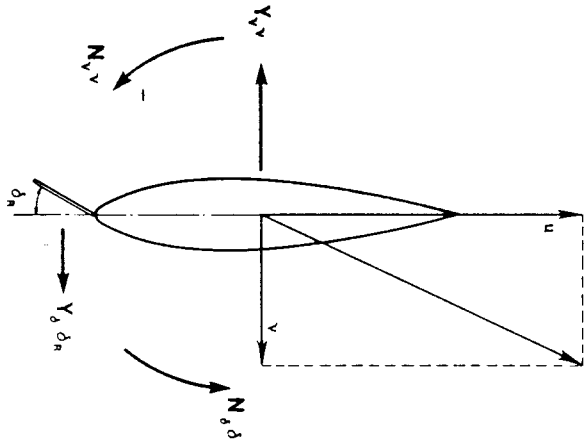

Figure 3: Rudder induced forces and moments.

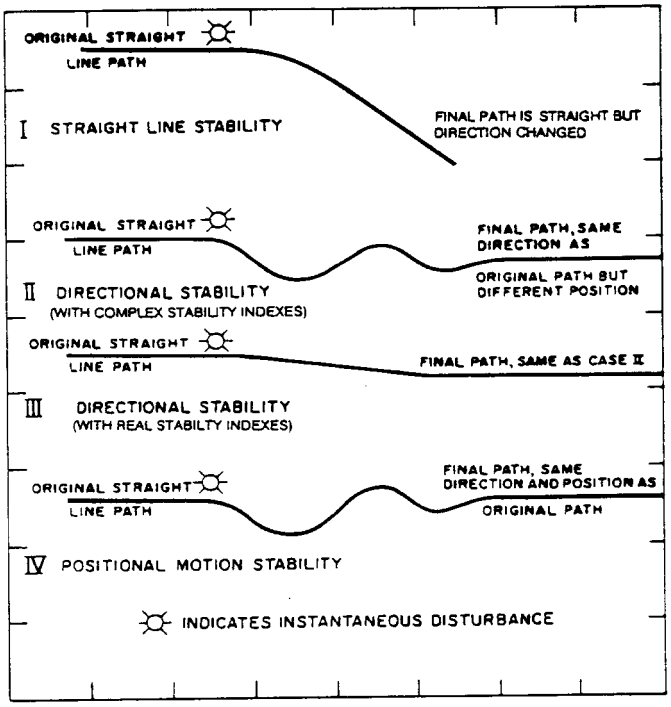

Figure 4: Various kinds of motion stability.

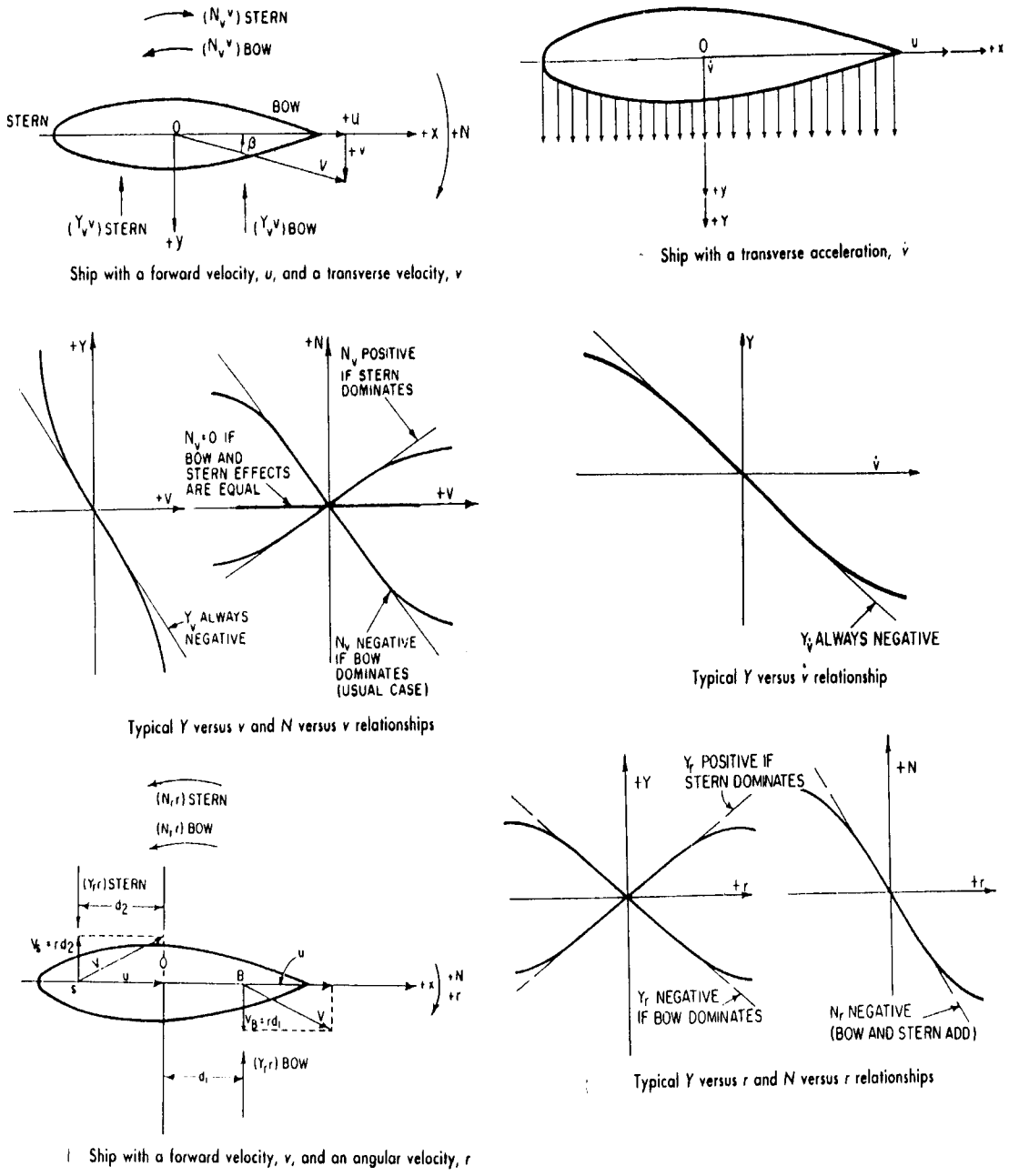

Figure 5: Explanation of signs of hydrodynamic derivatives.

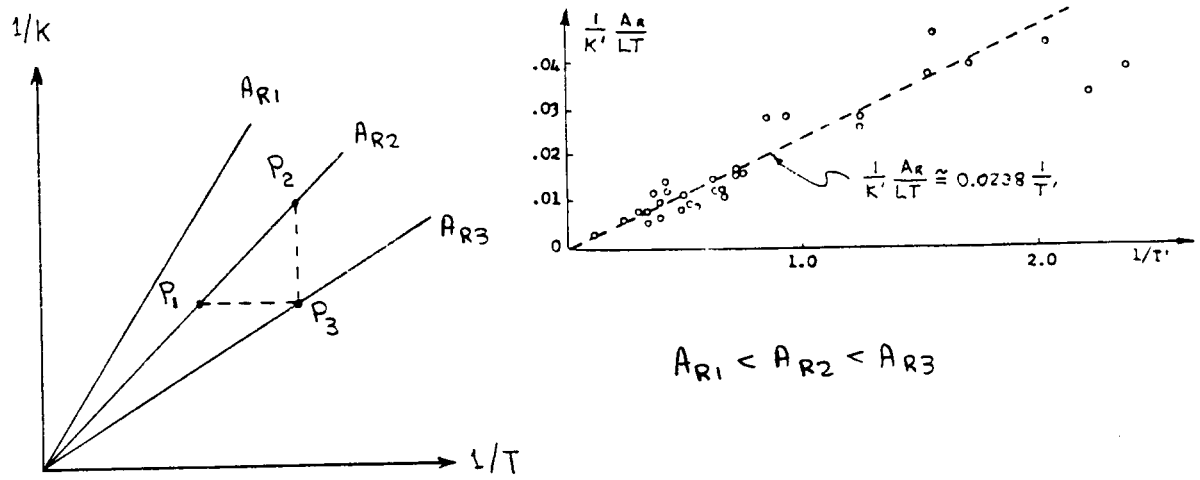

Figure 6: K–T diagram.

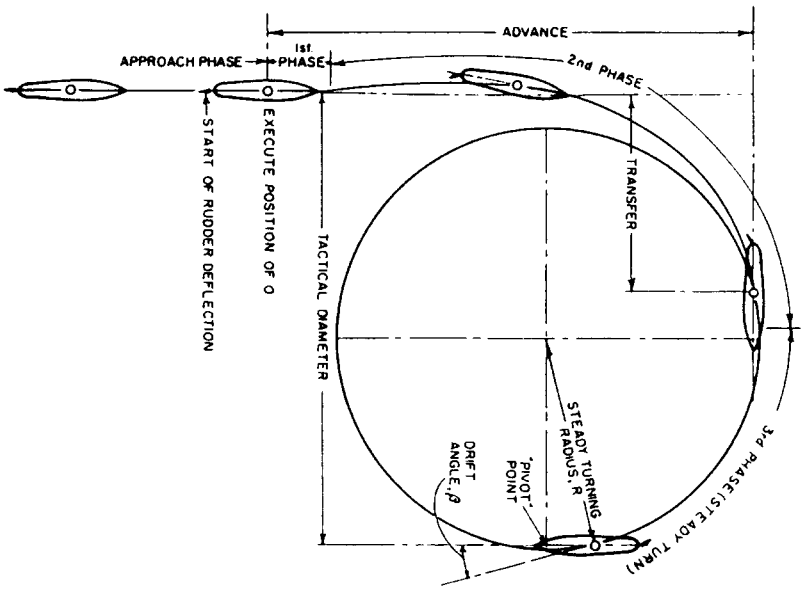

Figure 7: Turning path of a ship.

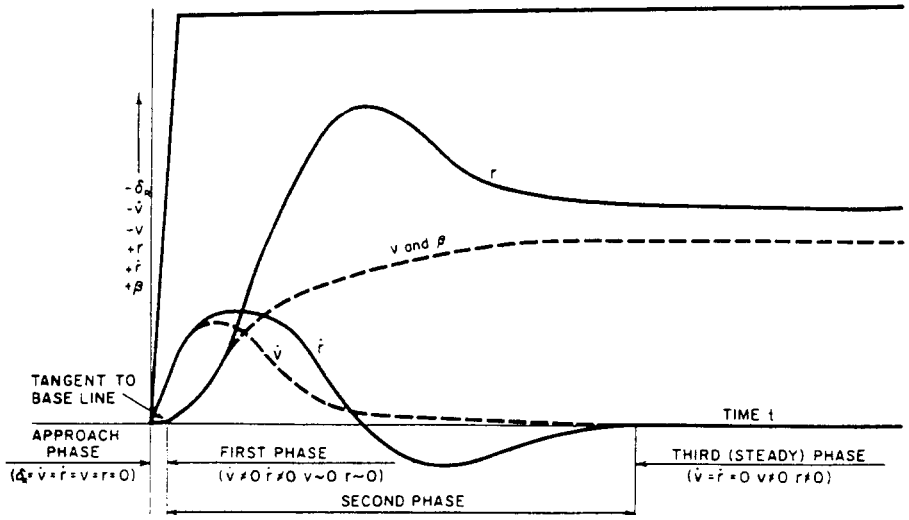

Figure 8: The three phases of a turn.

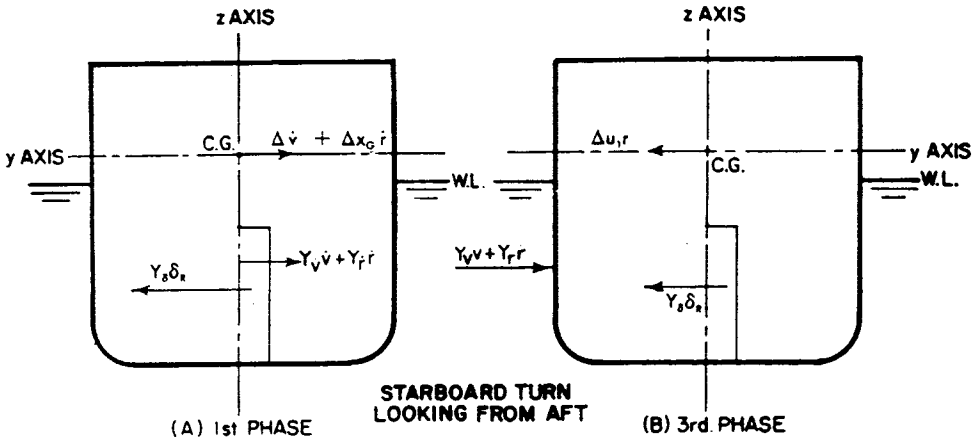

Figure 9: Forces in the yz–plane in a turn.

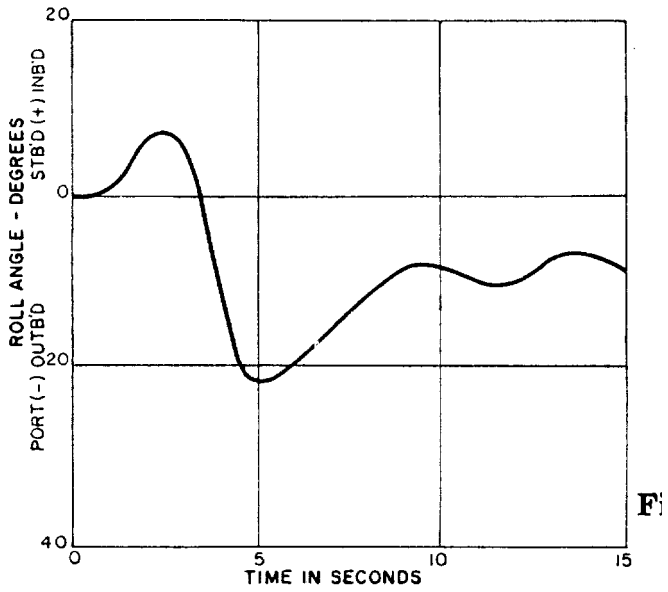

Figure 10: Heel angle for a starboard turn.

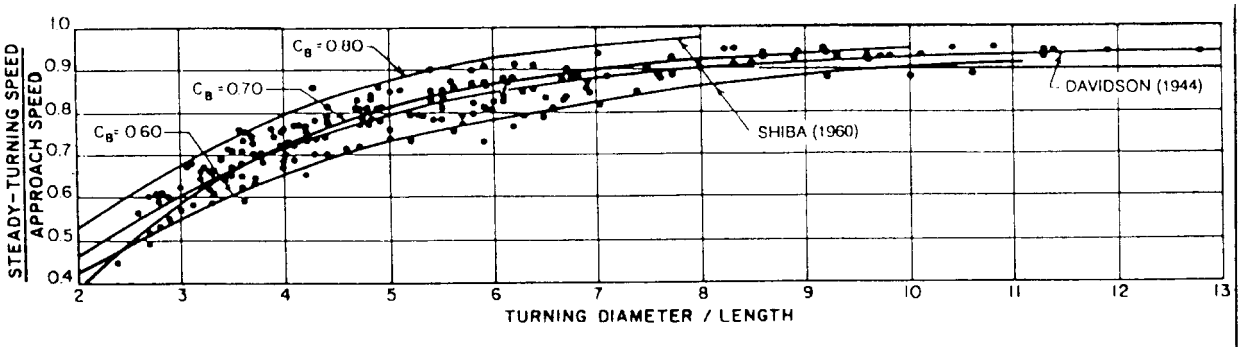

Figure 11: Speed reduction in a turn.

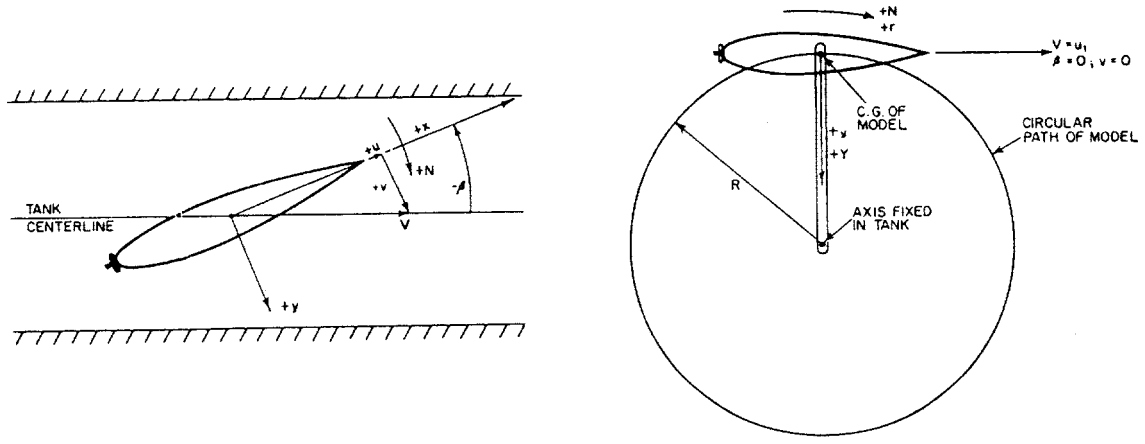

Figure 12: Straight line and rotating arm model tests.

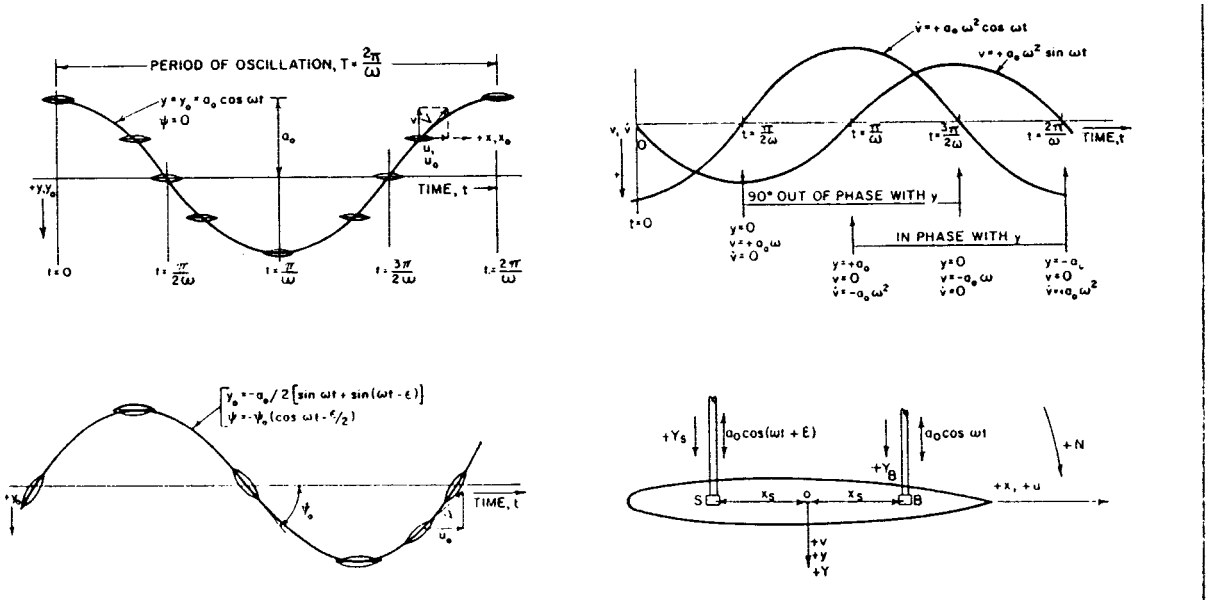

Figure 13: Planar motion mechanism tests.

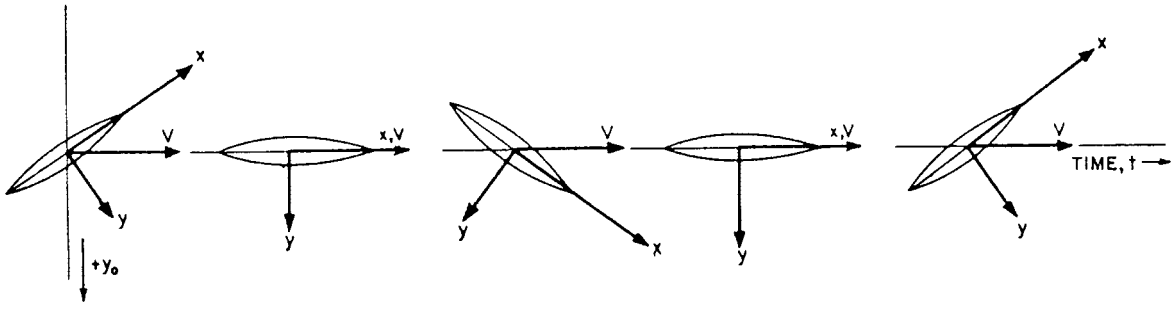

Figure 14: Oscillator tests.

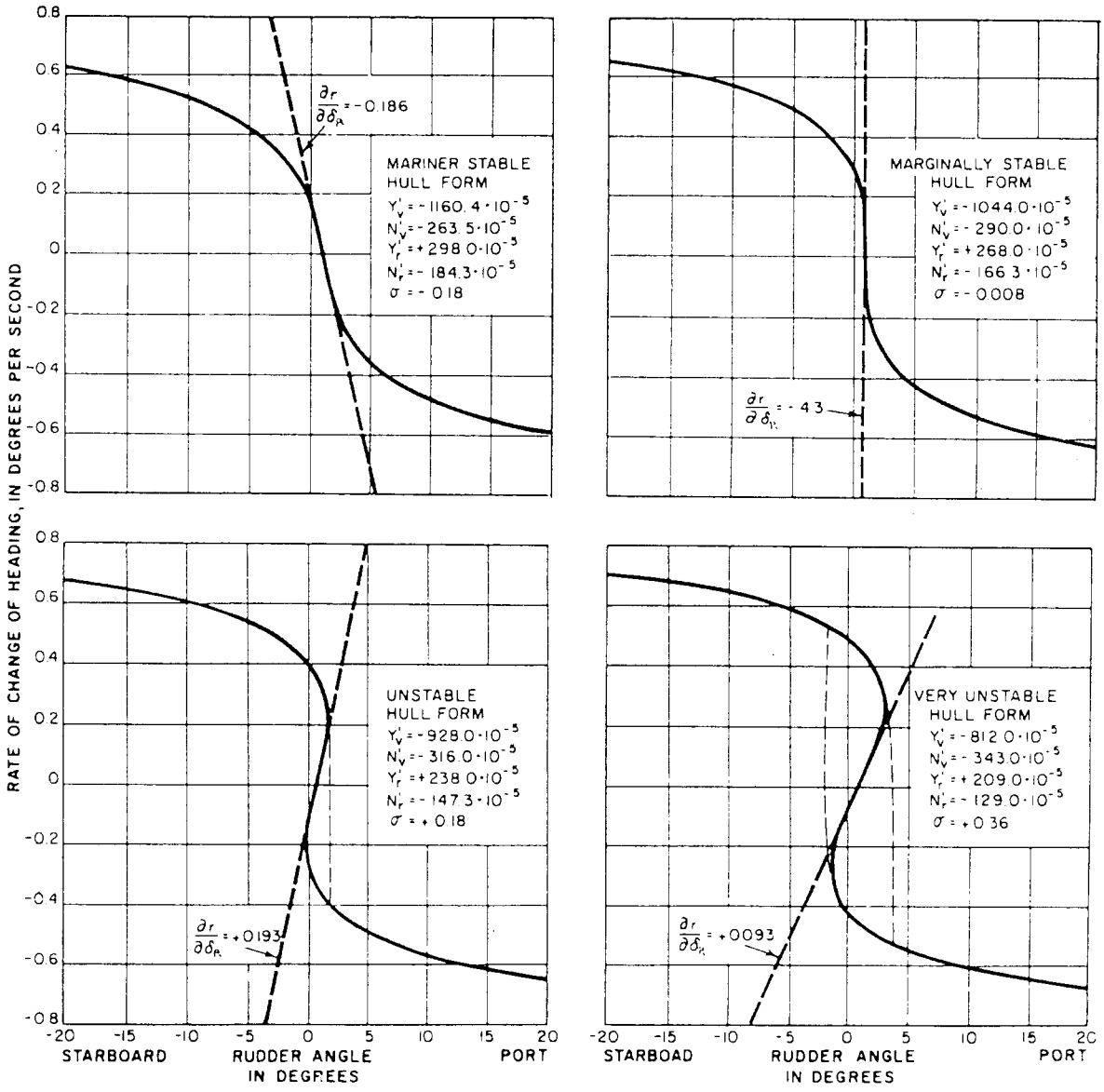

Figure 15: Spiral test maneuver results.

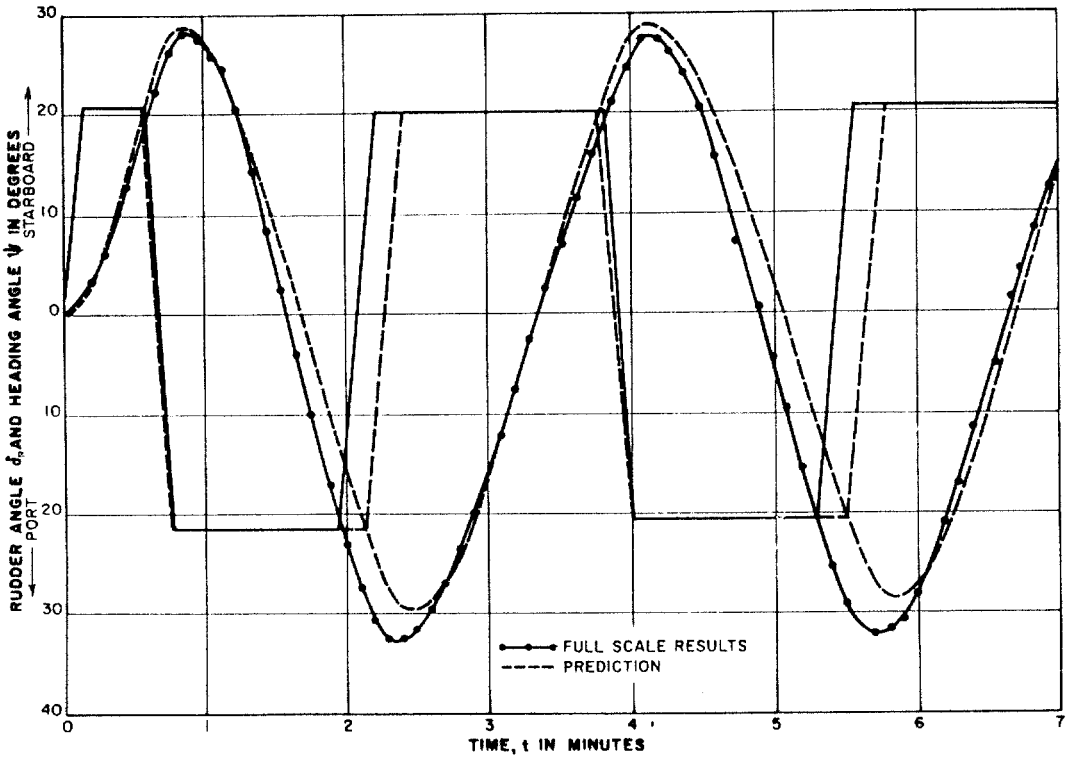

Figure 16: Zig–zag maneuver.

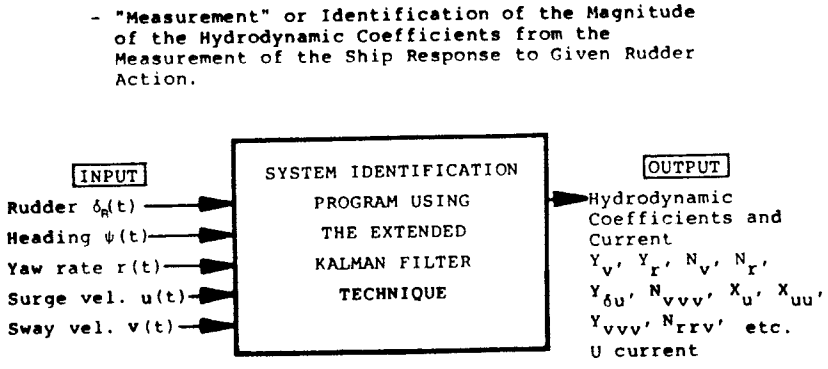

Figure 17: System identification.

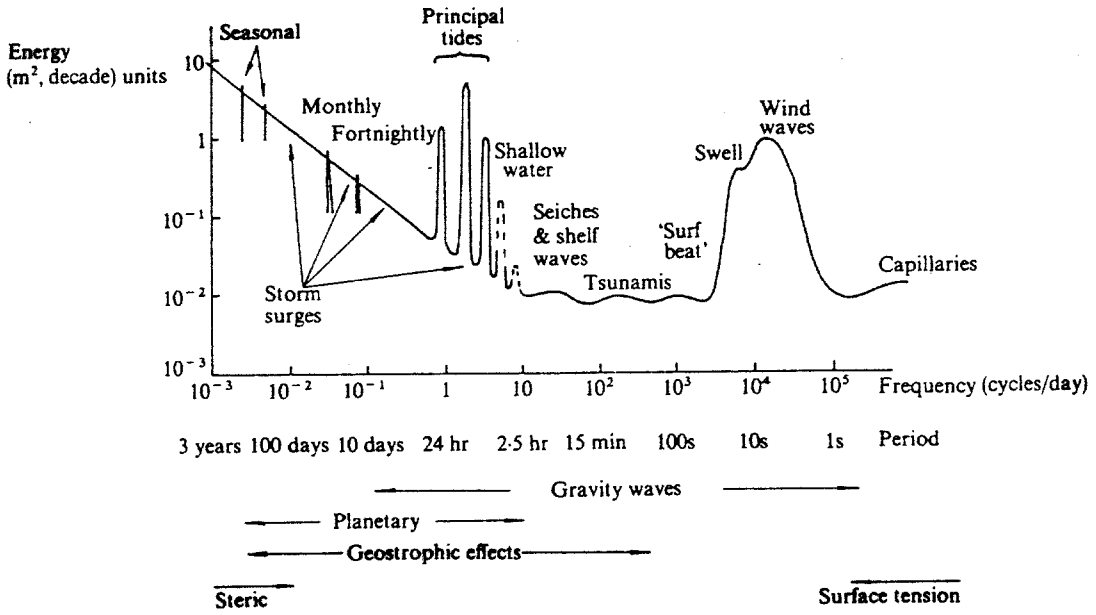

Figure 18: Energy versus frequency characteristics of wave systems.

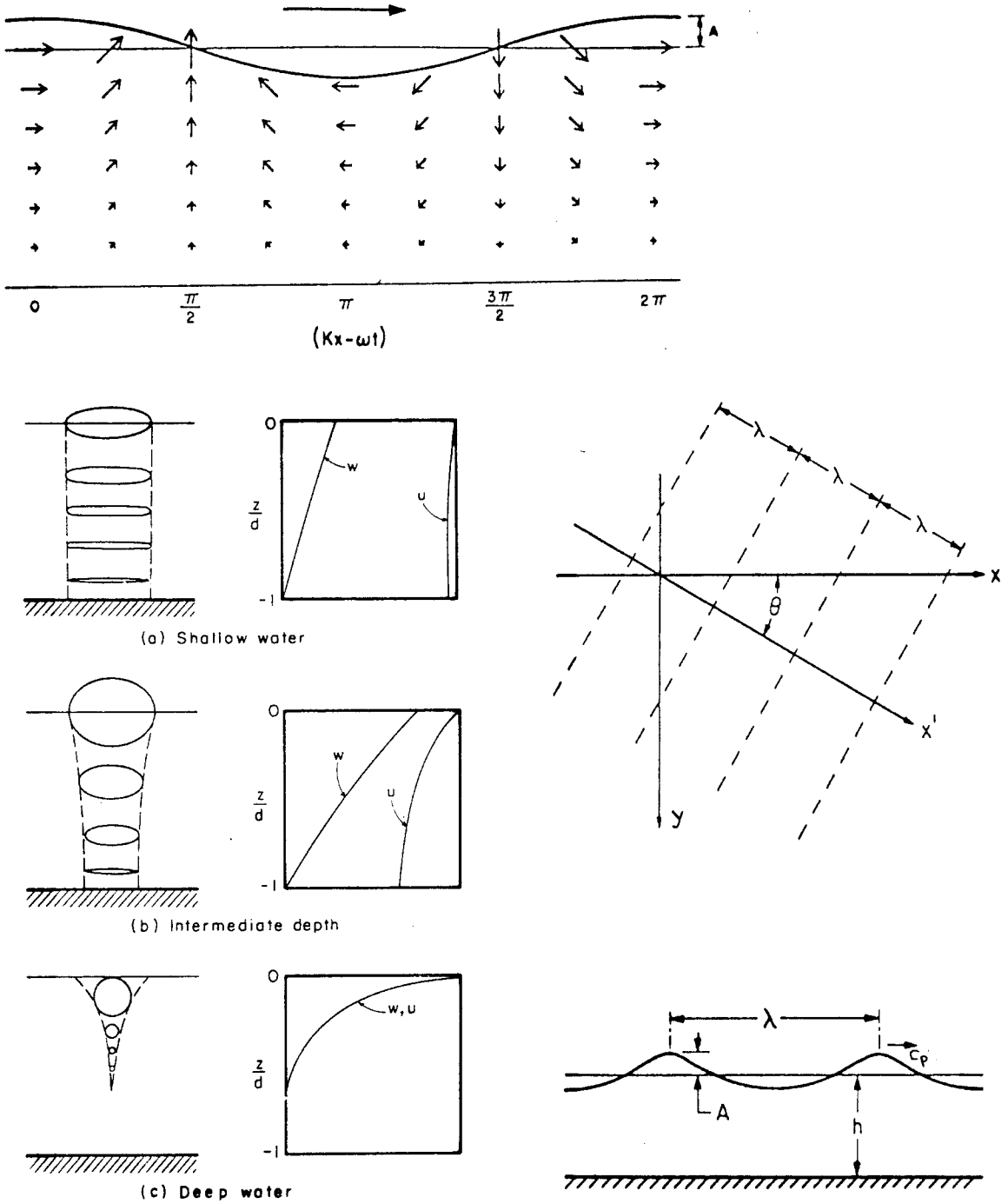

Figure 19: Definitions and velocity fields in waves.

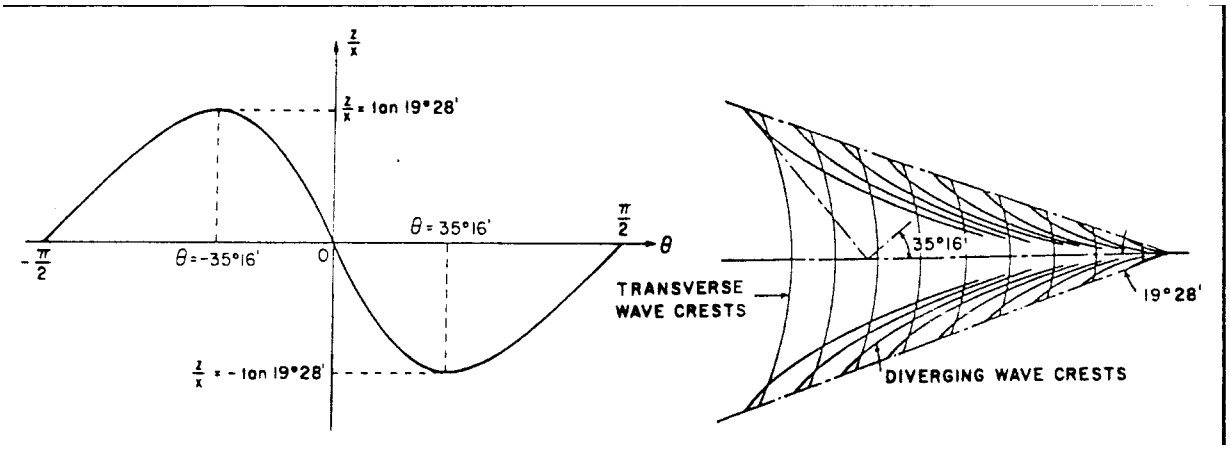

Figure 20: The Kelvin ship wave system.

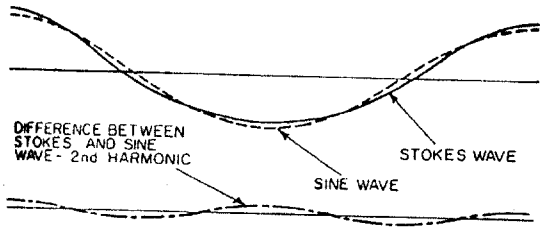

Figure 21: Sine wave and Stokes wave.

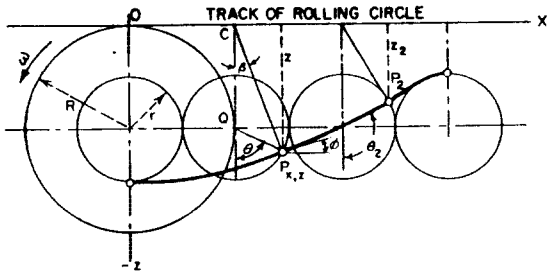

Figure 22: Trochoidal wave.

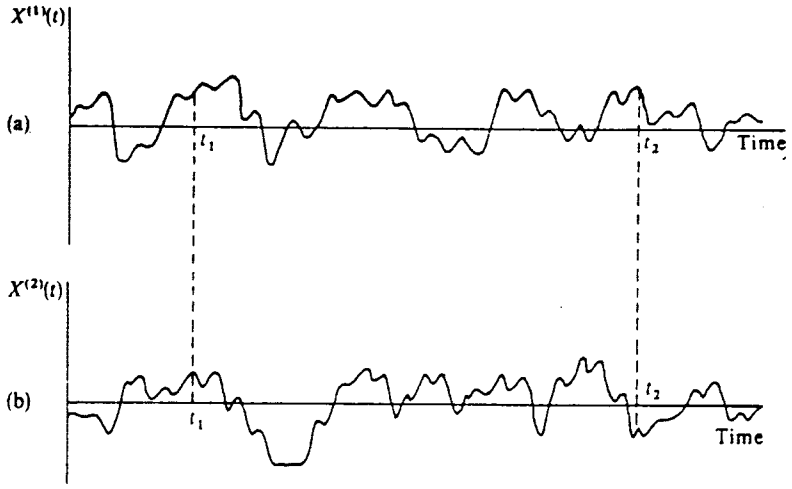

Figure 23: Two realizations of a random process.

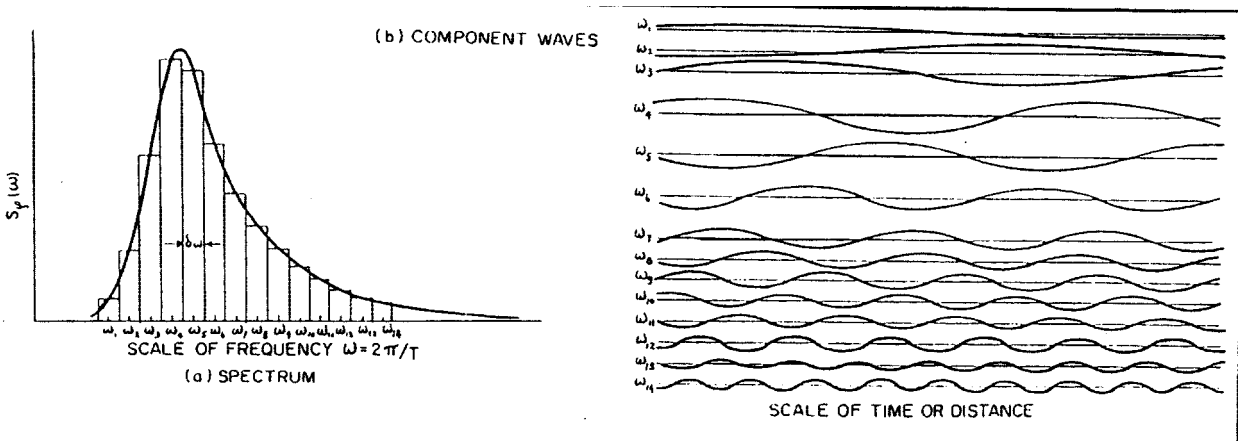

Figure 24: Typical spectrum of waves with individual components.

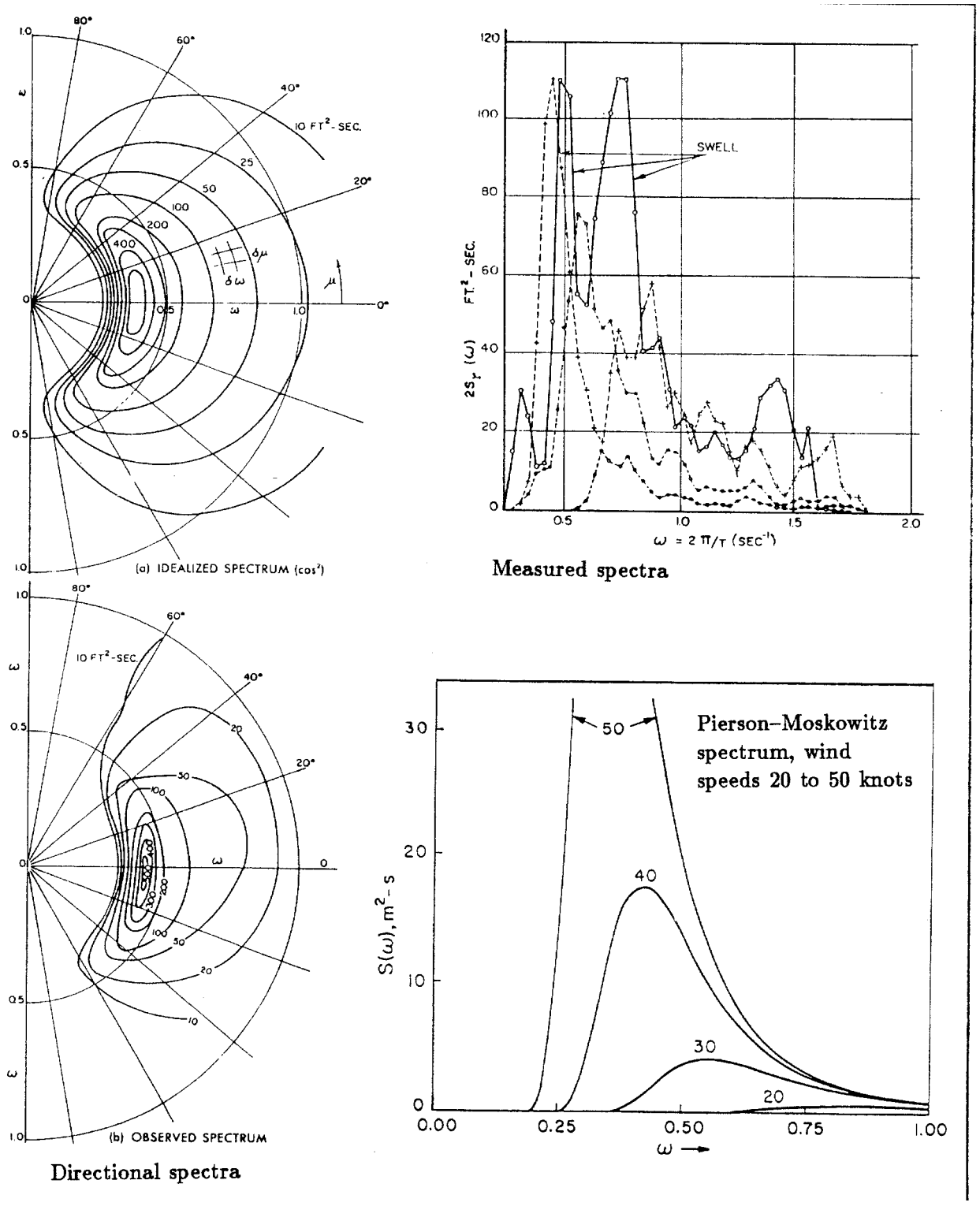

Figure 25: Typical sea spectra.

Wind Speed (knots)	Sea State (approx.)	Significant Wave Height (meters)	Average Period (seconds)	Average Wavelength (meters)
10	2	0.6	2.7	22
20	4	2.2	5.3	89
30	6	5.0	8.0	200
40	7	8.9	10.7	355
50	8	13.9	13.4	554

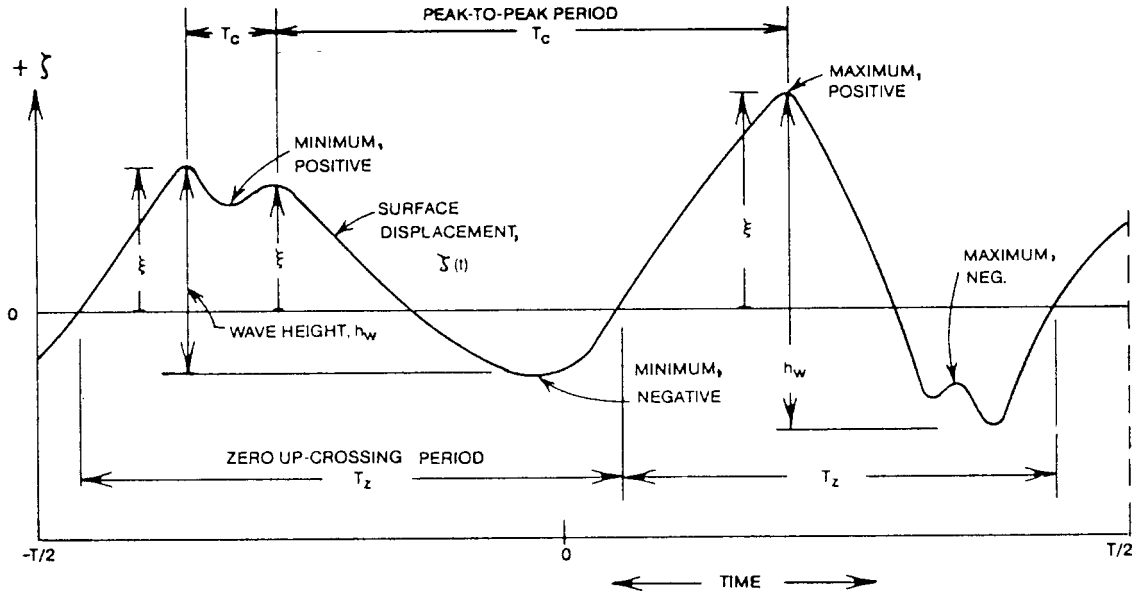

Figure 26: Typical wave record at a fixed point.

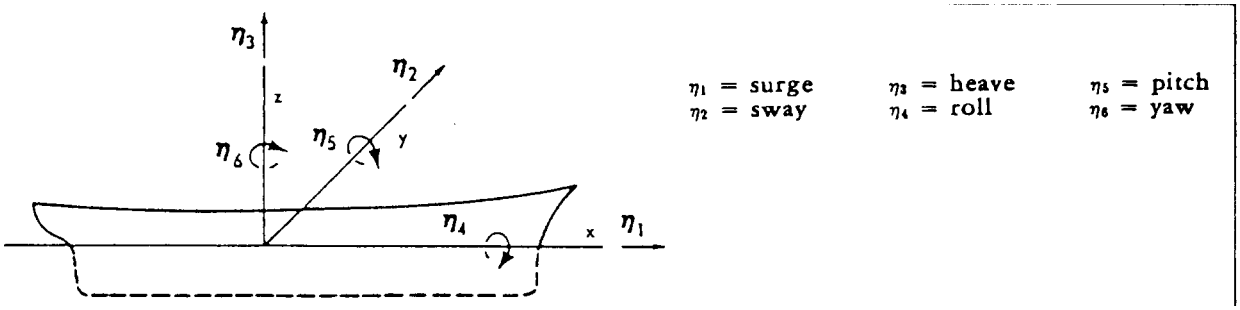

Figure 27: Definition sketch of body motions in six degrees of freedom.

$$A_{33} = \int a_{33}\, dx \qquad B_{33} = \int b_{33}\, dx$$

$$A_{35} = -\int x\, a_{33}\, dx - \frac{U_0}{\omega_e^2} B_{33} \qquad B_{35} = -\int x\, b_{33}\, dx + U_0\, A_{33}$$

$$A_{53} = -\int x\, a_{33}\, dx + \frac{U_0}{\omega_e^2} B_{33} \qquad B_{53} = -\int x\, b_{33}\, dx - U_0\, A_{33}$$

$$A_{55} = \int x^2\, a_{33}\, dx + \frac{U_0^2}{\omega_e^2} A_{33} \qquad B_{55} = \int x^2\, b_{33}\, dx + \frac{U_0^2}{\omega_e^2} B_{33}$$

$$C_{33} = \int c_{33}\, dx = \rho g \int B(x)\, dx$$

$$C_{35} = C_{53} = -\int x\, c_{33}\, dx = -\rho g \int x\, B(x)\, dx$$

$$C_{55} = \rho g \nabla \overline{GM}_L + LCF^2\, C_{33} \approx \int x^2\, c_{33}\, dx = \rho g \int x^2\, B(x)\, dx$$

$$F_{EX_3} = \overline{\zeta} \int_L e^{ikx}\, e^{-kT^*(x)} \left[c_{33} - \omega_0(\omega_e\, a_{33} - ib_{33})\right] dx$$

$$F_{EX_5} = -\overline{\zeta} \int_L e^{ikx}\, e^{-kT^*(x)} \left[x\left(c_{33} - \omega_0(\omega_e\, a_{33} - ib_{33})\right) - \frac{U_0}{i\omega_e}\, \omega_0\, (\omega_e\, a_{33} - ib_{33})\right] dx$$

where:

a_{33} is the sectional heave added mass
b_{33} is the sectional heave damping
c_{33} is the sectional restoring force $= \rho g\, B(x)$
$B(x)$ is the sectional waterline beam
$S(x)$ is the sectional area
$T^*(x)$ is the mean sectional draft or $\dfrac{S(x)}{B(x)}$
$\overline{\zeta}$ is the incident wave amplitude

Figure 28: Expressions for the coefficients in the equations of motion.

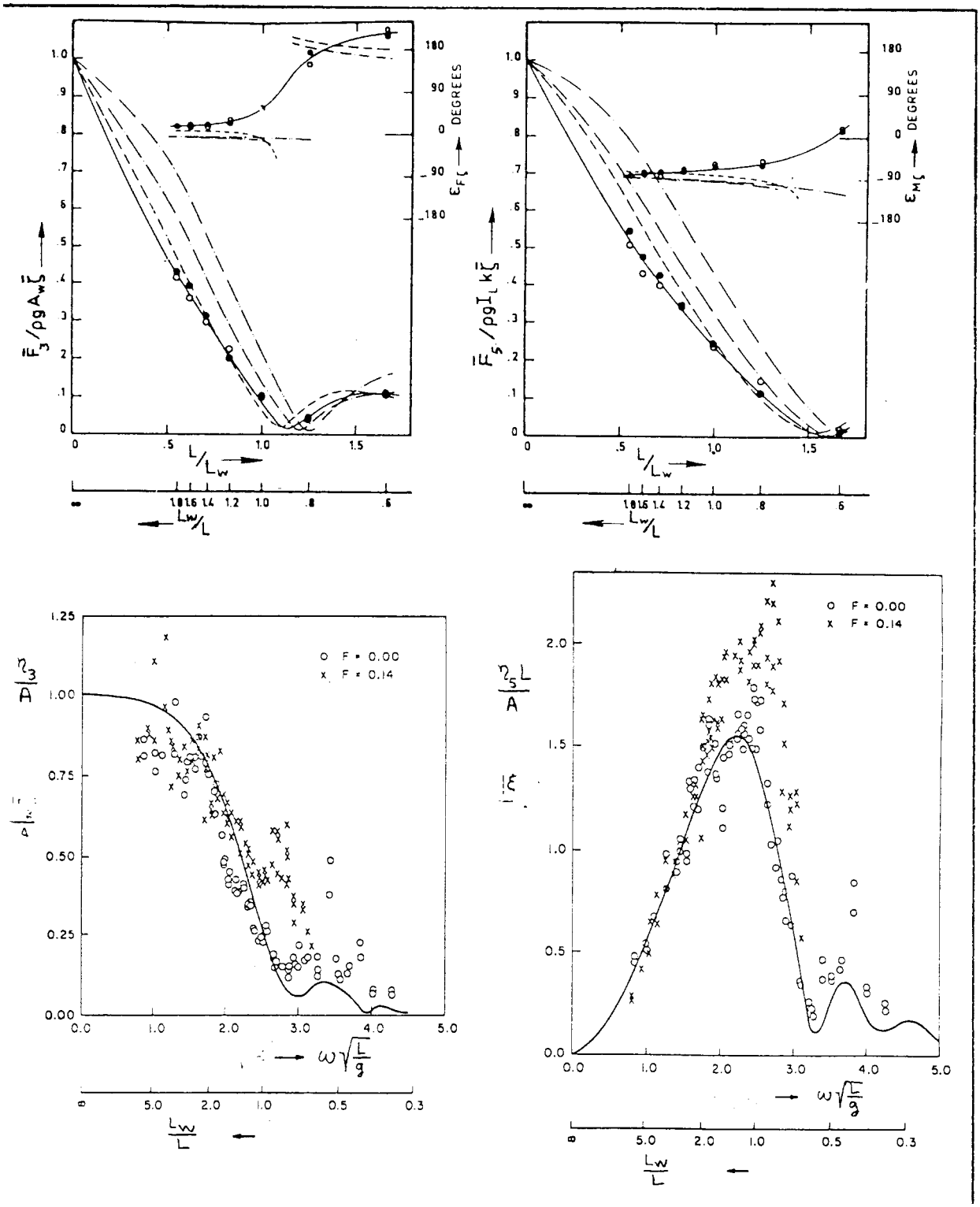

Figure 29: Heave and pitch exciting forces and motions in regular waves.

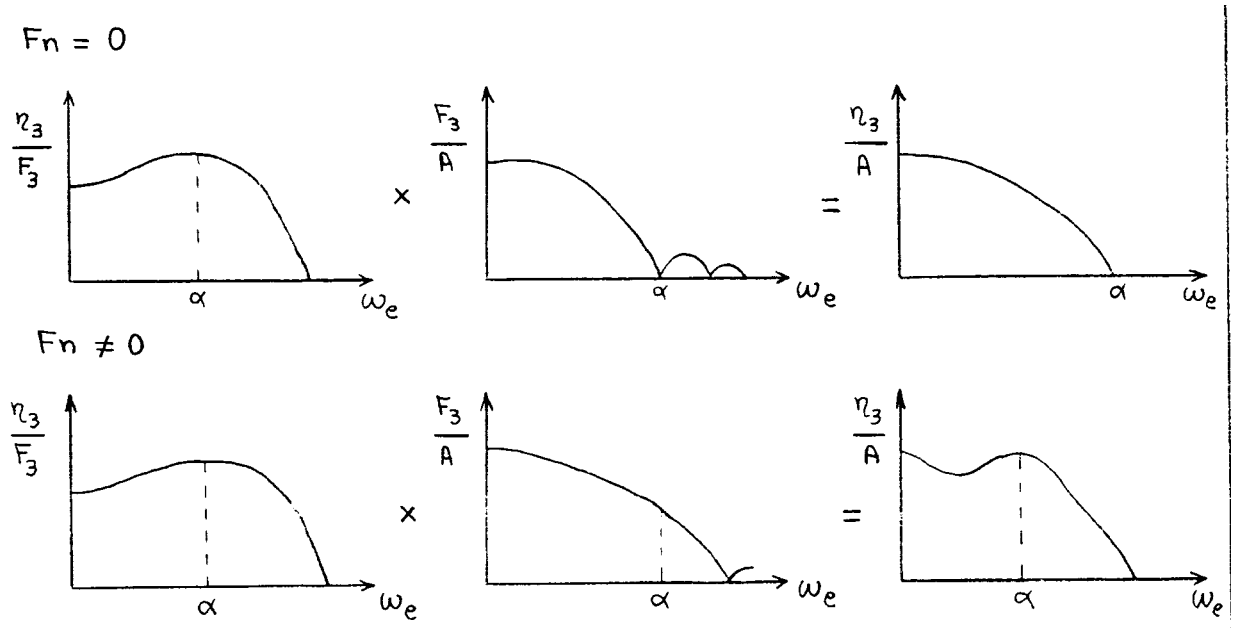

Figure 30: Influence of forward speed on heave RAO.

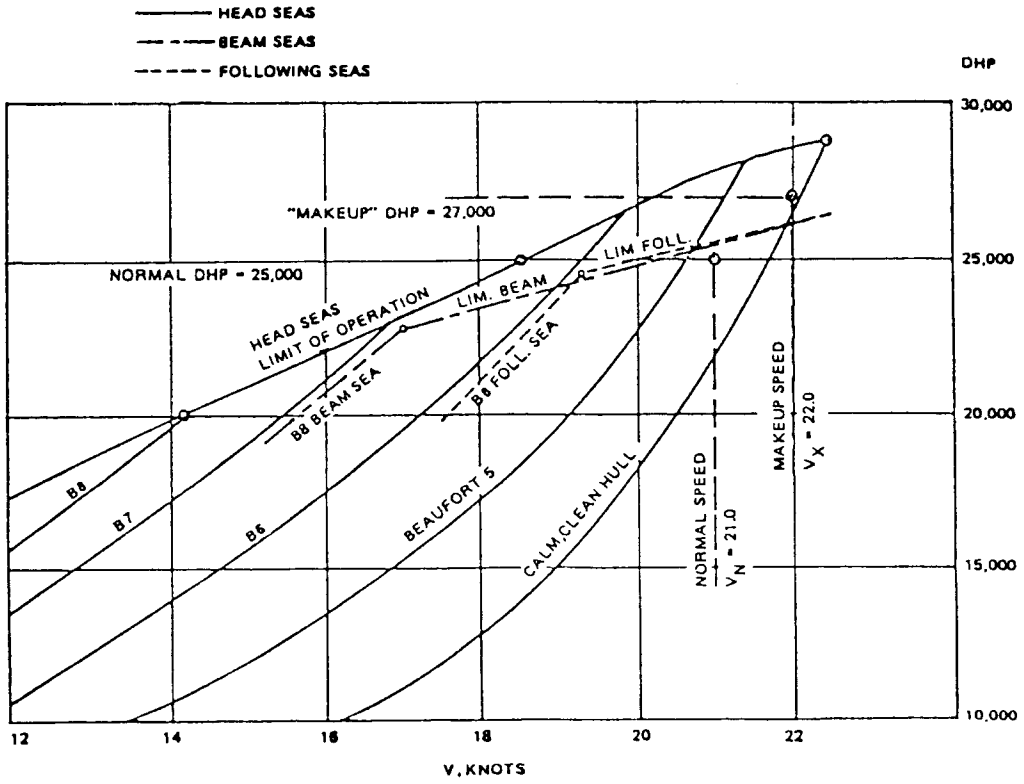

Figure 31: Typical service performance of a ship in rough seas.

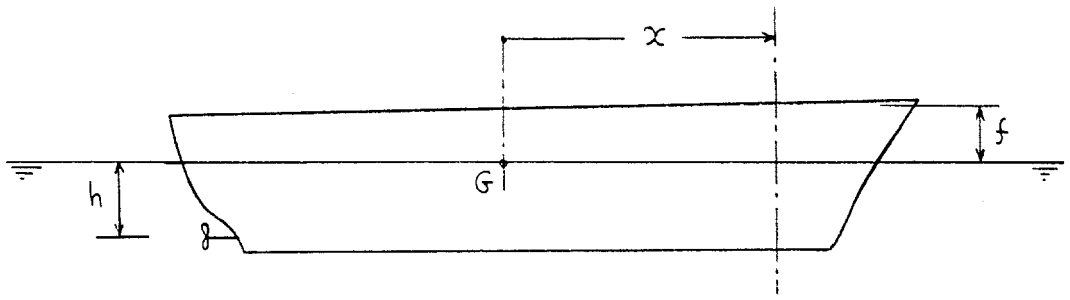

Figure 32: Definitions for propeller emergence and deck wetness.

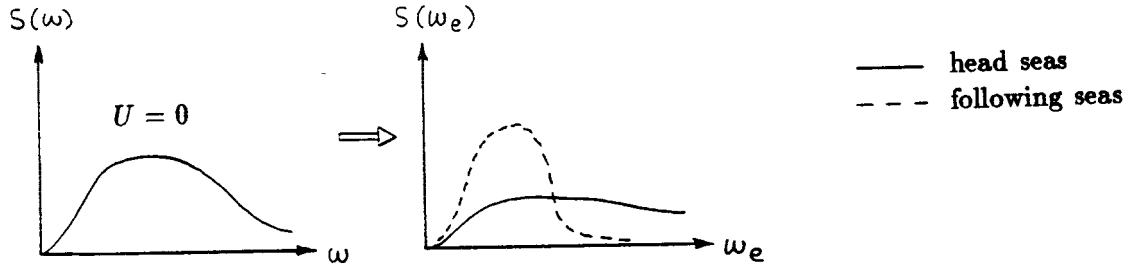

Figure 33: Transformations of sea spectrum.

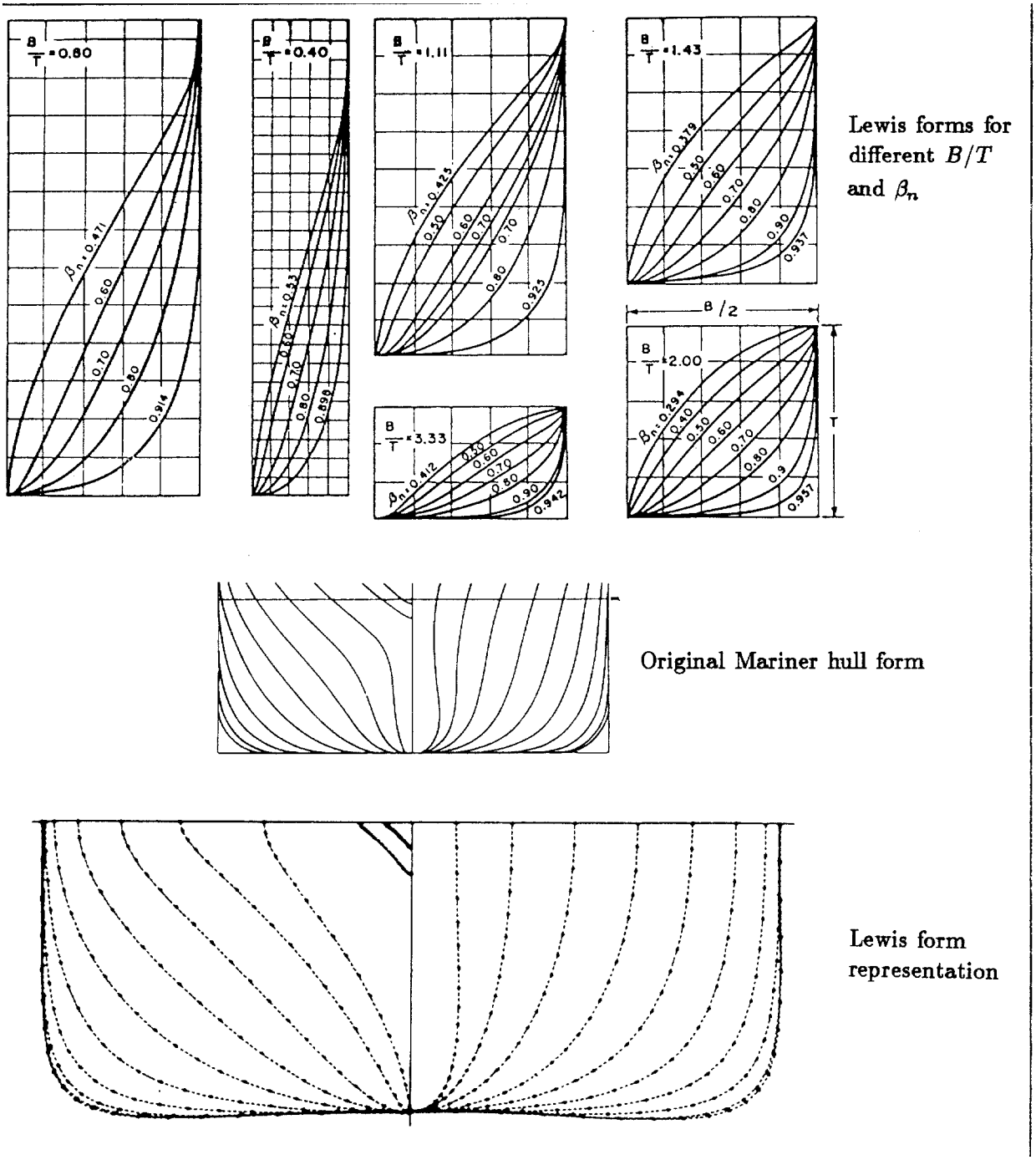

Figure 34: Lewis form representations.

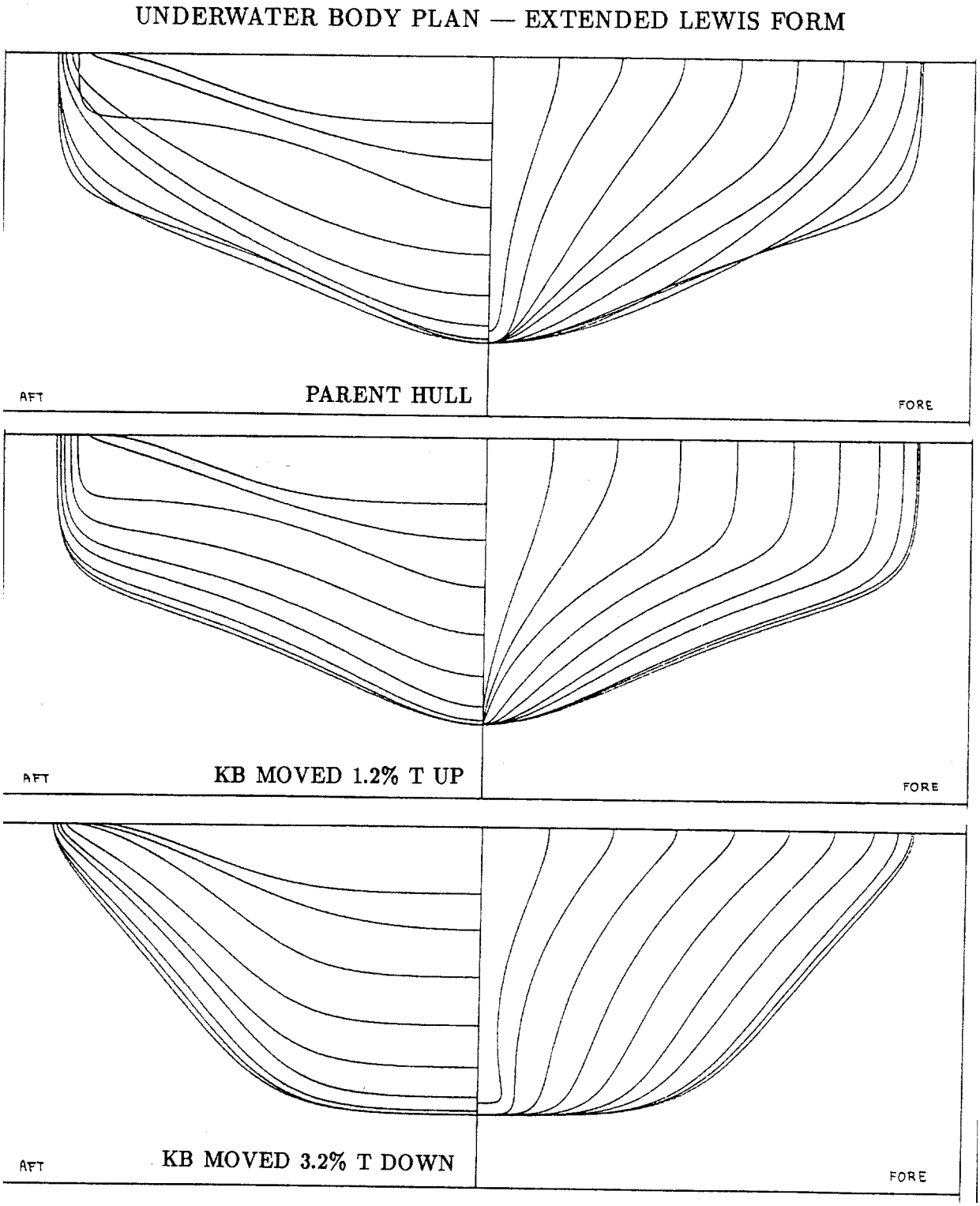

Figure 35: Extended Lewis form representations.

Criterion Response	Location	Criteria levels for		
		Launch	Recovery	Support
Pitch	About the center of gravity	3.0 deg		
Roll		5.0 deg		3.5 deg
Deck wetness	At F.P.	30 occurrences per hour		
Bottom slamming	15% L_{BP} from F.P.	20 occurrences per hour		
Vertical acceleration	Bridge	0.4 g		
Lateral acceleration		0.2 g		
Vertical velocity	Helicopter touchdown point	none	2.0 m/s	none

Figure 36: Typical seakeeping criteria.

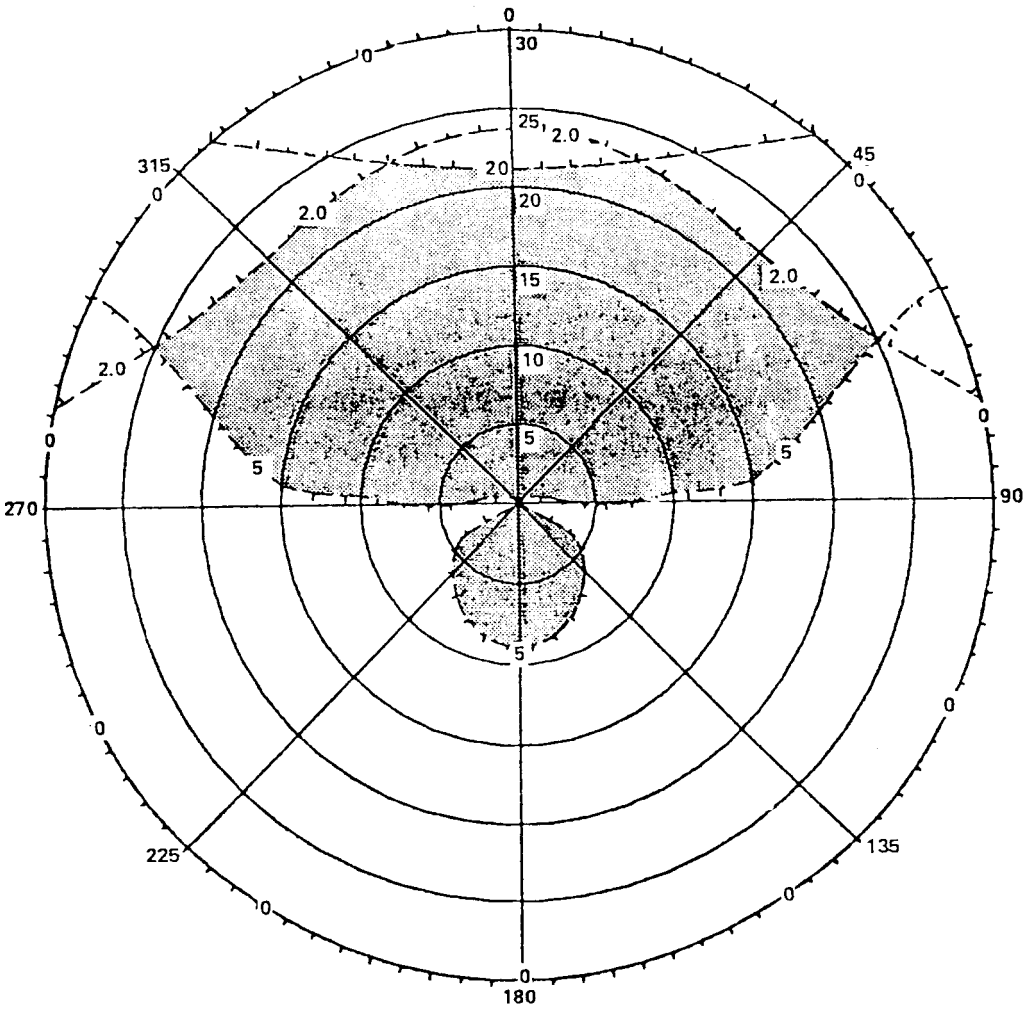

Figure 37: Typical performance assessment of helicopter landing.

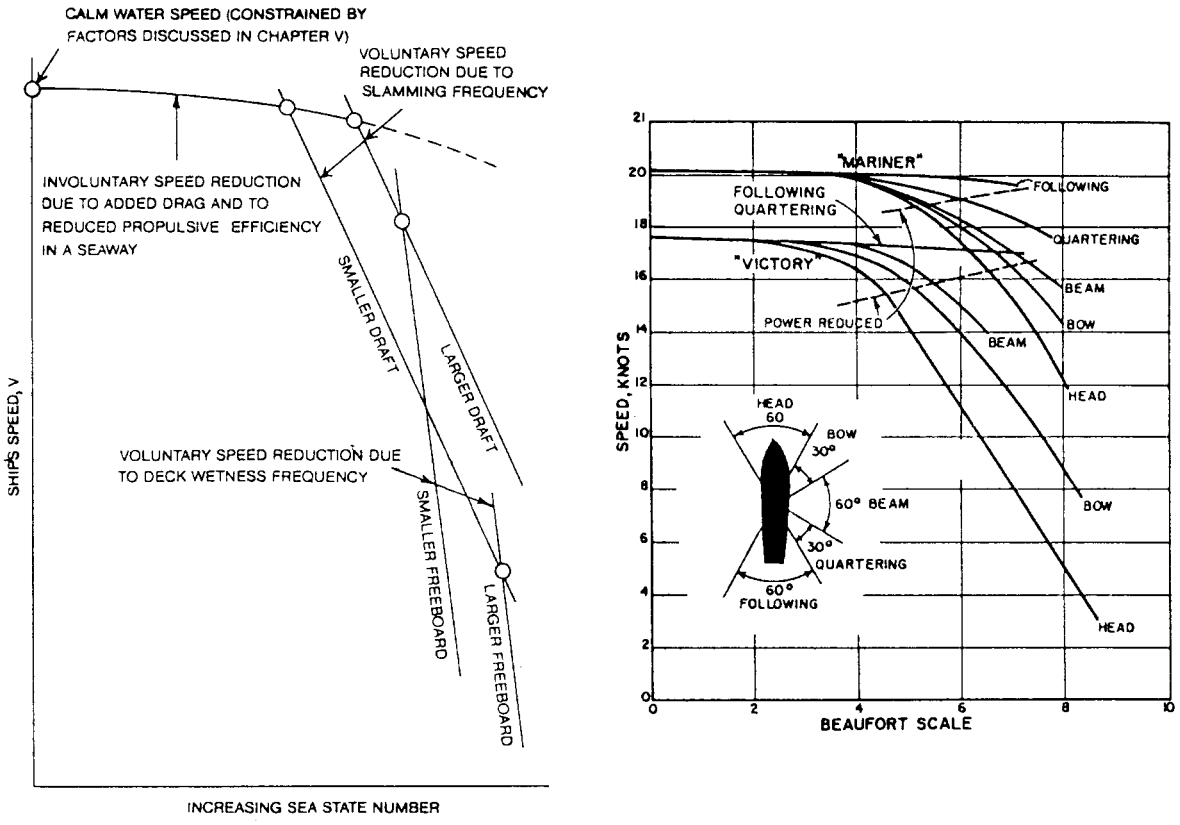

Figure 38: Speed reduction in rough seas.